“Precision timing detectors for High Energy Physics”

E. Bossini
(INFN-Pisa)

XXXX ciclo di dottorato in fisica sperimentale
Università di Siena
11 June 2025

Contact: edoardo.bossini@pi.infn.it

Lecture layout

- Particle detection - basics
- Need for precise timing detectors in High Energy Physics
- Introduction to timing concepts

- Overview of main detector technologies for timing :
  - MicroChannel Plate (MCP)
  - Silicon PhotoMultiplier (SiPM)
  - Low Gain Avalanche Diode (LGAD)
  - Diamond
  - 3D silicon
  - CMOS Monolithic Active Pixel Sensors (MAPS)
  - Gaseous detectors

- FEE & digitization

Lecture Objectives

- Get an overview of recent experimental requirements in terms of detector timing performance.
- Understand the main concepts connected to timing, the digitization techniques and understand the main sources of uncertainties.
- Acquire a broad knowledge on the main technologies able to provide sub-100 ps timing. Understand their operating principles, strengths and limitations. Get an insight of the latest developments and results in the field.

Particle interaction with matter

(just what you need to know today)

Detection of charged particles

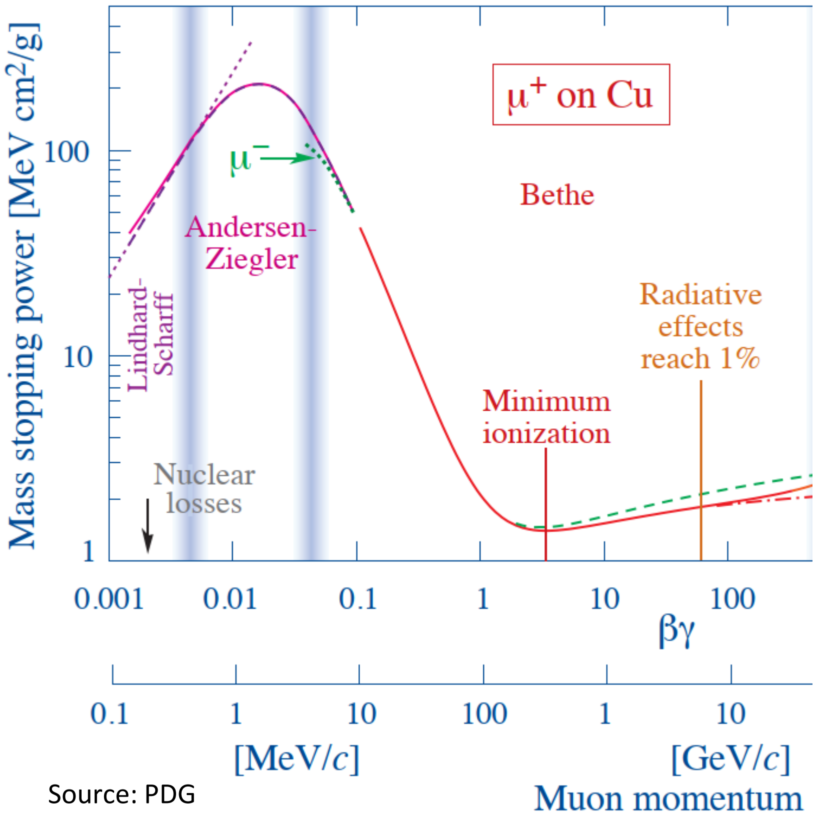

Source: PDG

Works great for heavy particle ($m \gg m_e$)

Three type of electromagnetic interactions for charged particle:

1. Ionization (of the atoms of the traversed material)
2. Emission of Cherenkov light
3. Radiative loss (Bremsstrahlung)
4. Emission of transition radiation (not discussed today)

The energy loss is described by the Bethe-Block formula + corrections:

$$\left\langle -\frac{dE}{dx} \right\rangle = K z^2 \frac{Z}{A} \frac{1}{\beta^2} \left[\frac{1}{2} \ln \frac{2 m_e c^2 \beta^2 \gamma^2 W_{\max}}{I^2} - \beta^2 - \frac{\delta(\beta\gamma)}{2} \right]$$

- At very low energy only empirical models available
- $\beta\gamma < 3 \rightarrow dE/dx \propto 1/\beta^2$
- $\beta\gamma \simeq 3$ minimum → MIP (Minimum Ionizing Particle)
  $\rightarrow dE/dx \text{ @ } MIP \sim 1.5 - 2\ MeV\ cm^2/g$
- $\beta\gamma > 3$ logarithmic rise limited by density correction
  dE/dX ≃ 2 MeV cm2/g

Detection by ionization loss

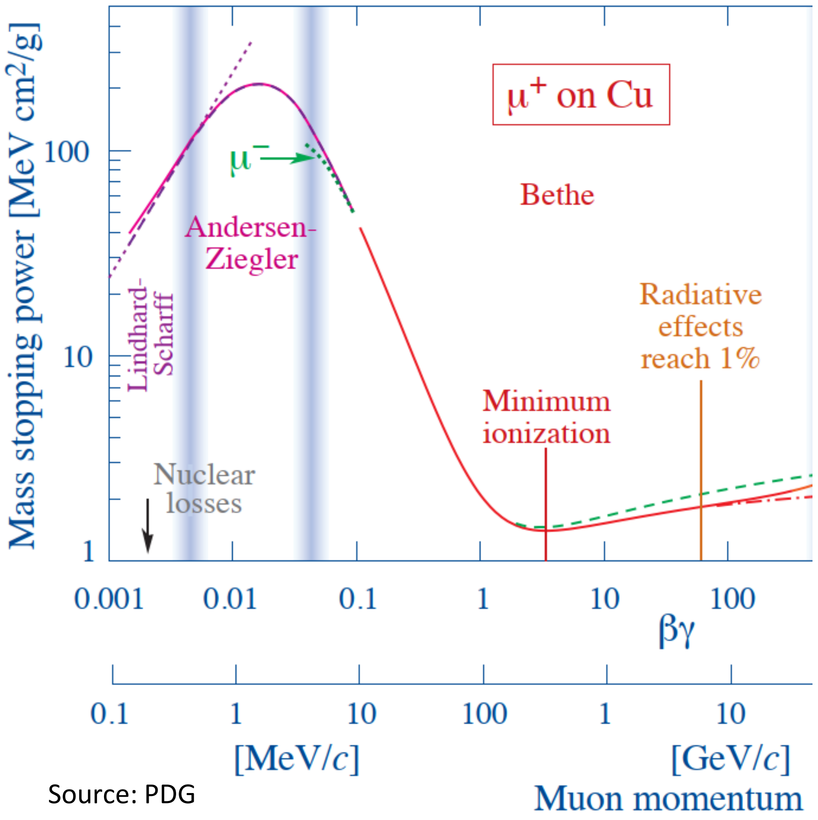

Source: PDG

Very mild dependence on the absorber, when scaled for the absorber density

Energy loss rate depends on the particle speed. In the MIP region a proton of 10 GeV/c release the same energy of Pion of 1 GeV/c!

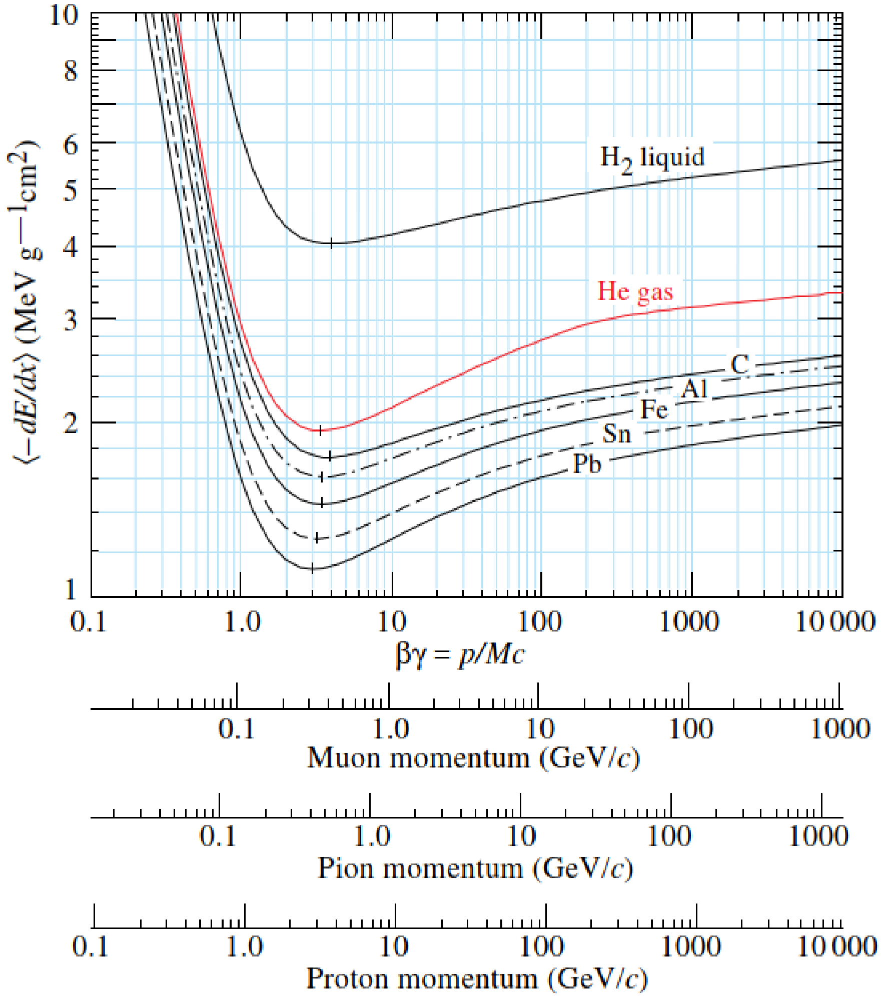

Works great for heavy particle ($m \gg m_e$)

Detection by ionization loss

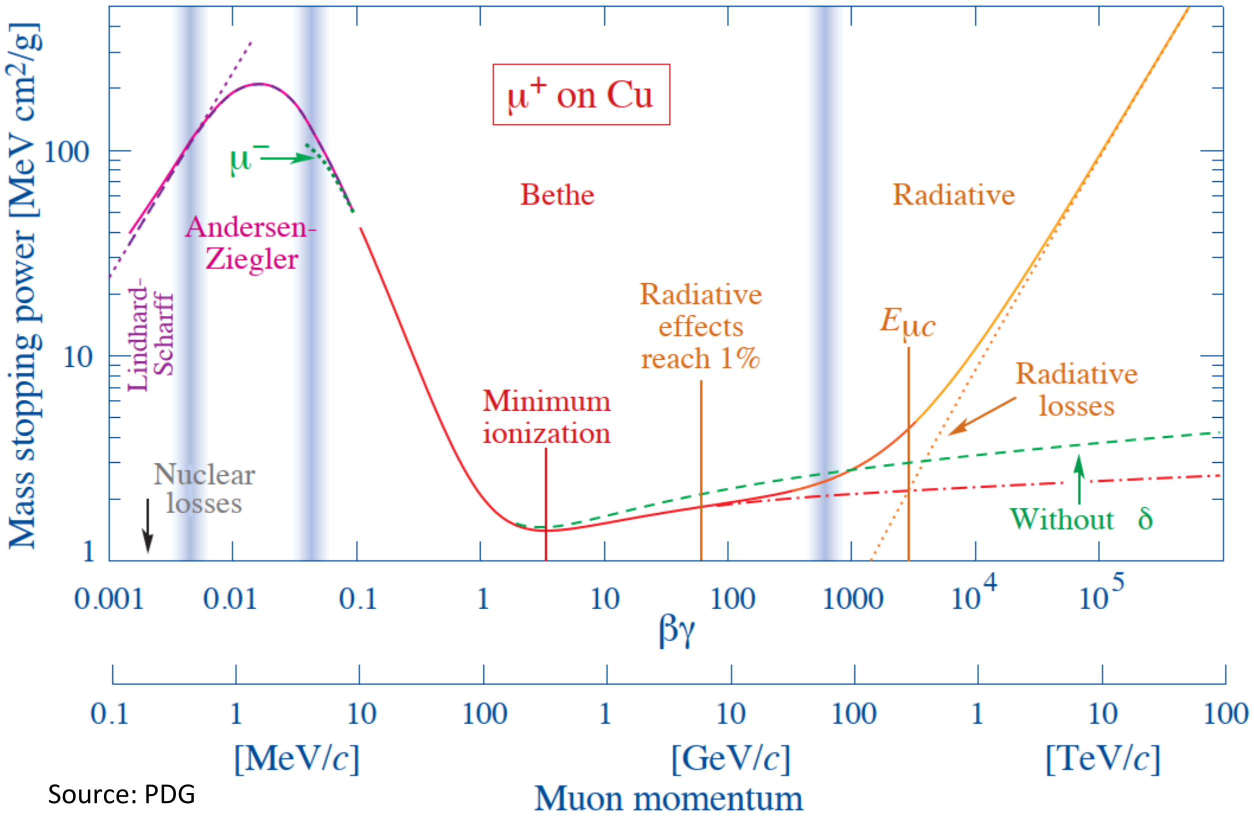

Source: PDG

At higher energies radiative loss dominate (**Bremsstrahlung**). The critical energy depend on the particle mass ($dE/dx_{bre} \;\propto E/m^2$)

For muons $E_C \sim 200\ TeV$. ~Not relevant for us, but in case of high energy electrons $E_C \sim 10\ MeV$!

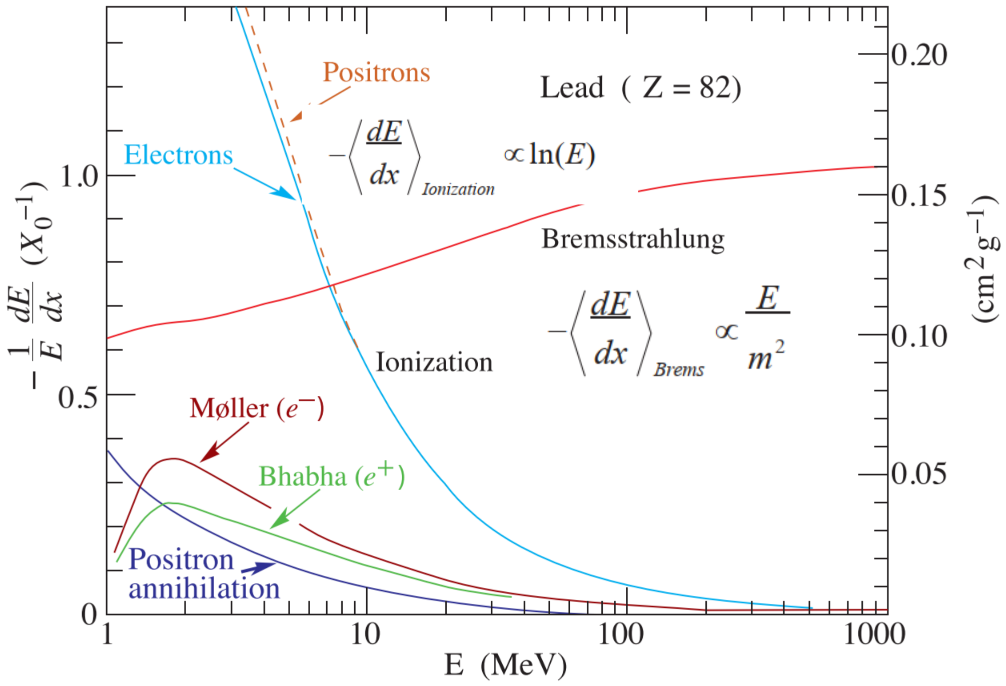

Works great for heavy particle ($m \gg m_e$)
Radiative losses are not so relevant for thin detector, since the emitted photon can escape undetected

Source: PDG

UNIVERSITÀ DI SIENA 1240

Total energy release in thin absorbers

You might expect a gaussian distribution of the energy released in each thin layer of the detector.
However, electrons can be directly hit by a traversing particle, transferring a lot of energy (up to several MeV) in a single collision:

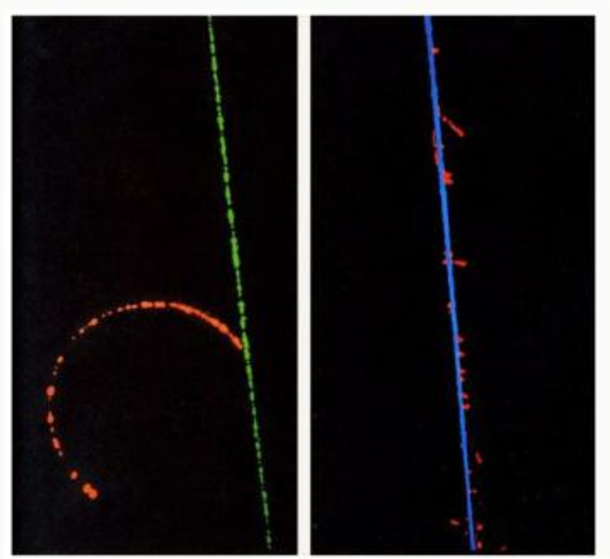

- Knocked-out electrons are called delta ray or delta electrons
- Nearly always ~perpendicular to particle trajectory
- Produce secondary ionization, greatly increasingly local dE/dx
- In gas detectors can curl in magnetic field
- In solid state detectors can distribute signal over more strips/pixels with larger cluster

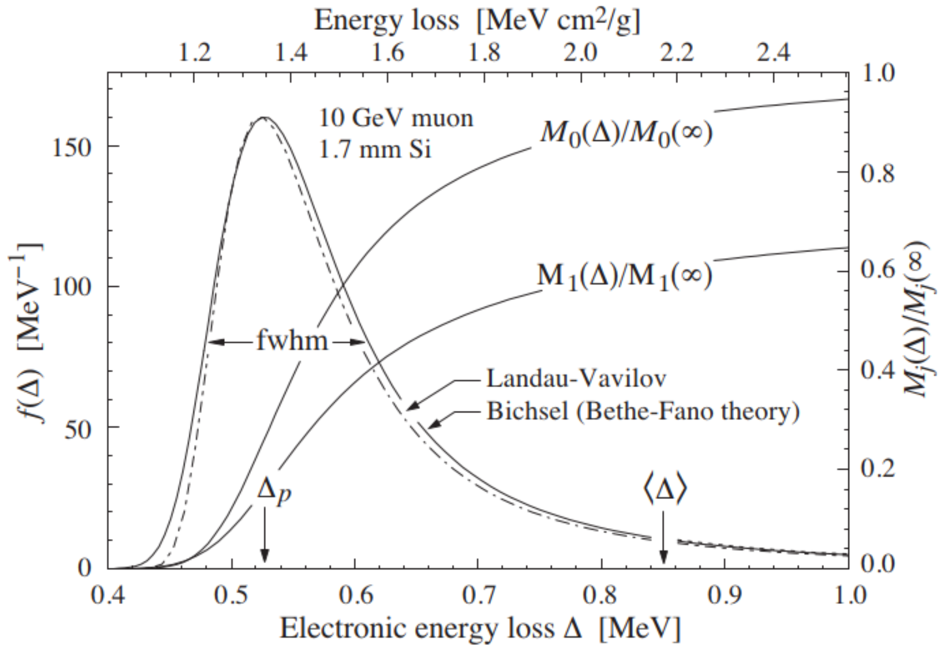

Energy loss is a statistical process:

- Average loss expressed by Bethe-Bloch
- Including the delta electrons, the distribution becomes broader, with a long tail for higher energy losses
- Final distribution for thin material is a “Landau”, with a mean energy loss different from most probable value (MPV)

Cherenkov radiation

EM radiation is emitted by a charged particle in a medium where the particle speed is greater than the speed of light in that material.

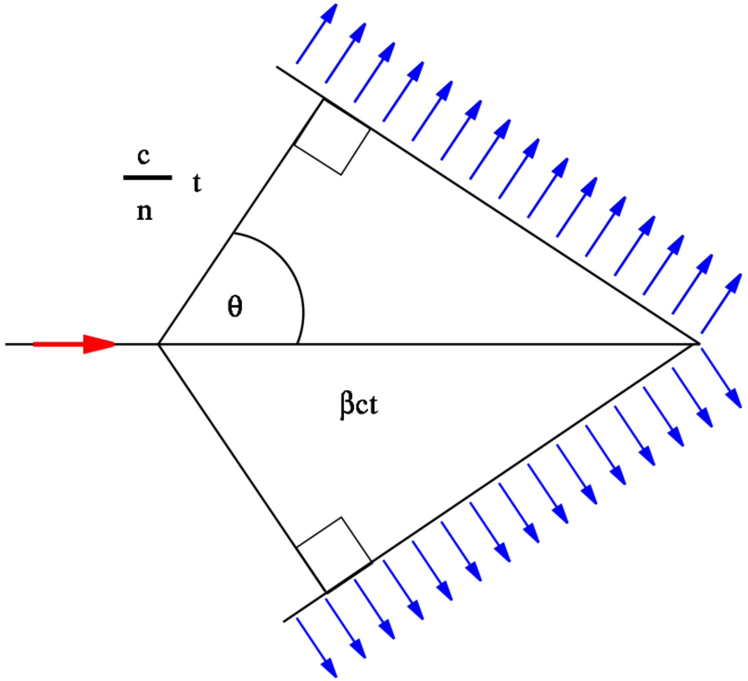

$$-\left\langle \frac{dE}{dx} \right\rangle_{Cherenkov} \propto z^2 \sin^2 \theta_c \qquad \cos\theta_c = \frac{1}{n\beta}$$

- Threshold condition: Cherenkov happens only if $\beta \geq 1/n$
- Radiation is emitted with a characteristic angle (n is refractive index of material)
- Measure of θ_C lead to a measure of β (harder when β~1)
- If you have an independent measure of the momentum, you can do PID

- Energy loss by Cherenkov is <1% of ionization loss
- Emission of 200-1000 photon/cm in the visible spectra
- $\frac{1}{\lambda^2}$ wavelength distribution -> Near UV photons favored

$$\frac{d^2N}{d\lambda dx} \propto \frac{1}{\lambda^2} \sin^2\theta_C$$

Photon interaction

A photon is removed from the beam after one single interaction either because of total absorption or scattering. Three main processes:

- Photoelectric
- Compton
- Pair production

$$I(x) = I_0 e^{-\mu x}, \quad \mu = \frac{N}{A} \sum_{i=1}^{3} \sigma_i$$

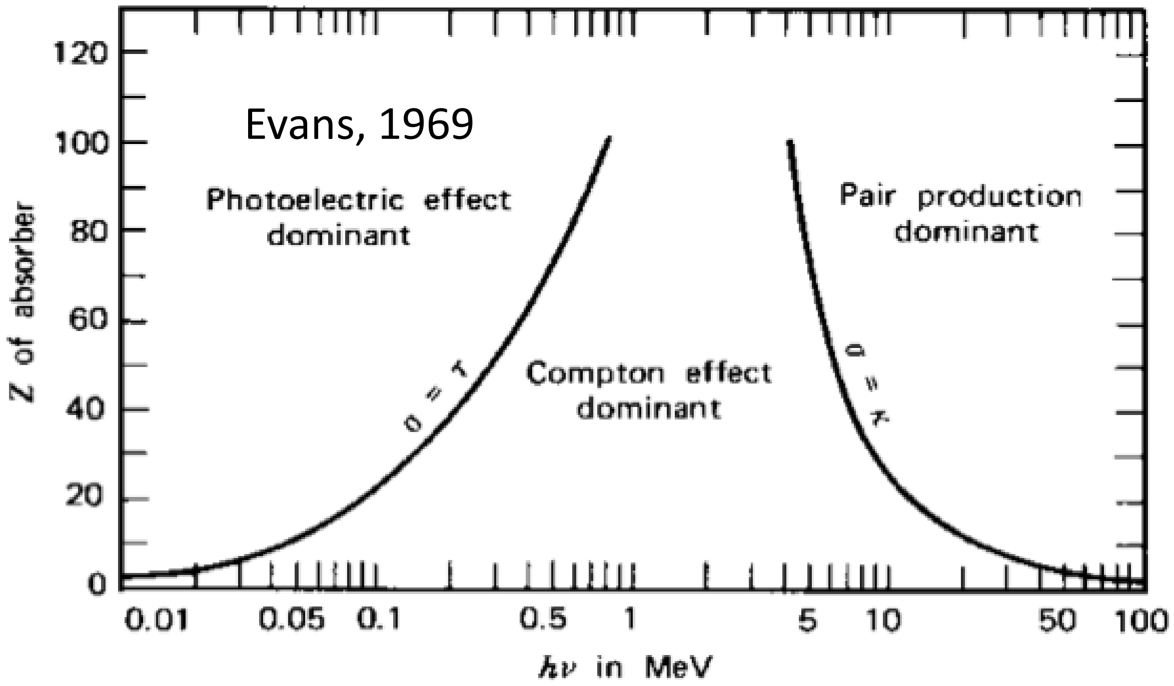

The knocked-out electrons or the pair will then generate secondary ionization in the absorber

- Compton should be (usually) avoided since the scattered photon can exit from the detector
- Photoelectric and pair production cross section raise faster with the absorber Z

Use high-Z material to enhance cross section and reduce Compton probability.

Neutral particle: make them interact with nuclei or the electrons of the absorber (strong or weak interactions), then detect the charged particles generated by the interaction!

Why we need precise timing detectors?

High Luminosity colliders

A major challenge faced by High luminosity accelerators is the large pileup, represented by multiple simultaneous independent collisions. In the HL-LHC an average number of 200 simultaneous pp collisions per bunch crossing is foreseen.

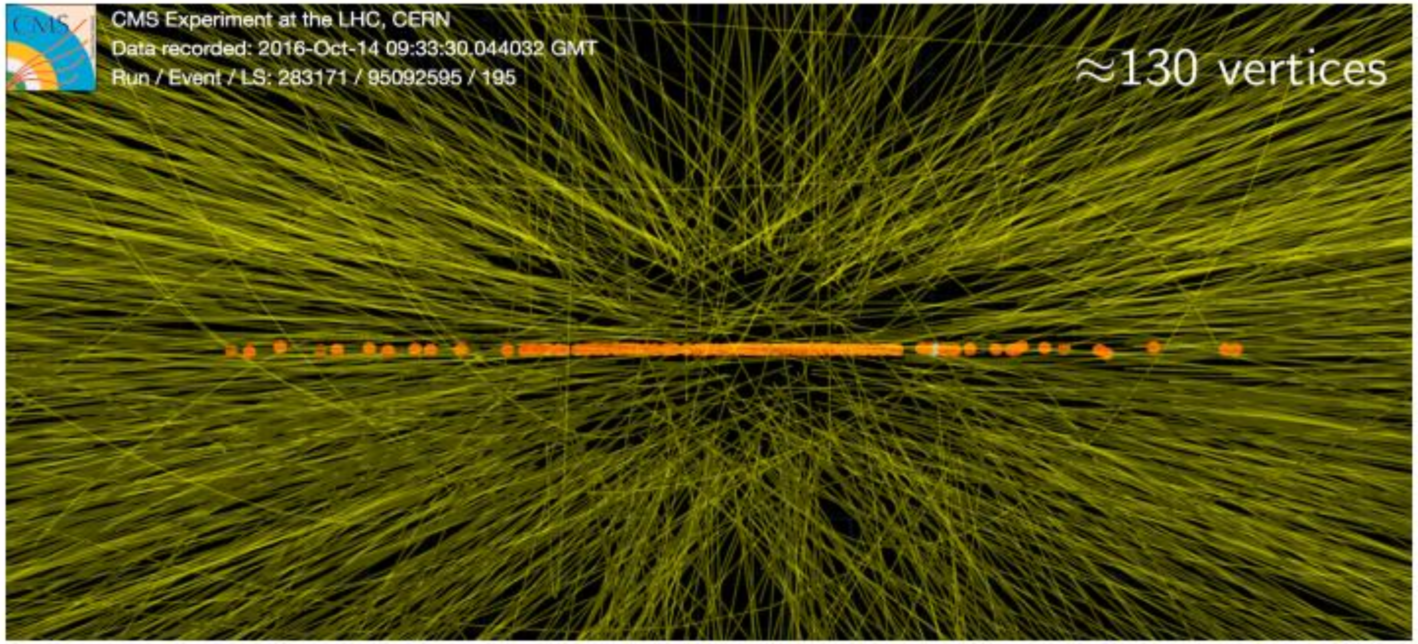

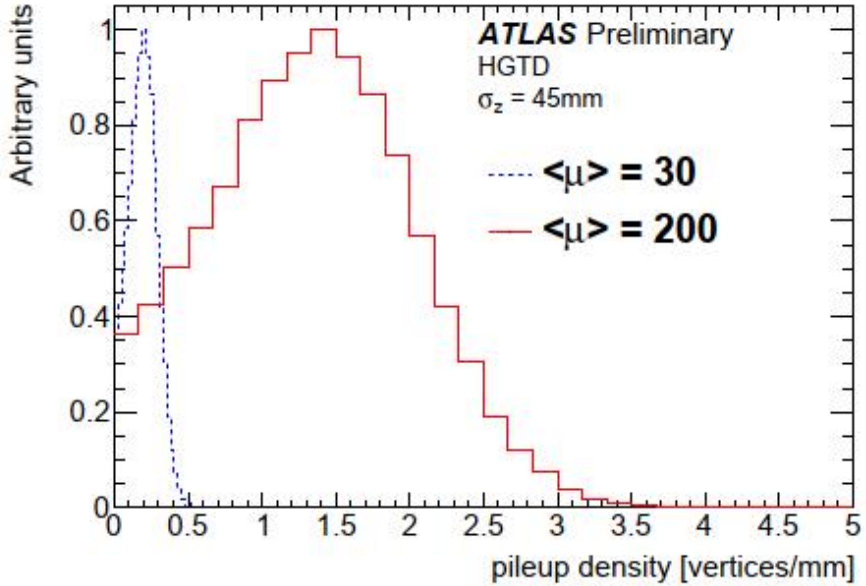

Beam spot longitudinal RMS will be 45 mm, with an expected average pile-up $\langle \mu \rangle = 200 \ \rightarrow 1.6$ vertices/mm n average!

High Luminosity colliders

The two colliding bunches will take approximately 180ps to cross each other -> vertices not separated in space can be separated in time!

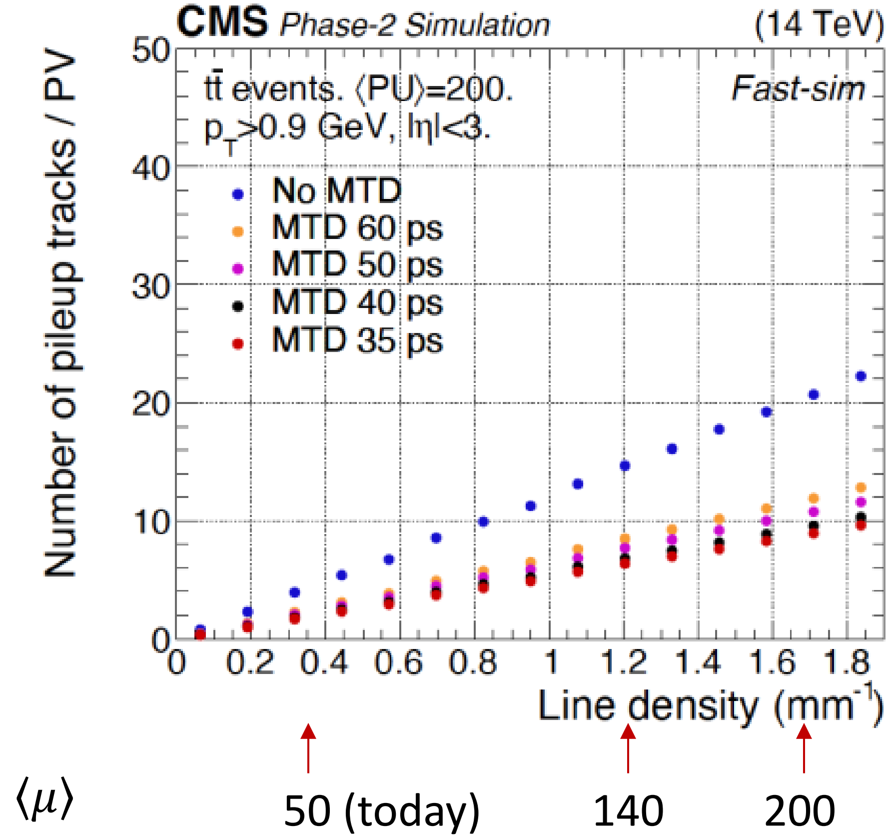

4D vertex reconstruction

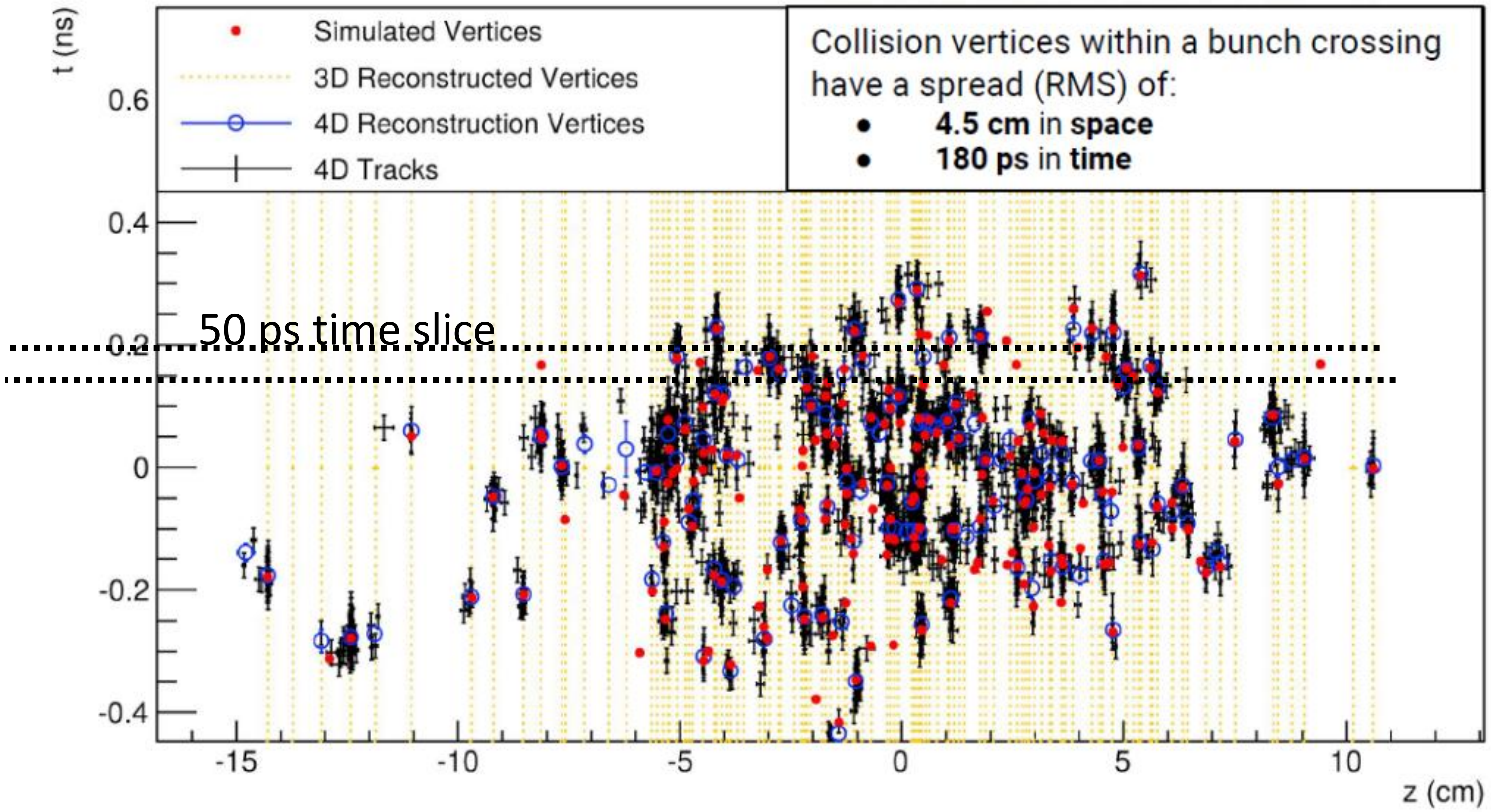

ATLAS HGTD

Particles created in high energy inelastic collision are mainly generated in the forward direction, parallel to beam direction. This imply that a precise timing detector is mainly needed in the forward region.
The ATLAS High Granularity Timing Detector (HGTD will indeed cover timing measurements for charged particles in the forward region ($2.4 < \eta < 4.0$)

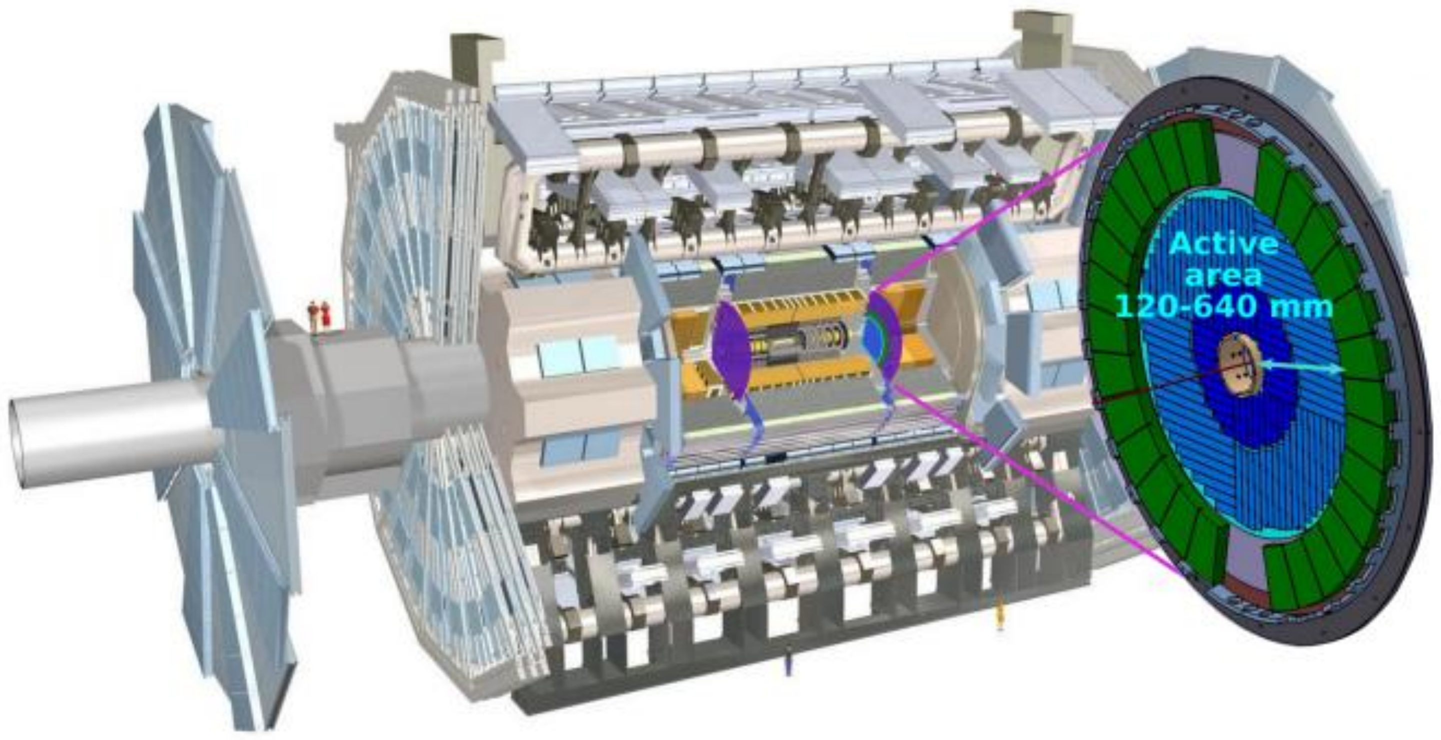

- Two endcap disks at $z = \pm 3.5$ m
- $6.3\ \mathrm{m}^2$ active area, with a radius $120\text{mm} < R < 640\text{mm}$
- Expected radiation up to $3.7\text{x}10^{15}\ n_{eq}/cm^2$, 4.1 MGy TID
- Detector technology :Si-based LGAD, with expected resolution of 30ps/track
- Pixel segmentation 1.3mm x 1.3 mm to achieve an occupation <10%

CMS MTD

CMS is developing a new endcap (forward) calorimeter, HGCAL. It will provide timing information on particle clusters. Moreover, a new timing layer (MIP Timing Layer, MTD) will provide an ~hermetic coverage.

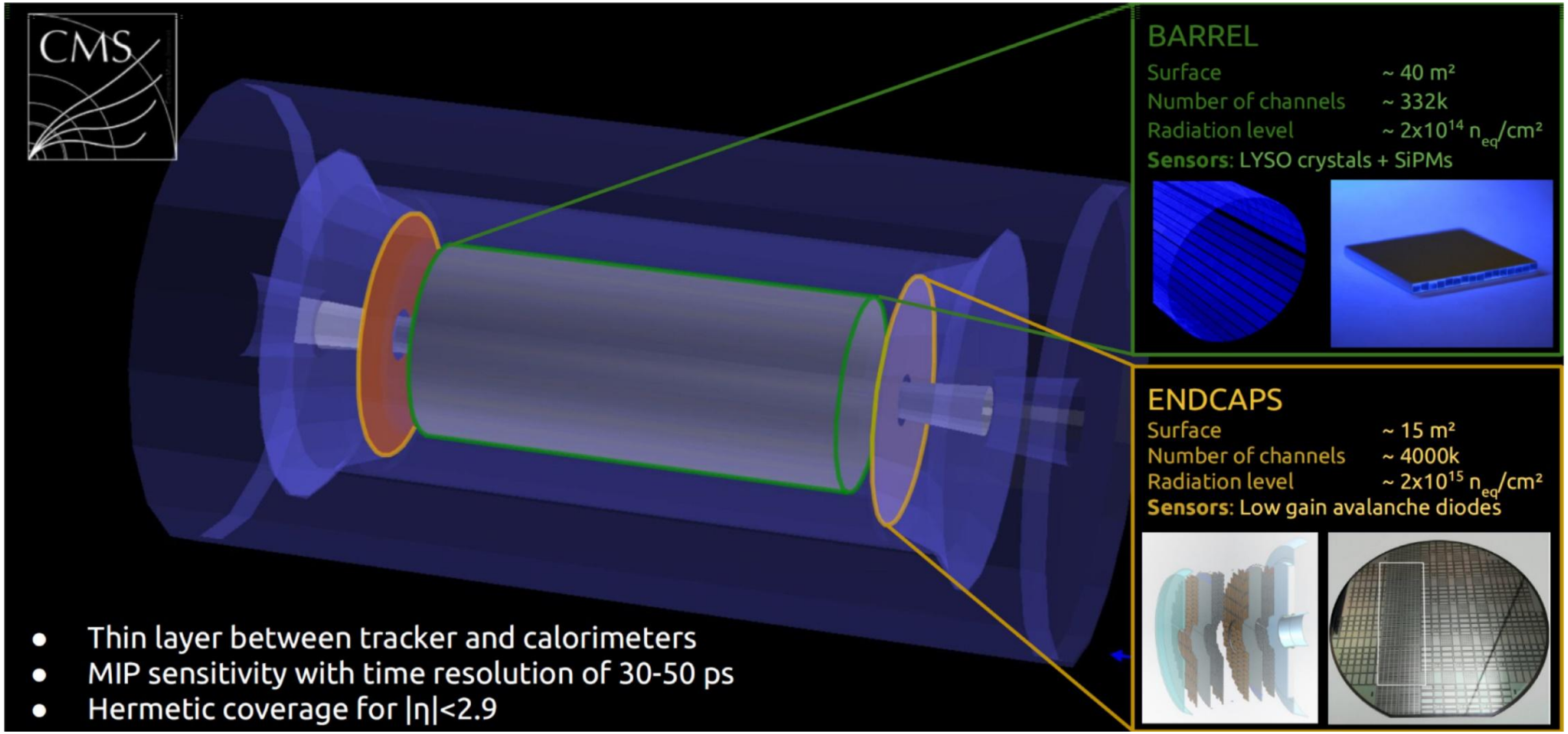

PID through dE/dx

B-physics experiments (Belle-II, LHCb, PANDA) require excellent, high-efficiency PID, especially in the π-k discrimination.

ALICE TPC

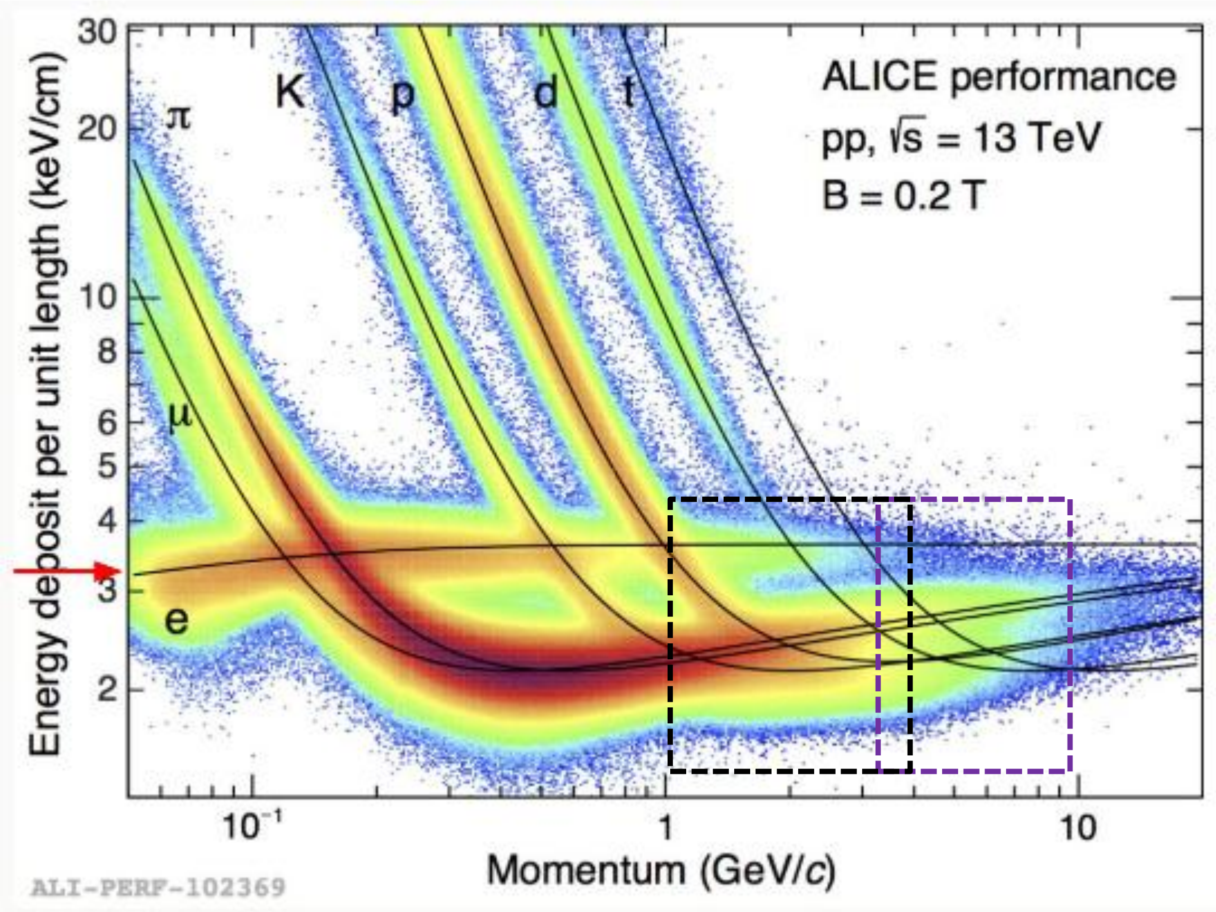

Particle Identification (PID) can be carried out by performing simultaneous measurement of the particle momentum (i.e. with a tracker inside a magnetic field) and dE/dx

- Efficient identification for momentum below ~1 GeV/c
- Need very good resolution at greater energies (or alternative measurement…)

PID with Time Of Flight

In the sub-GeV range this is usually attained by a combined measurement of the particle momentum (tracking in magnetic field) and dE/dx (ionization). At higher energy and higher particle rate Time Of Flight (TOF) detector can be used.

Tracking (momentum) + de/dx & TOF

ALICE TOF, MRPC

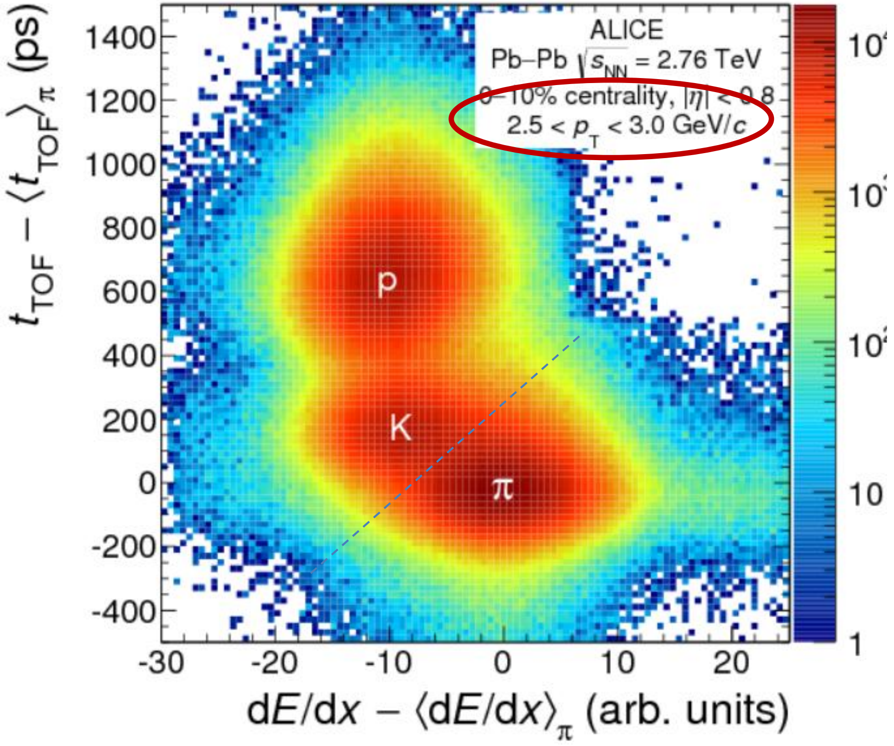

Tracking (momentum) + Cherenkov (speed)

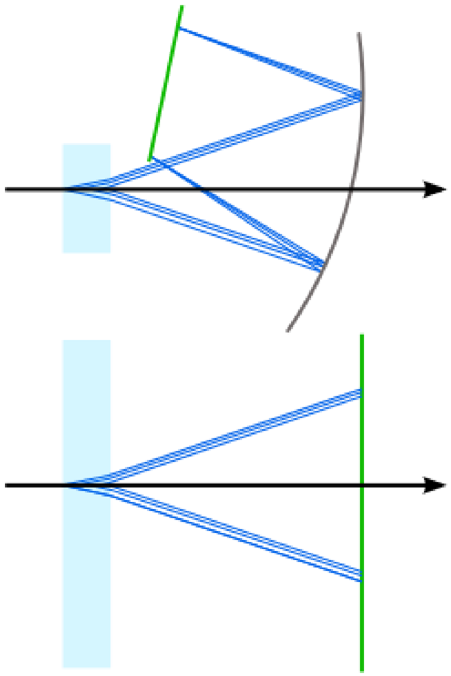

The radius of the ring can be used to reconstruct the speed of the particle -> PID when coupled with the momentum measurement

In the 1-5 Gev/c range the Cherenkov threshold can be used (no signal Cherenkov effect from K)

RICH (Ring Imaging Detector)

PID-DIRC

Existing RICH geometries are poorly matched to the required physical sizes, location within the detector, rate requirements, and the secondary particle momentum range at B Factories.

TOF detectors must cover the full solid angle and occupying a limited amount of detector volume, usually in between other detector layers. They also should have a reduced mass, often being in front of high precision electromagnetic calorimeters

Detection of Internally Reflected Cherenkov light

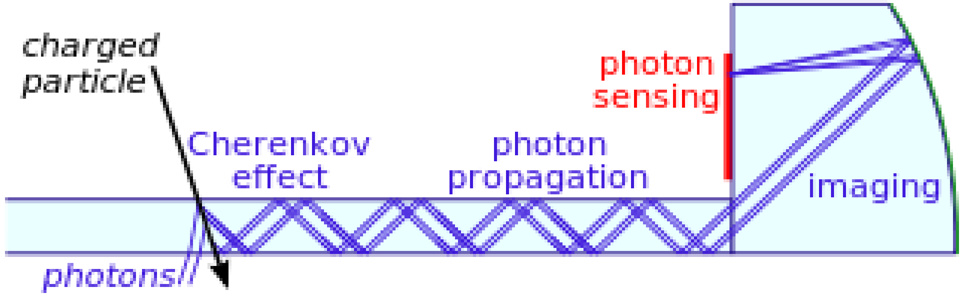

PID-DIRC

Existing RICH geometries are poorly matched to the required physical sizes, location within the detector, rate requirements, and the secondary particle momentum range at B Factories.

TOF detectors must cover the full solid angle and occupying a limited amount of detector volume, usually in between other detector layers. They also should have a reduced mass, often being in front of high precision electromagnetic calorimeters

Detection of Internally Reflected Cherenkov light

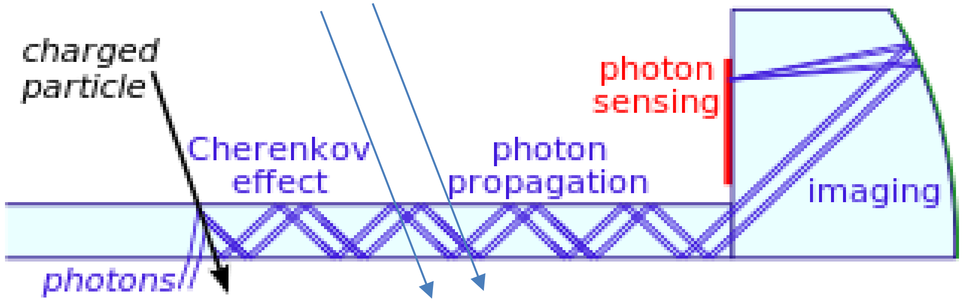

PID-DIRC

Existing RICH geometries are poorly matched to the required physical sizes, location within the detector, rate requirements, and the secondary particle momentum range at B Factories.

TOF detectors must cover the full solid angle and occupying a limited amount of detector volume, usually in between other detector layers. They also should have a reduced mass, often being in front of high precision electromagnetic calorimeters

Detection of Internally Reflected Cherenkov light

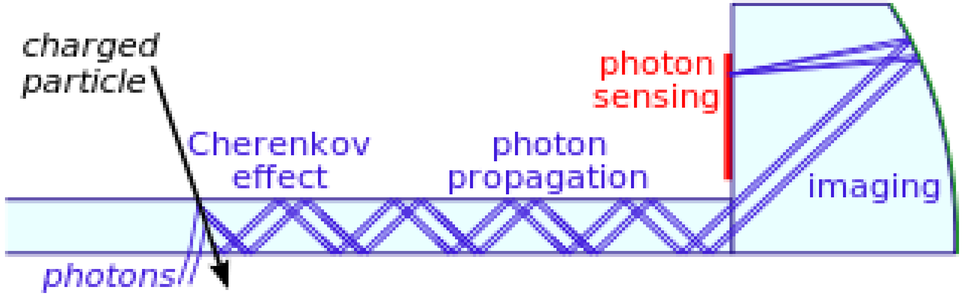

Double measure: TOF + Cherenkov angle!

Depending on the resolutions achieved, when combined with direct angular measurements, this single photon timing can provide:

- spatial separation of events along the bar
- a reliable tag of beam crossings (4 ns at PEP-II) -> can be used as reference for other TOF measurement
- background rejection at high rates
- separation of some reflection and direction ambiguities
- a measurement of the wavelength photon by photon-> chromatic dispersion correction
- a measurement that convolves the Cherenkov polar angle and the overall particle Time-of-Flight (TOF)

Example of future DIRC: TORCH

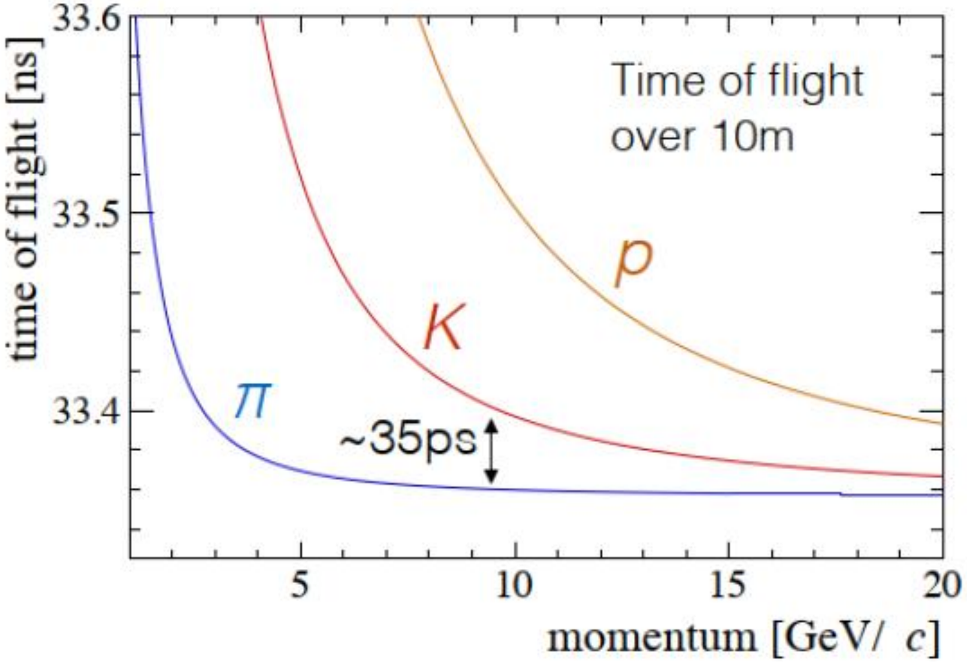

A resolution of 10 ps is needed to provide efficient π-k discrimination up to 10 GeV/c.

3 regions for π-k PID, momentum measurement in conjunction with other sub-detectors:

1. Below 1 Gev/c -> Energy deposition
2. 1-5 GeV/c -> Cherenkov Threshold or TOF
3. Up to 10 Gev/c -> precision TOF and/or cherenkov

Simulated LHCb performance with the TORCH DIRC detector

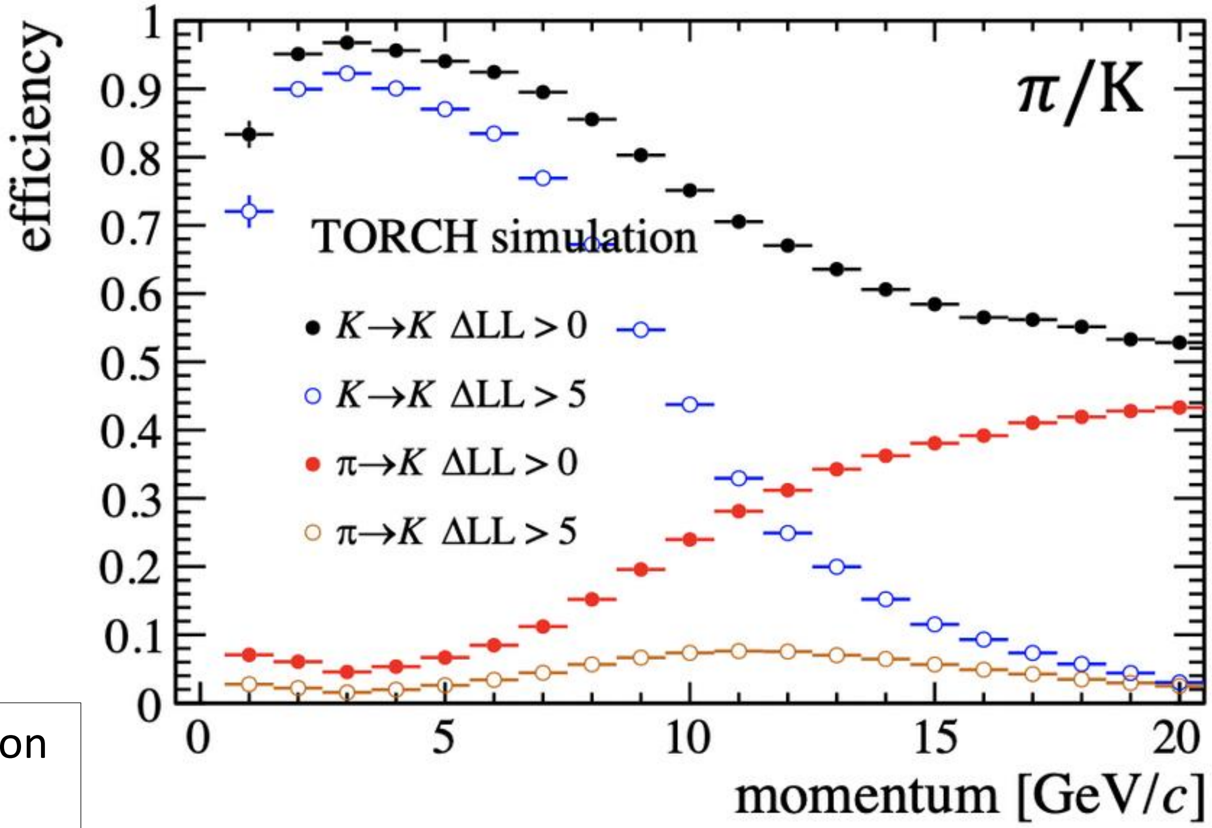

Medical applications (1)

Time Of Flight Positron Emission Tomography (TOF-PET)

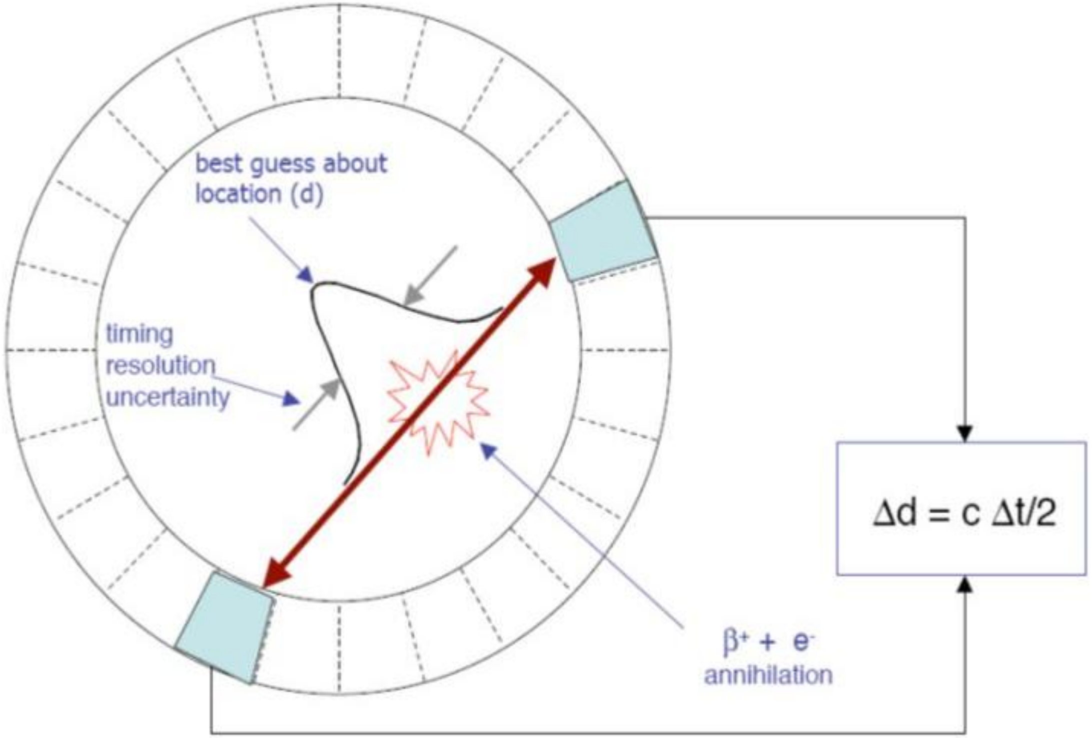

- Radioactive β^+ marker provided to patient
- Positron annihilation generate 2 back-to-back 0.511 MeV photons
- Reconstruction of decay vertex through the difference in photons propagation time
- Resolution of 100ps or better is needed to achieve 1-2 cm resolution

Medical applications (2)

Prompt gamma beam monitoring

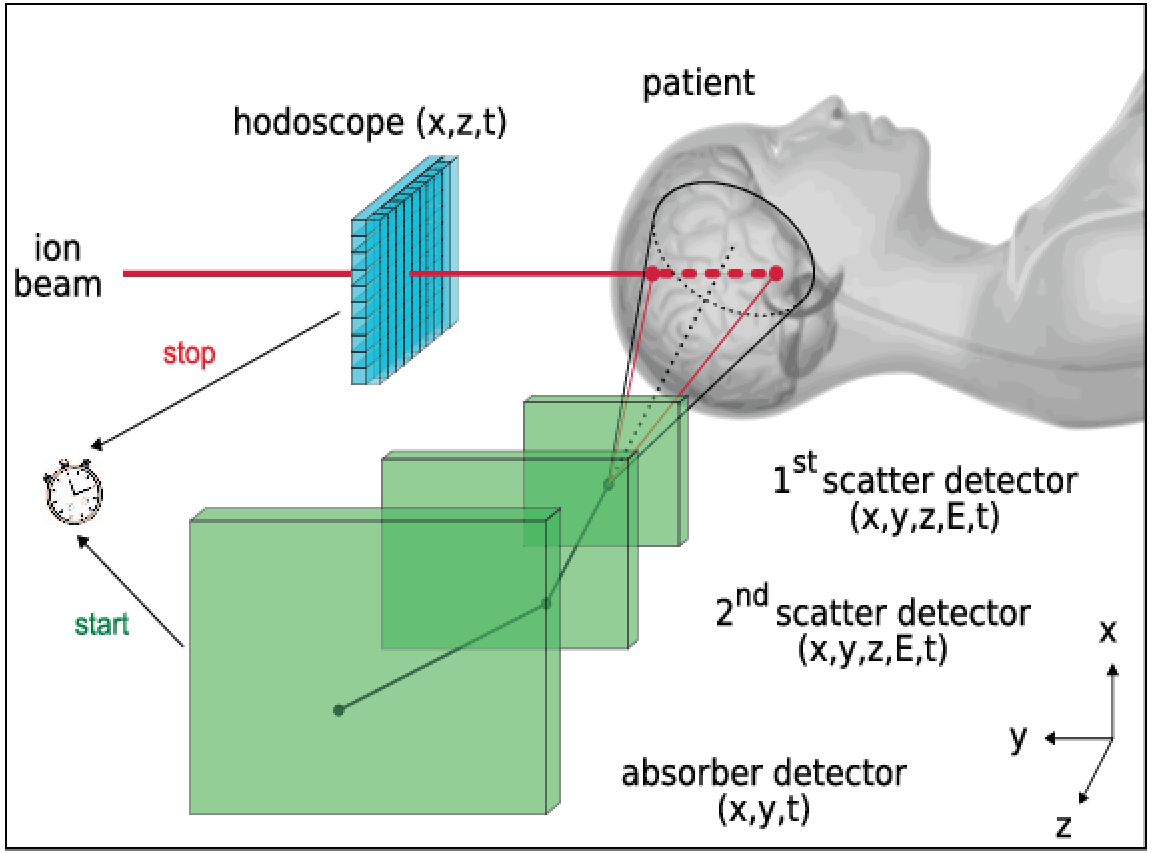

Hadron therapy requires real time dose control, especially for recent FLASH therapy protocols.

Prompt gammas (1-7 MeV range) are release by ions in the patient tissue:

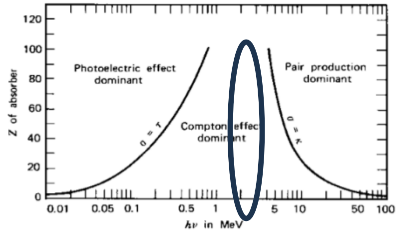

- ➢ Tracking the gamma trajectory can be difficult and affect by large uncertainties
- ➢ Measure of the gamma timestamp enhance the measurement accuracy
- ➢ Beam reference or an additional detector can be used to determine the timestamp and position of the incoming particle
- ➢ Using high resolution timing it is possible to acquire a precise 3D reconstruction of the dose profile
- ➢ The beam detector must be radiation hard and with low material budget
- ➢ Gamma detector like the one used for TOF-PET

Space applications

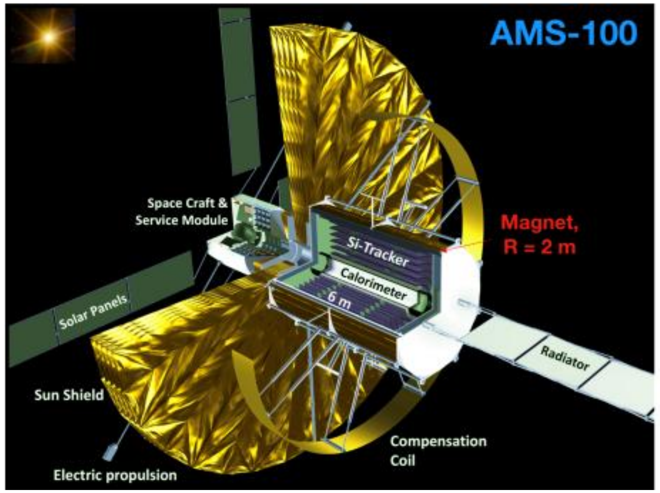

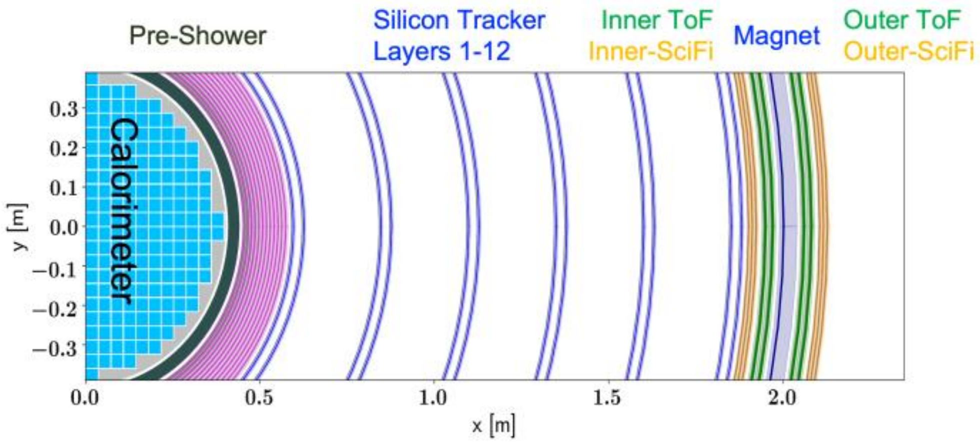

Tracking in space dominated by Silicon Microstrip detectors (SIMS), due to the operating constraints (power, weight, number of readout channels,…)

If timing is combined with the tracker additional benefit are achieved:

1. overcome the occurrence of "ghost" hits in SiMS detectors.
2. 4D tracking
3. Opens to 5D measurement (position, time, dE/dx)

Advantages of a precise timing layer:

1. identification of back-scattered particles from calorimeters
2. Improve track finding algorithm
3. opportunities for large-acceptance CR detectors for which pile-up event suppression is challenging
4. improved e/p identification with precise TOF measurements.

Many R&D ongoing, like ADA-5D.

In practice, precise (<100ps) timing open up a new dimension. Similar to move from 2D to 3D event reconstruction!

Precise timing: CONCEPTS

How to measure the particle time?

Direct collection of the charges created through ionization:

- e/ions pairs in gas
- e/h pairs in solid state detectors

Internal amplification of charge is possible for some detector technologies

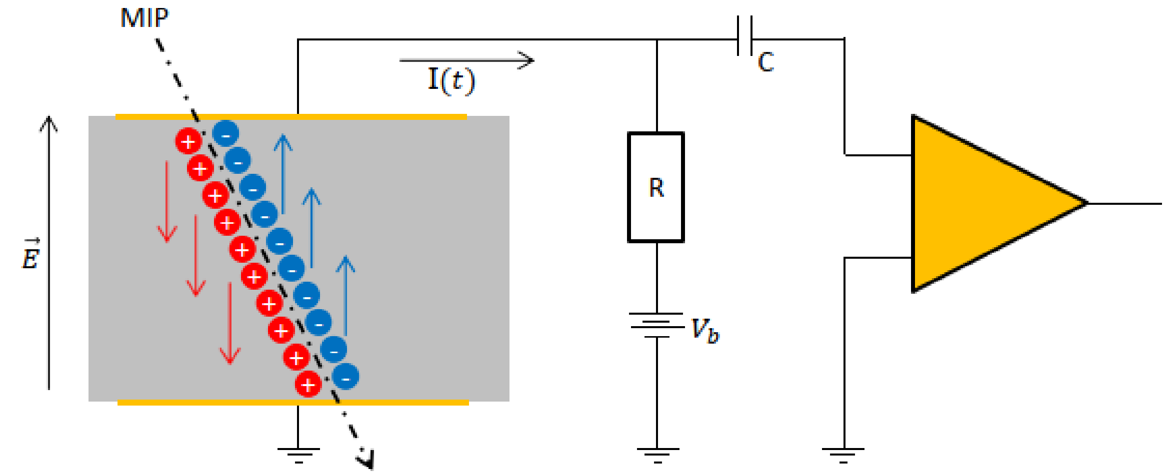

Generation and detection of optical or UV photon:

- Cherenkov
- Conversion of ionization energy into photon (scintillators)

Optical photons are converted back into an electron with a photocathode (PMT like) or in the bulk of a solid-state detector (SiPM like), then charge amplification is attained through different processes.

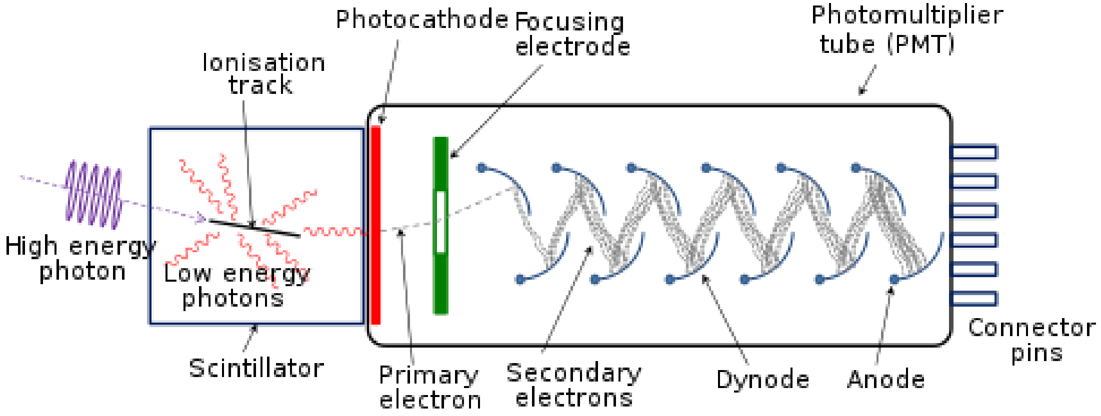

Some detectors can work in both ways!

What to measure?

When comparing performance of the detectors is always good to have a common reference, if possible.
A low energy heavy ion will release much more charge compared to a MIP, and the performance of the detector will be (usually) better!

Commonly we use two “standard” in quoting our results:

- MIP resolution
  - Often (but not always!!!) the final target
  - Performance can be easily scaled to other energy ranges
  - All contributions to the final resolution are present

Don’t get fooled!!

- Single Photon Time Resolution (SPTR) /Time Transit Spread (TTS):
  - Applicable only to light sensitive detectors
  - Factor out the photon production and transport process
  - Very useful to characterize part of the sensor
  - If photon production and transport introduce negligible time uncertainty the final detector resolution with scale as $\sqrt{N_{ph}}$ generated.

How to test?

UNIVERSITÀ DI SIENA 1240

Laser

UV lasers with $\sigma_t \ll 100$ fs are available (for example IRAMIS facility @ CEA Saclay), but any ps laser can do the job.
Can be used on indirect detectors as well in some direct detector (i.e., not diamonds)
Can be tuned to generate a single photon or emulate the energy release of MIP
They don't consider several aspects that we will discuss later.

My opinion: only an indication of the possible (best case) performance on the detector

Cosmic rays

Always available «for free», but it can require time for statistics. Energy and particle type may vary but they can be assumed dominated by muon MIP

Test Beam

Require long praparation and a dedicated facility. By far the most precise results can be obtained.

There are facilities all over the world that can generate a large variety of particles at different energies (CERN, DESY, PSI, FERMILAB, ...).

Time precision

The time precision, σ_t, is due to several main contributions:

$$\sigma_t^2 = \sigma_{sensor}^2 + \sigma_{jitter}^2 + \sigma_{walk}^2 + \sigma_{digit}^2 + \sigma_{drift}^2$$

- σ_{sensor} <- is the contribution due to the sensor:
  - Interaction point uncertainty
  - Local Landau energy fluctuation
  - Electrical field non-uniformities
  - …
- σ_{jitter} <- electronic noise and signal characteristics
- σ_{walk} <- fluctuation of signal amplitude, mainly linked to total energy release fluctuation
- σ_{digit} <- signal digitization
- σ_{drift} <- environmental changes or aging

And many other effects play role in large detectors:

- Clock distribution
- Cross talk effect between pixels/channels
- Baseline oscillation or other instabilities
- Charge sharing in multi-channel detectors
- Chromatic effect (Cherenkov /scintillators)
- Calibration

Usually $\sigma_{digit}, \sigma_{drift}$ can be made negligible, however, as we will see, the digitization technique can have a huge impact on the σ_{walk}

Sensor contribution

Scintillator emission time

Interaction point in the photocathode

We'll see later many more examples

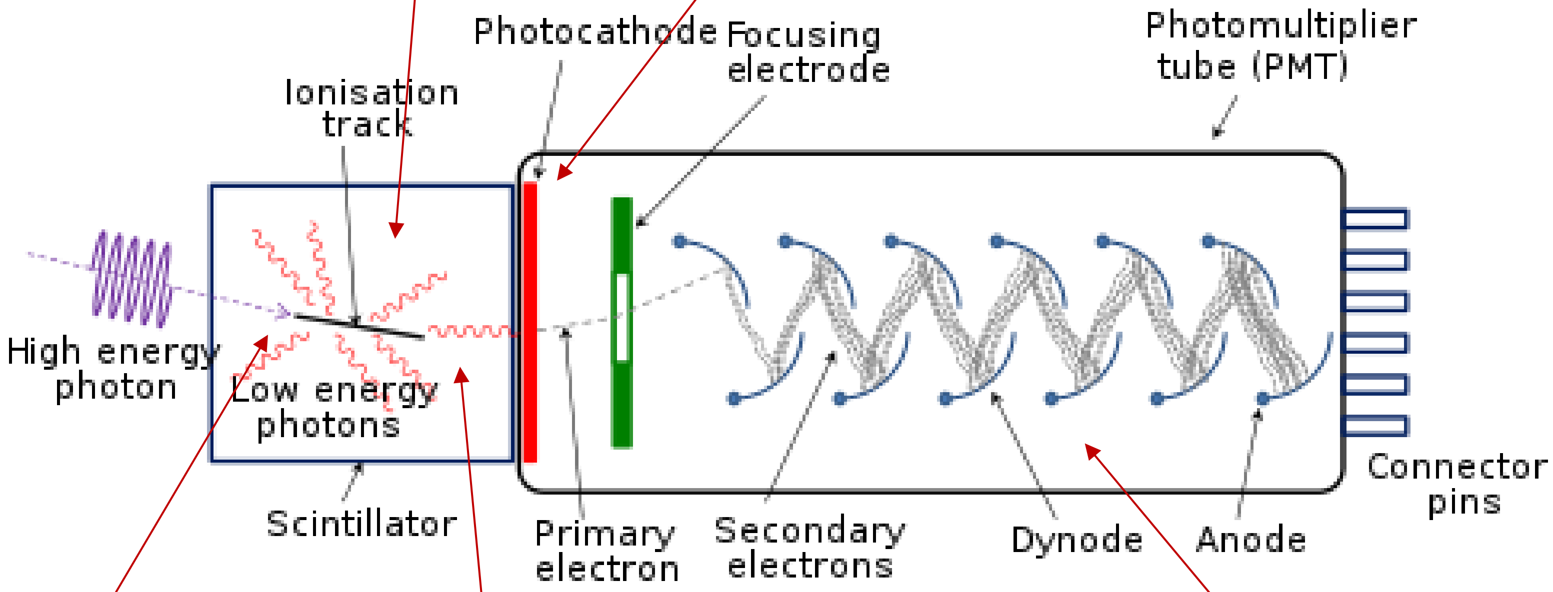

Photon path to photocathode

Path difference of the secondary electrons
Differences in the local electric field

Interaction point

Result: scintillators+PMT not the best choice for timing…

Jitter contribution

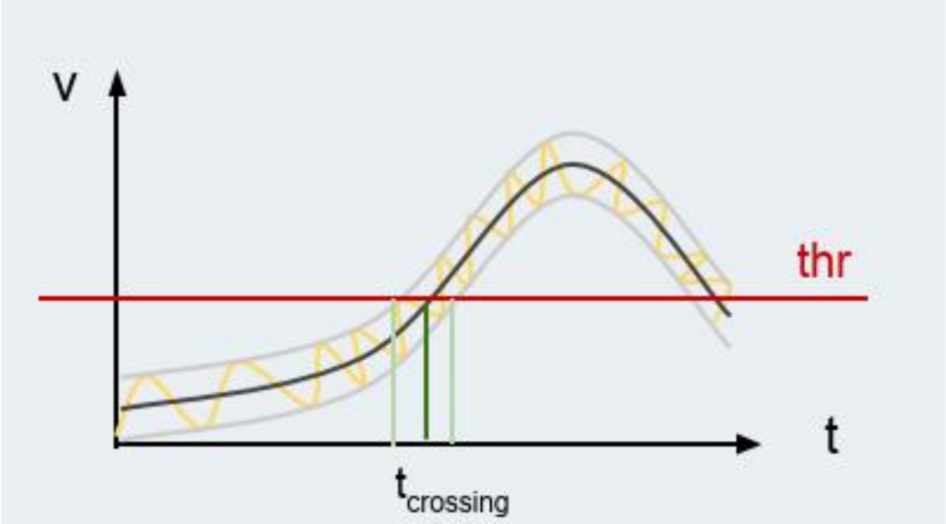

$$\sigma_{jitter} \sim \frac{\sigma_V}{dV/dt} \sim 1.25\frac{\Delta t_{0.1-0.9}}{SNR}$$

Where the Signal to Noise Ratio (SNR) is defined as the ratio between the amplitude V_{max} and the noise σ_V:

$$SNR = \frac{V_{max}}{\sigma_V}$$

The rise (fall) time $\Delta t_{0.1-0.9}$ is the time needed by a positive (negative) signal to rise (fall) from 0.1 V_{max} to 0.9 V_{max}.

$$\sigma_t = \frac{\sigma_n}{\left|\frac{dV}{dt}\right|}$$

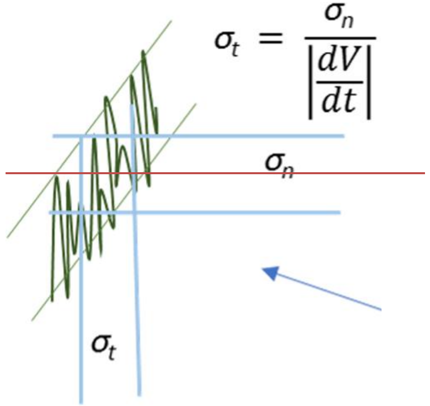

Needs optimization of detector, electronics and their coupling!
First stage of amplification play the crucial role

FAST OR PRECISE?

Fast is mandatory only at high rates

Time walk

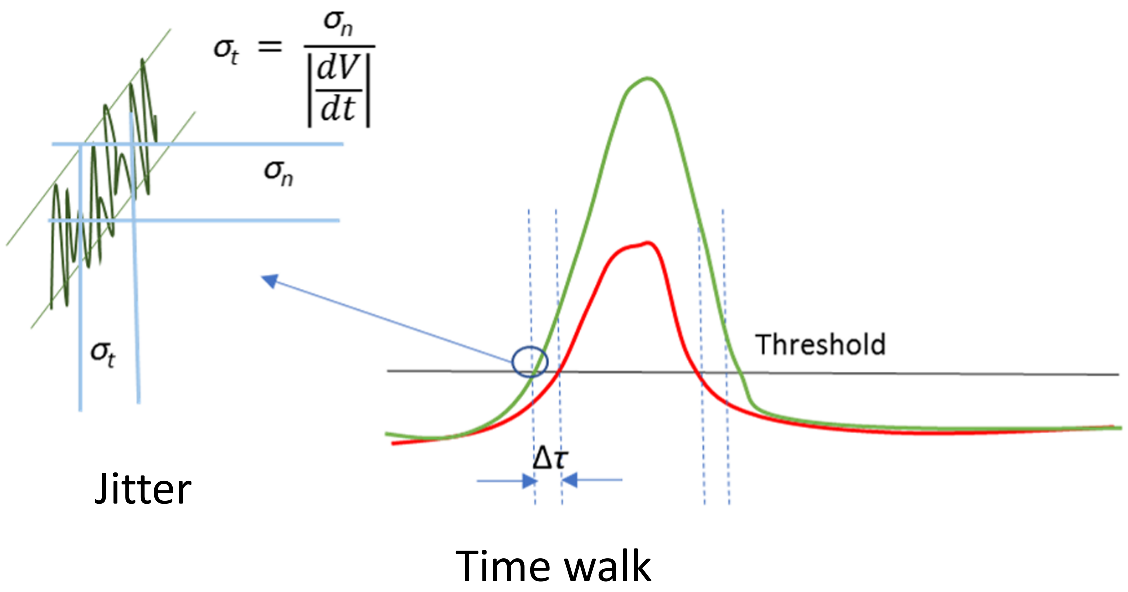

George M. Williams, Jr. Allegro MicroSystems

Requirements for a good timing :

- High SNR and slew rate of the sensor signal
- Signal shape must be constant
- Possibility to perform time walk correction
  - Parallel signal charge measurement
  - CFD or offline normalized threshold
  - Time over Threshold
  - Cross correlation
  - Neural network

Time walk will be the main source of uncertainty, if not properly corrected!
If no correction are available, at least put the threshold as low as possible…
Typology of time walk correction depends on the digitization:

- ➢ Discriminator + Time to Digital Converter
- ➢ Sampler (i.e., oscilloscope)

TW correction: CFD ONLINE

Signal shape depends on sensor characteristics and electronics. A good sensor and electronics should keep it constant -> CFD can remove the time walk effect.

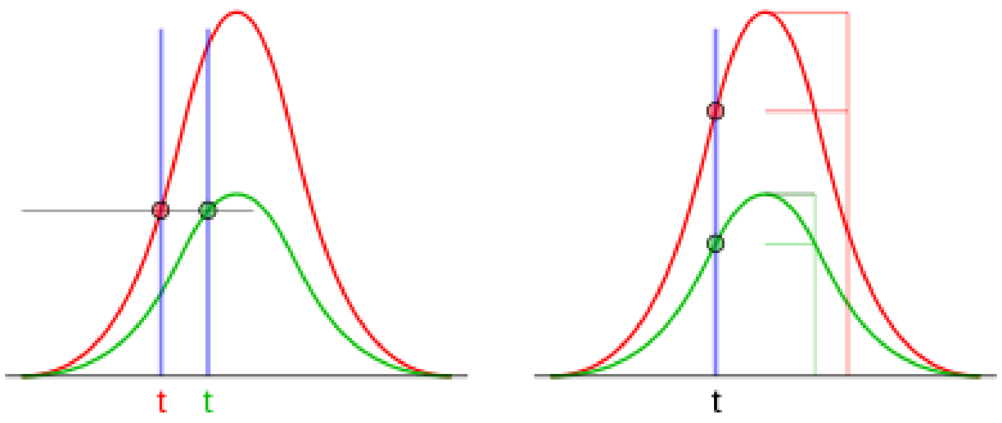

CAEN N605

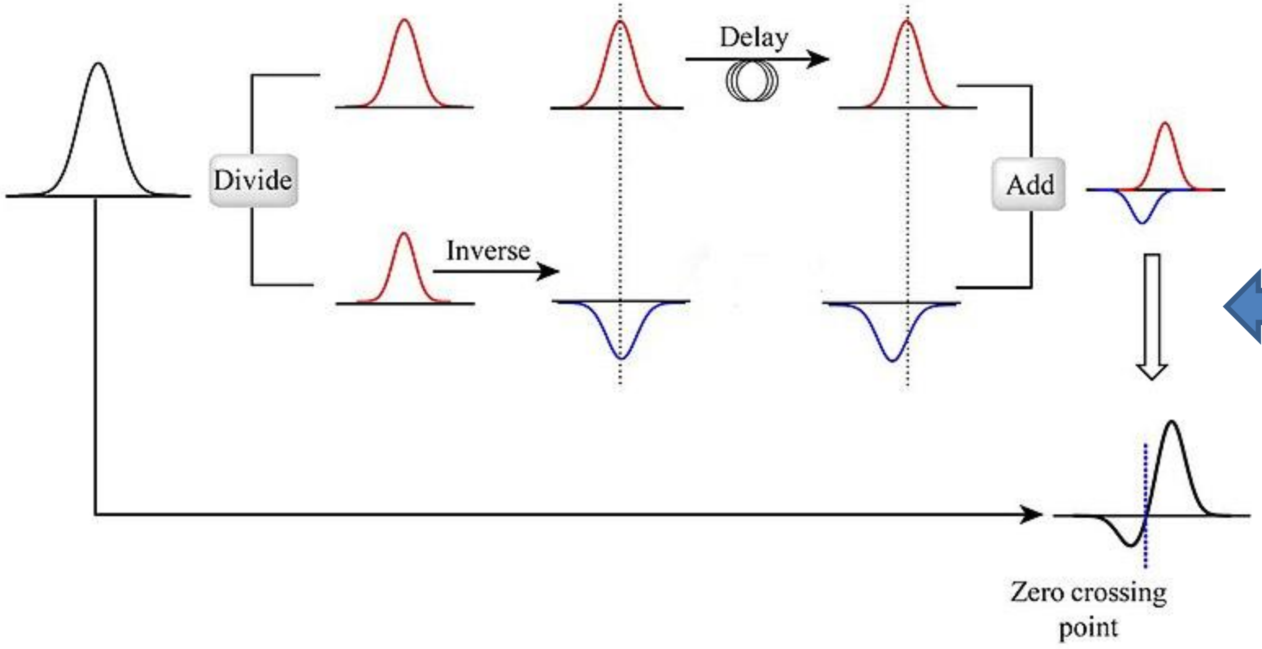

Problem in online computation: the threshold is usually crossed **before** the maximum amplitude is reached!

Digitization electronics : CFD + Time to Digital Converter (TDC)

TW correction: OFFLINE CFD

Offline CFD requires to store several samples of the signal:

- Baseline
- Leading edge
- Maximum

No need for the tail!

30% good compromise:

- Close to start
- Linearity
- Far from baseline oscillation

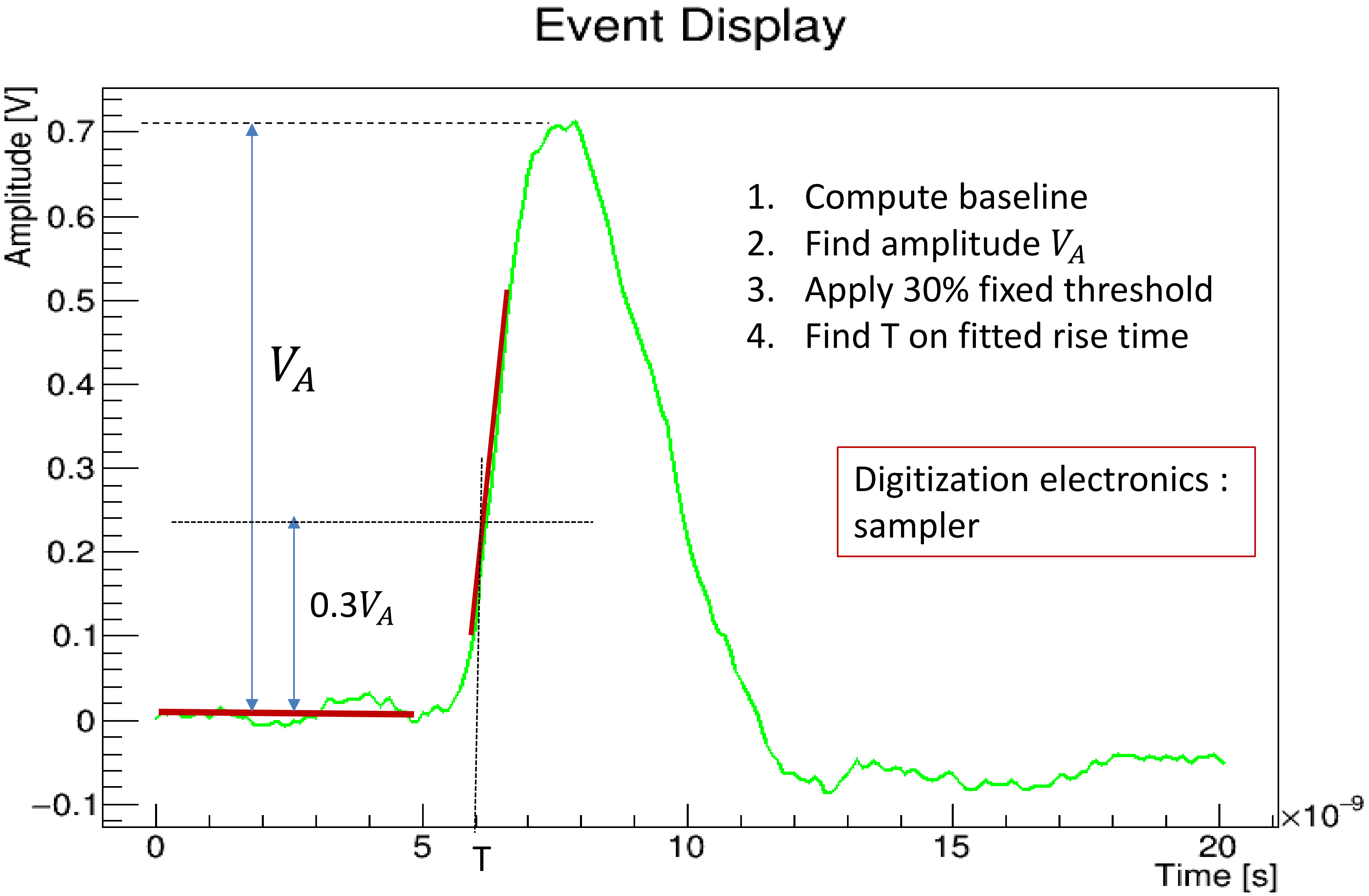

1. Compute baseline
2. Find amplitude V_A
3. Apply 30% fixed threshold
4. Find T on fitted rise time

Digitization electronics : sampler

Online and offline CFD not working if signal is saturated (i.e., due to electronics clamping)

TW correction: TOT correction (or similar)

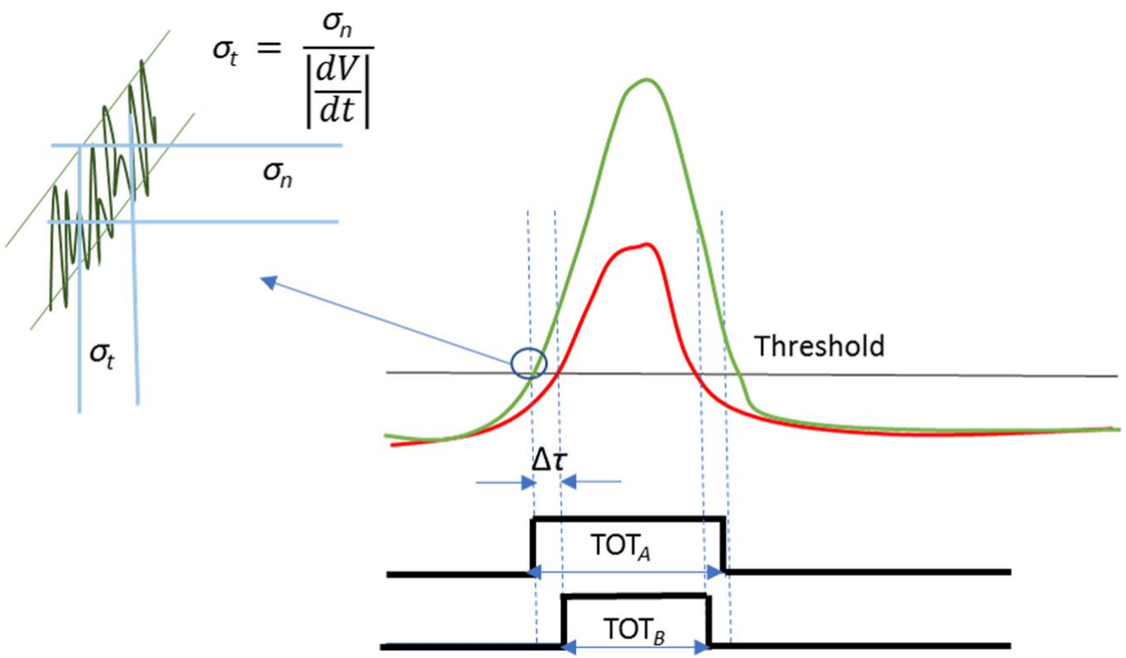

Time Over Threshold (TOT) discriminator have an output linked with the time the signal stay above a given threshold.

Digitization electronics :
"TOT" Discriminator + TDC
with dual edge sensitivity

It can be generalized to every device which output duration is somehow linked to the signal charge/amplitude.

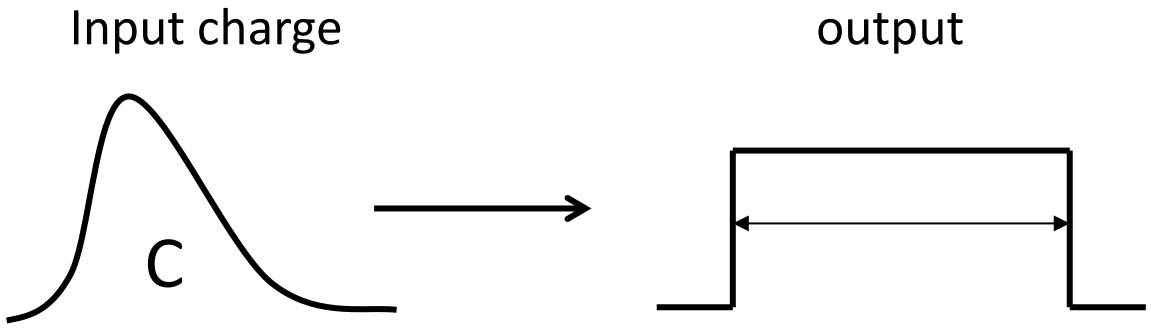

$$W = f(Q)$$

Widely used because of the high rate capability and low data payload

“TOT” example : NINO chip

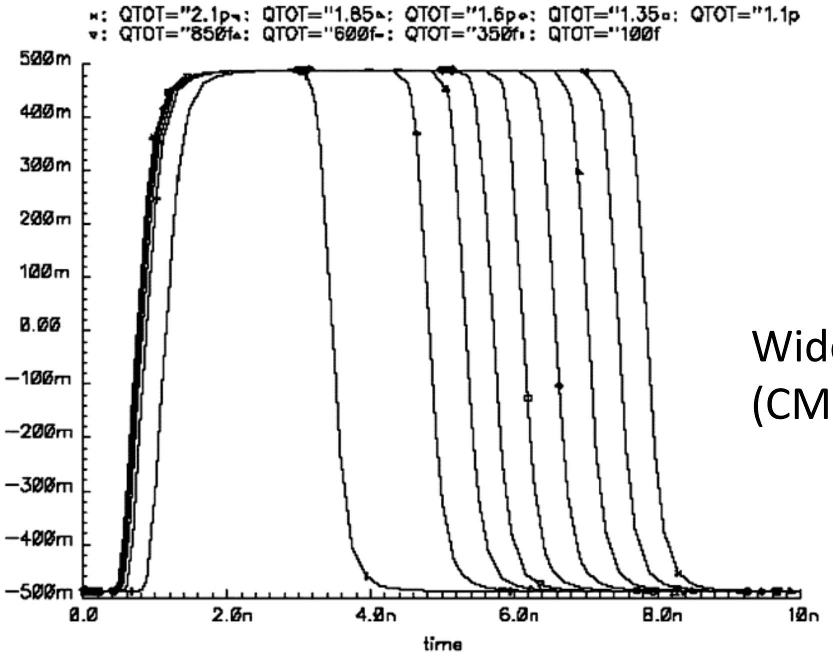

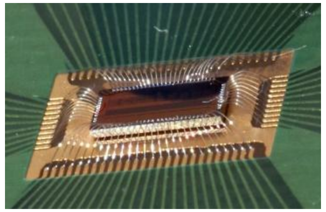

Widely used at CERN (CMS,TOTEM,ALICE,…)

Parameter	Value
Peaking time	1ns
Signal range	100fC-2pC
Noise (with detector)	< 5000 e- rms
Front edge time jitter	< 25ps rms
Power consumption	30 mW/ch
Discriminator threshold	10fC to 100fC
Differential Input impedance	40Ω< Zin < 75Ω
Output interface	LVDS

Input charge

NINO output

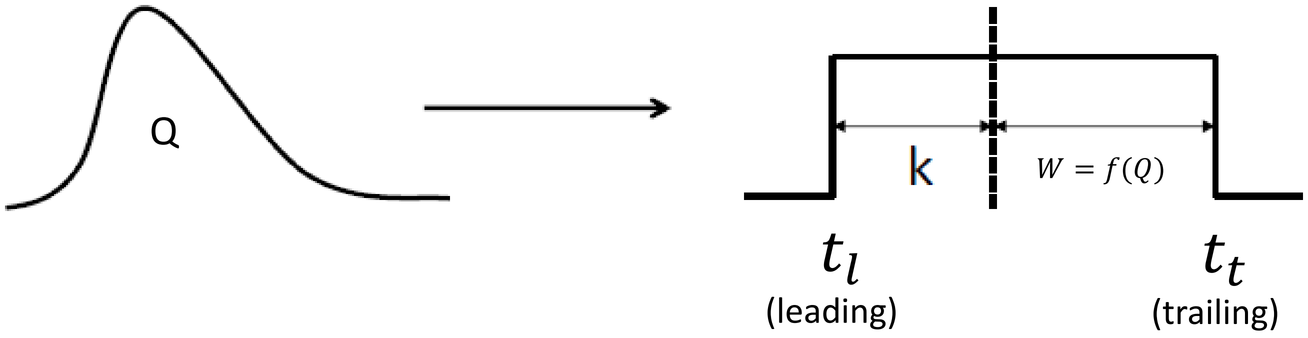

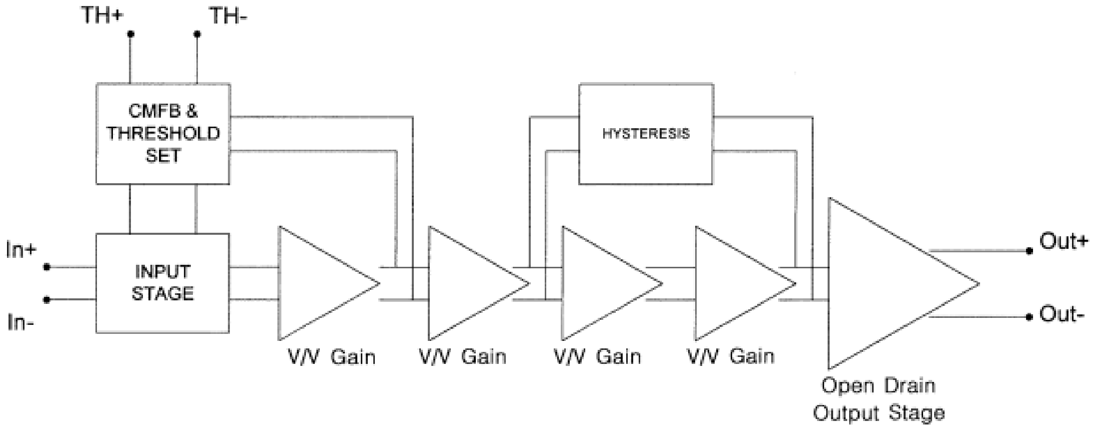

Example of TOT correction (2)

$$\sigma_t = \frac{\sigma_{12}}{\sqrt{2}} = 193\ \text{ps}$$

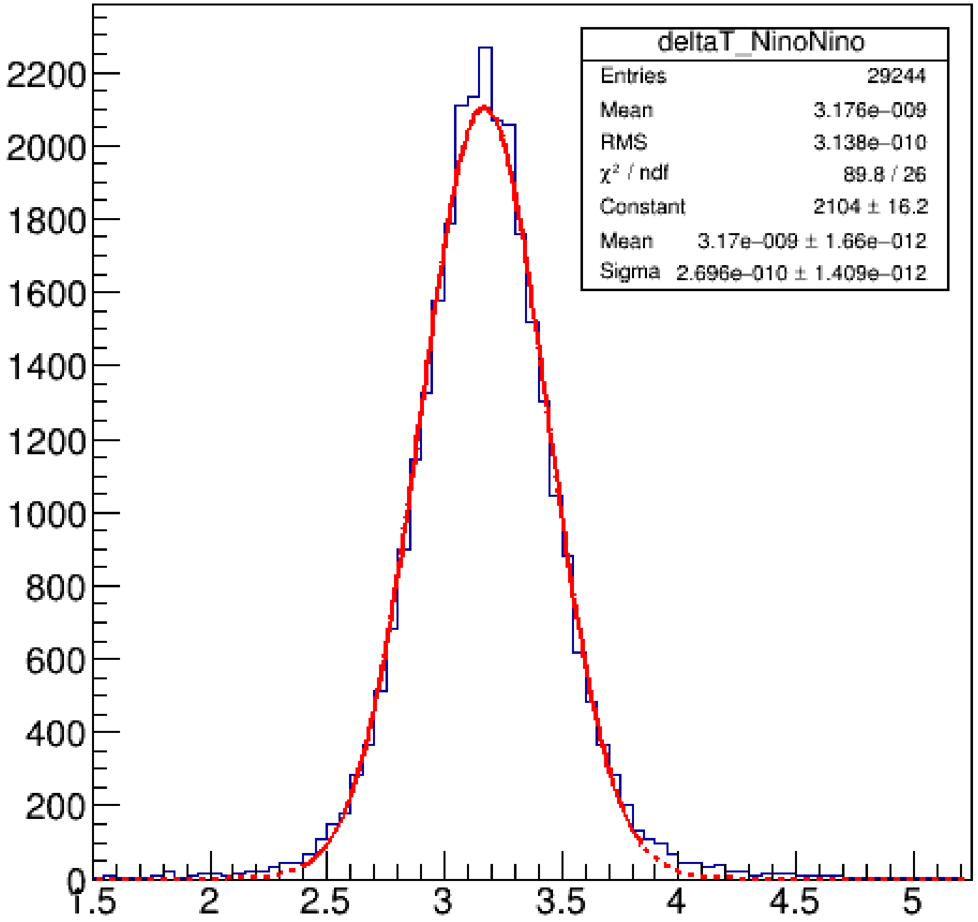

$\Delta T_{raw}[ns]$

Example of TOT correction (1)

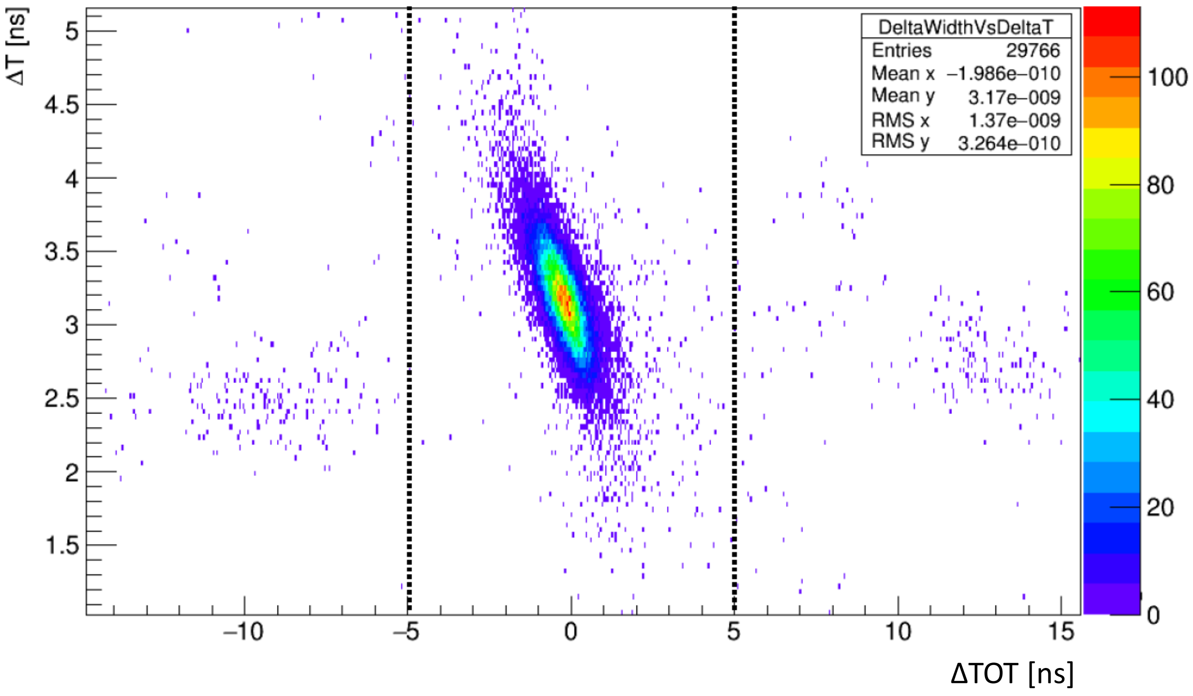

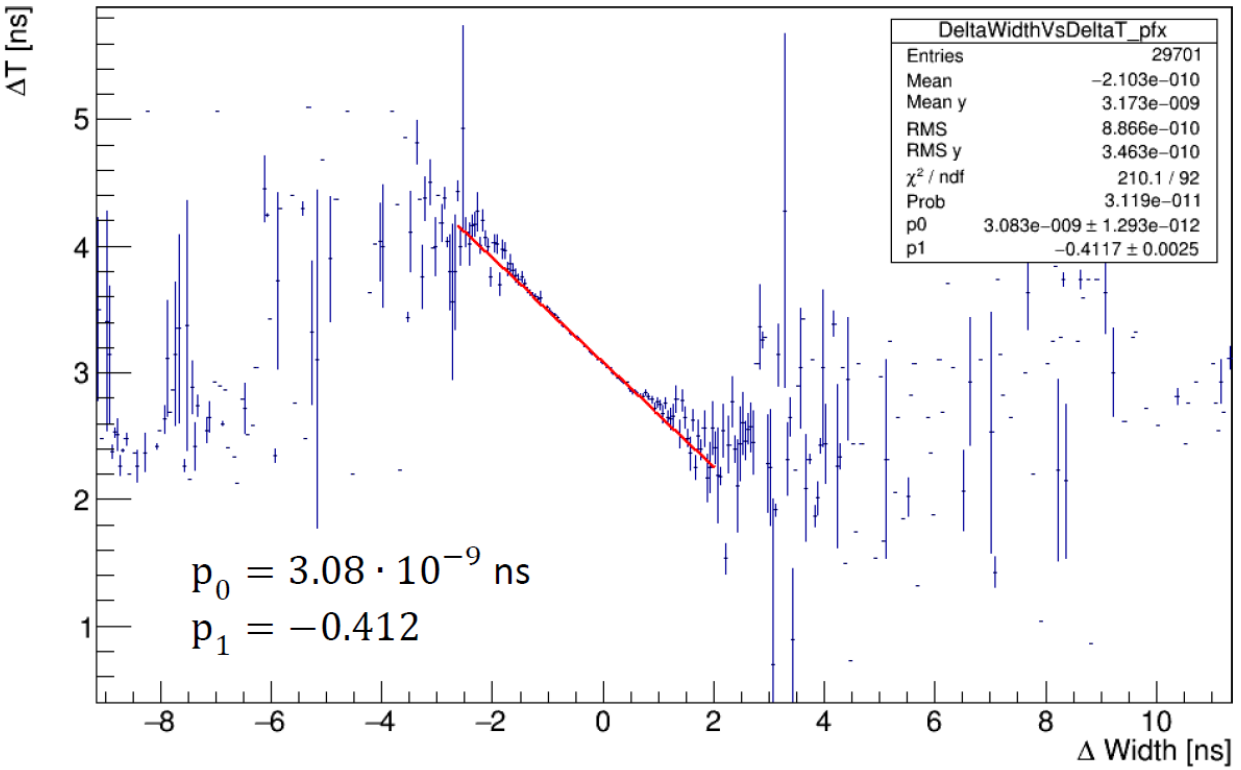

$$\Delta T_{corr} = \Delta T_{12} - p_1 * \Delta W + p_0$$

Device Under Test (DUT):

- Two diamond detector digitized with NINO

Example of TOT correction (2)

$\sigma_t = \frac{\sigma_{12}}{\sqrt{2}} = 193$ ps

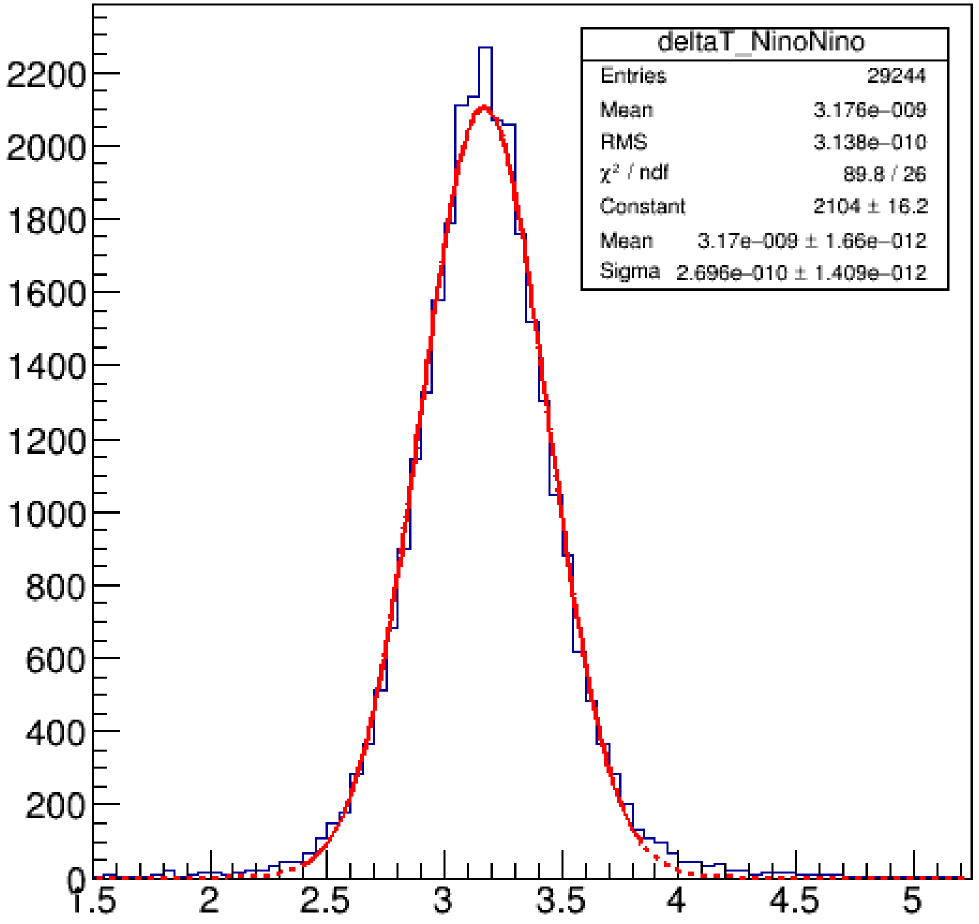

$\Delta T_{raw}[ns]$

$\sigma_t = \frac{\sigma_{12}}{\sqrt{2}} = 127$ ps

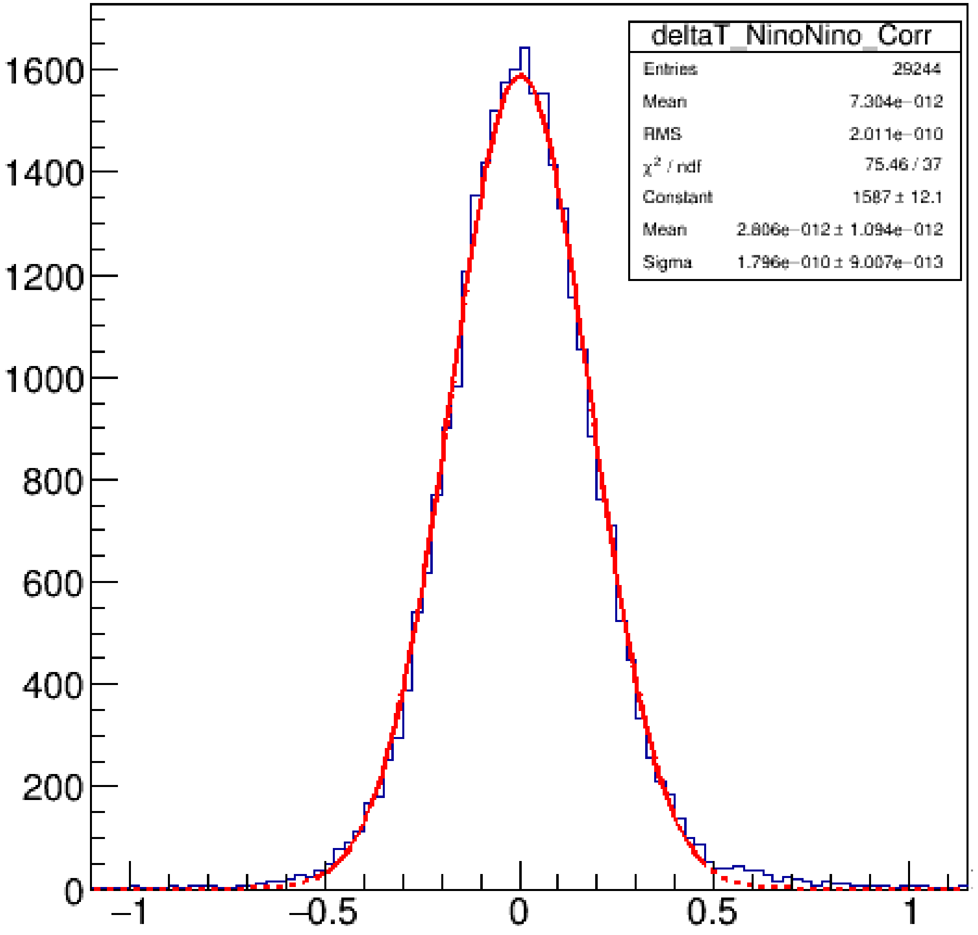

$\Delta T_{corr}[ns]$

CROSS correlation

The correlation of the signal with a template can be used to compute the arrival time.
A template can be generated averaging many normalized signal waveform (green band in figure)

The template is translated over the signal to find the maximum of the correlation:

$$c[j] = \sum s[t_i]\ g[t_{i+j}]$$

This process is time consuming, so this process is repeated in a small time window defined using CFD.

The advantage of the cross-correlation method is that the information of all the sampled points can be included in the computation whereas other algorithms only uses a few points.

Digitization electronics : sampler

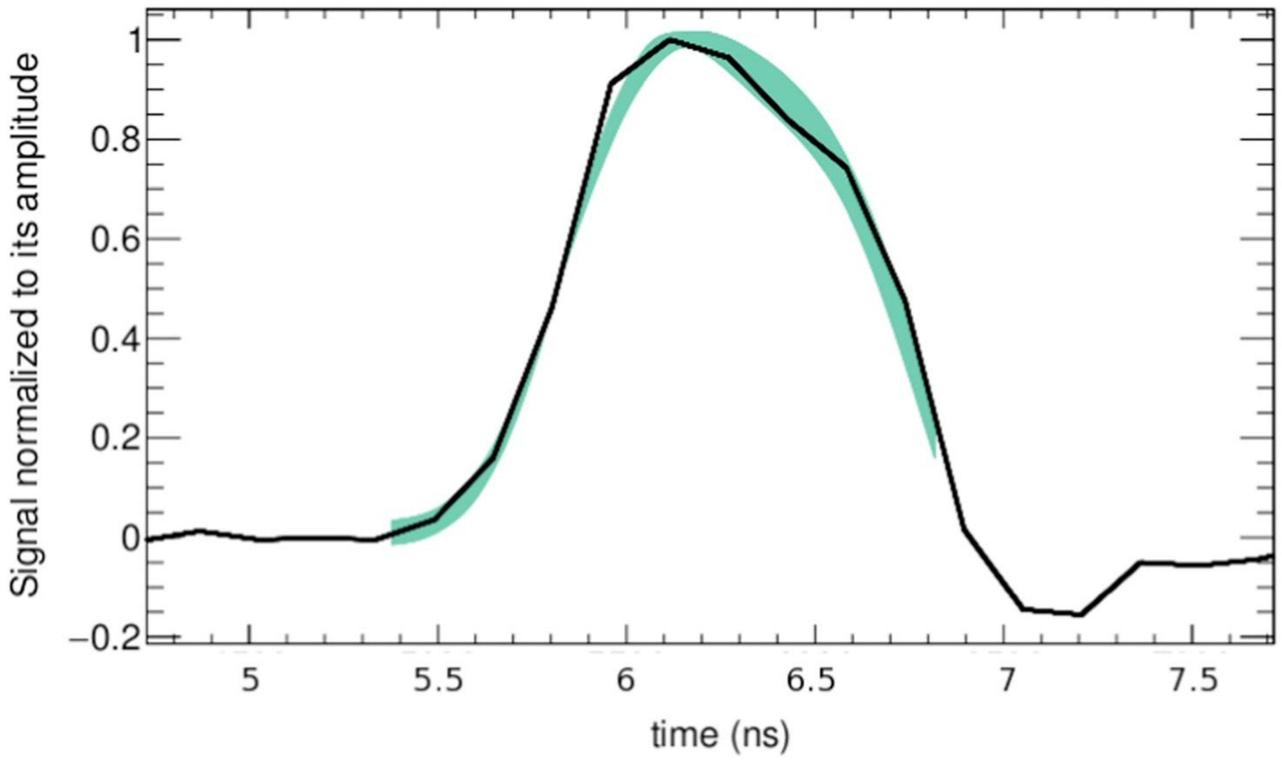

Measurements of timing resolution of ultra-fast silicon detectors with the SAMPIC waveform digitizer
http://dx.doi.org/10.1016/j.nima.2016.08.019

Performance comparison

[Timing performance of diamond detectors with Charge Sensitive Amplifier readout](), CERN-TOTEM-NOTE-2015-003

	Offline method	ΔT_{12} fitted-value, (ΔT_{12} RMS), [resolution]
1	Simple Threshold	1450 (1490) [1025] ps
2	Position of the Maximum	719 (754) [508] ps
3	Normalized Threshold (70%)	467 (491) [330] ps
4	Normalized Threshold (50%)	353 (359) [250] ps
5	Normalized Threshold (30%)	336 (341) [238] ps
6	Fitted Normalized Threshold (35%)	308 (315) [217] ps
7	Offline CFD	306 (298) [210] ps
8	Extrapolation of normalized Threshold	277 (281) [196] ps

Example with two diamond detector, signal amplified with Cividec C6 Amplifiers and readout with oscilloscope
RMS on the time difference between two signals with respect to the signal amplitude.

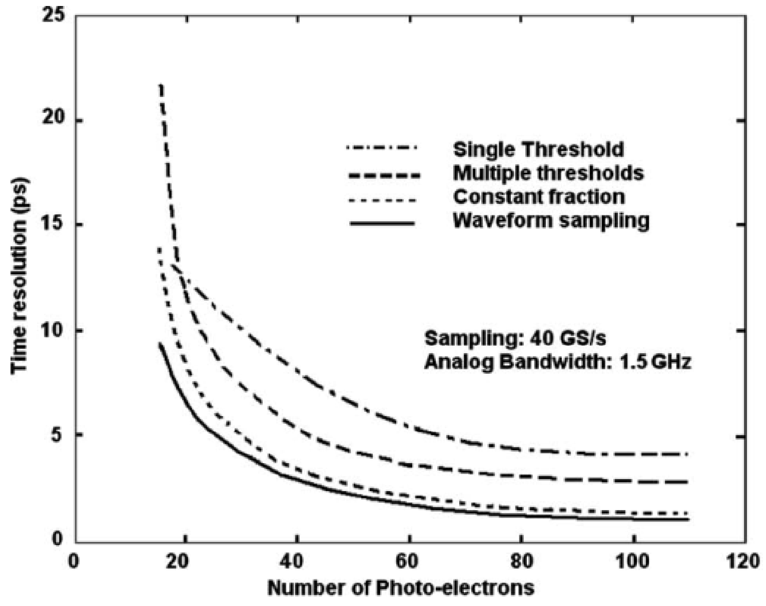

Many other algorithms are possible, but usually with *similar* performance.

MCP test
J. F. Genat et al., NIM A, 607 (2009) 387-393

Measurements of timing resolution of ultra-fast silicon detectors with the SAMPIC waveform digitizer
http://dx.doi.org/10.1016/j.nima.2016.08.019

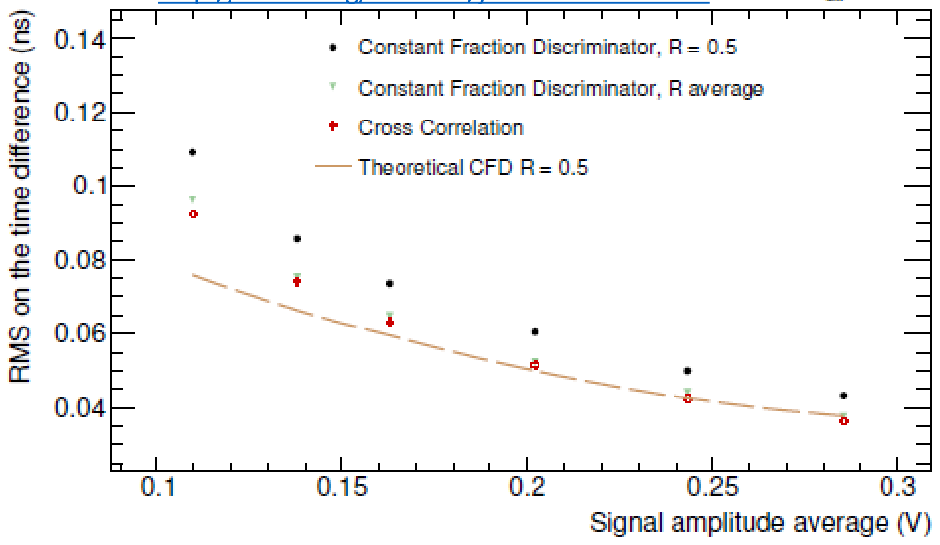

Laser tests with 300 μm USFDs read-out with Cividec C2 BDA, acquired using the SAMPIC chip at 6.4 GS/s.

MicroChannel Plate (MCP)

From PMT to MCP

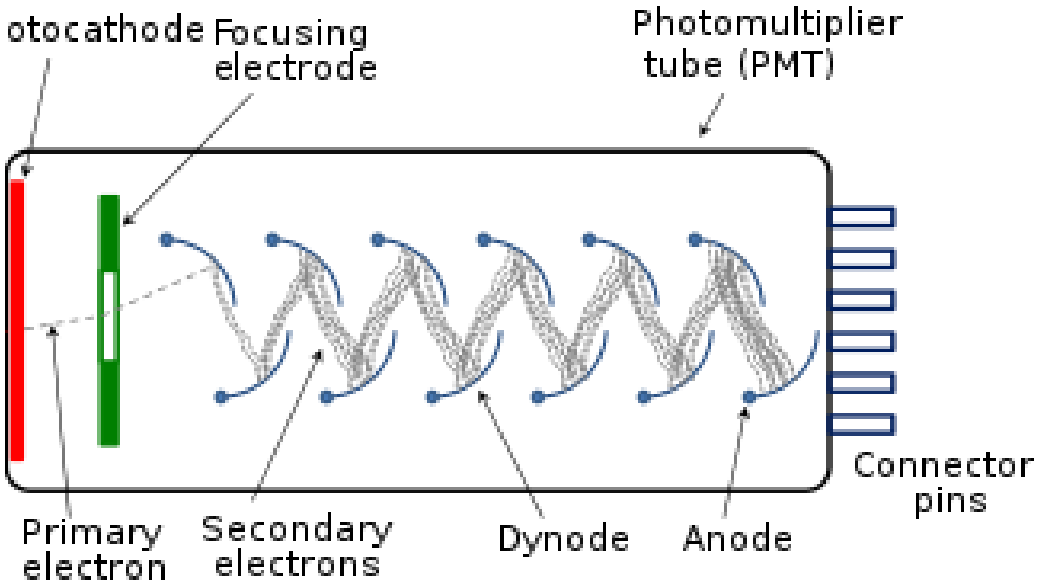

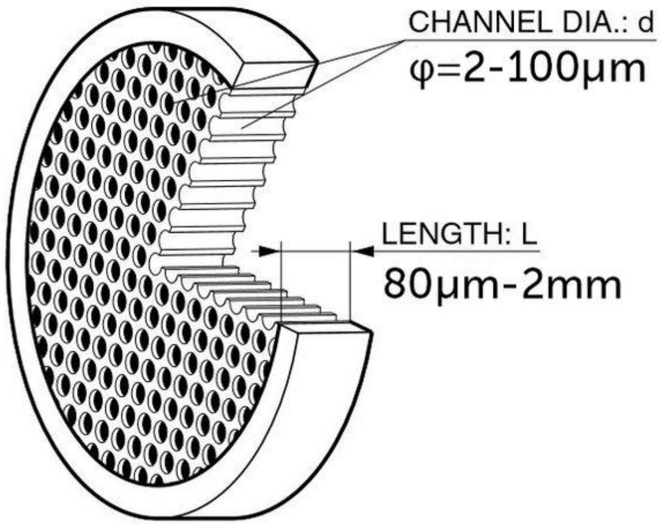

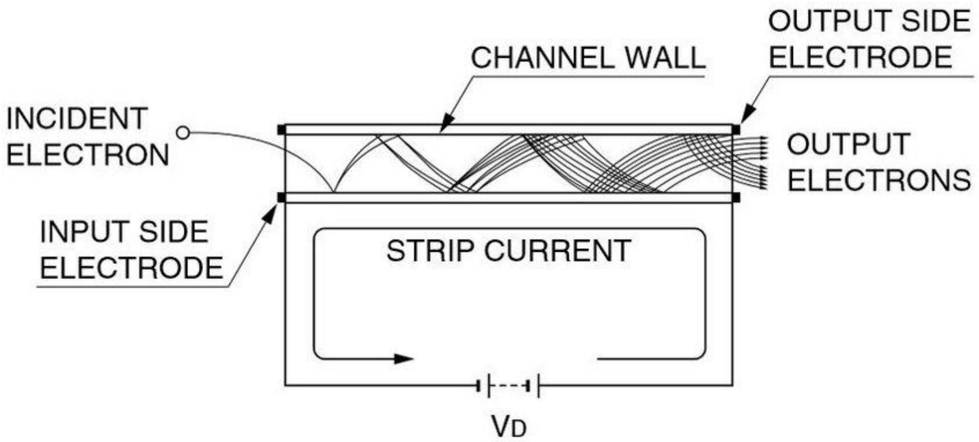

If possible, scintillator must be replaced with Cherenkov radiator!

MCP

Micro-Channel-Plate

- Tiny electron multipliers
  Diameter 2-100μm, length 80μm-2mm
- High gain
  10^6 for two-stage type
- Fast time response
  Pulse raise time ~50-400ps, TTS < 50ps
- can operate under high magnetic field (~1.5T)

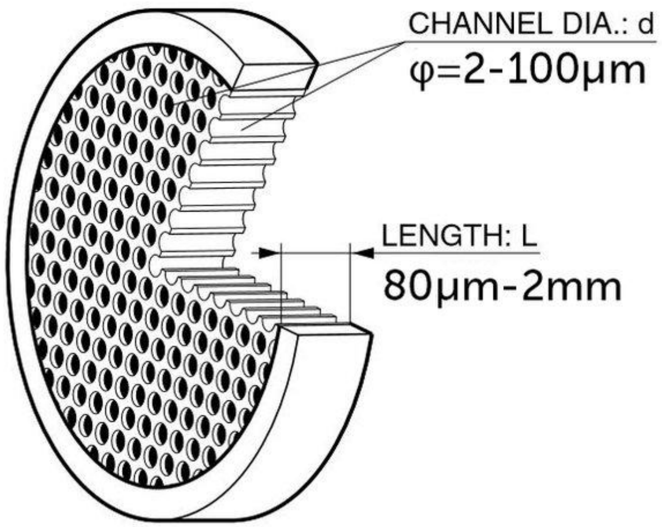

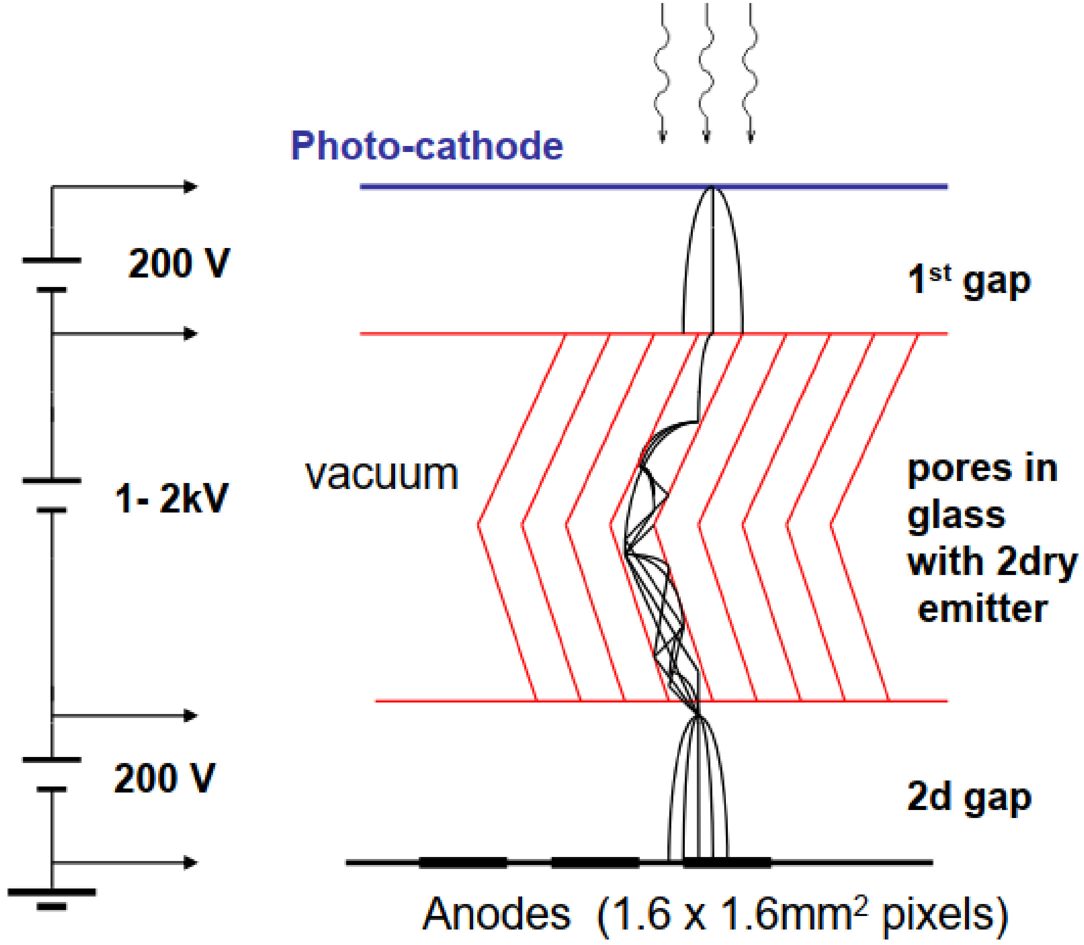

Jean-Francois Genat, Fast Timing Workshop, Lyon, Oct 15th 2008

TTS resolution

Va’vra 2020 J. Phys.: Conf. Ser. 1498 012013

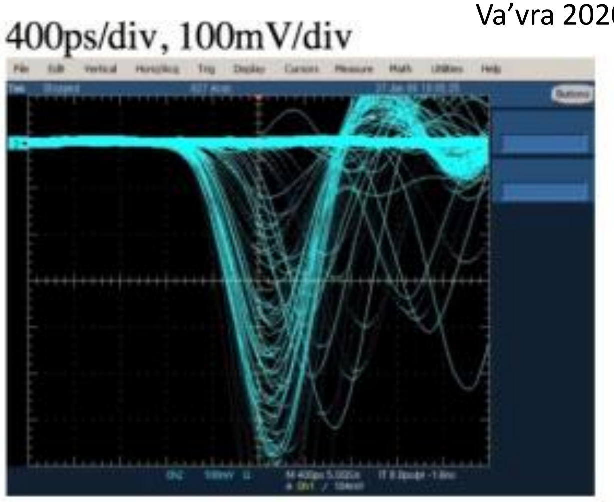

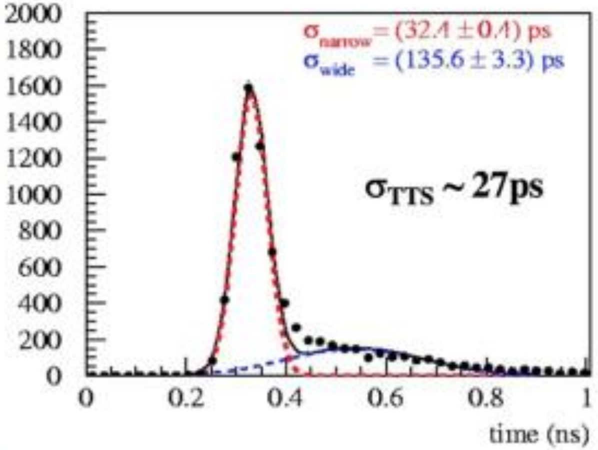

Planacom 85013-501 MCP, gain $\sim 10^6$.
Readout with Philips 715 CFD + LeCroy 2248 TDC
Laser test $\sigma_{TTS} = \sqrt{((32^2 - \sigma^2_{Laser} - \sigma^2_{Electronics})} \sim 27$ ps.

BELLE-II TOP DIRC NIMA, Volume 941, 11 October 2019, 162342

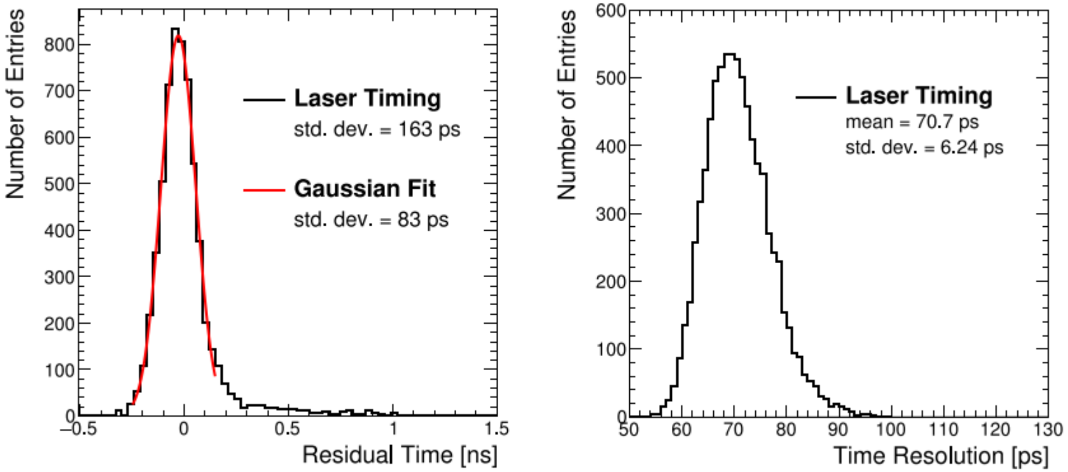

Hamamatsu R10754-07-M16, multichannel 4x4, gain 2x10^5
Readout with custom asic sampler + FPGA SoC reco code
Laser test

Beam test	-	-	< 10 ps/track *	[7,8,9]
Laser test	-	-	~27 ps/photon *	[21, 22]
PANDA Barrel test	10 MHz/cm^2 * (laser)	~20 C/cm2 *	-	[15, 16, 17]
Panda Endcap	~1 MHz/cm^2 ** (photons)	-	-	[38]
TORCH test	-	3-4 C/cm^2 *	~90 ps/photon *	[37]
TORCH	10-40 MHz/cm^2 ** (photons)	5 C/cm2 **	~70 ps/photon **	[34, 35, 36, 37]
Belle-II	<4MHz/MCP *** (photons)	-	80-120 ps/photon***	[32]

Va’vra 2020 J. Phys.: Conf. Ser. 1498 012013

TTS resolution

Va'vra 2020 J. Phys.: Conf. Ser. 1498 012013

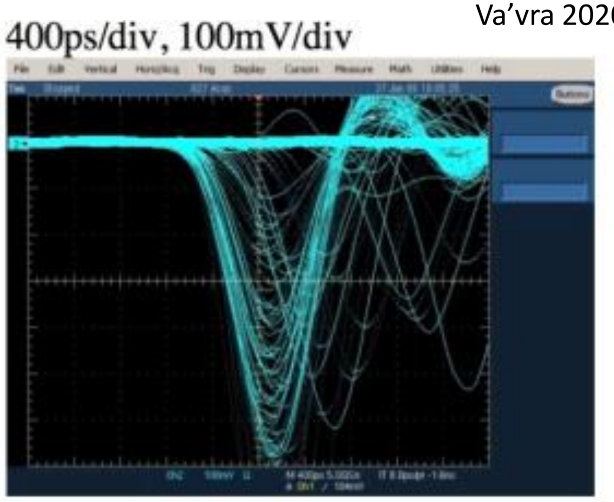

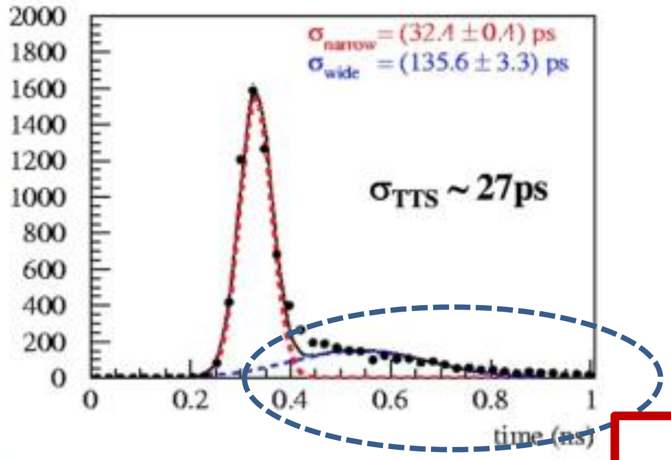

BELLE-II TOP DIRC NIMA, Volume 941, 11 October 2019, 162342

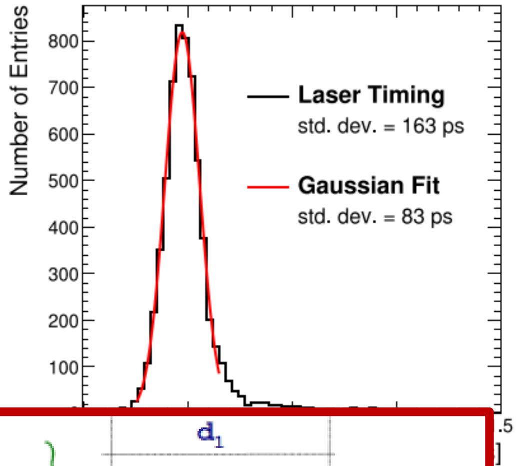

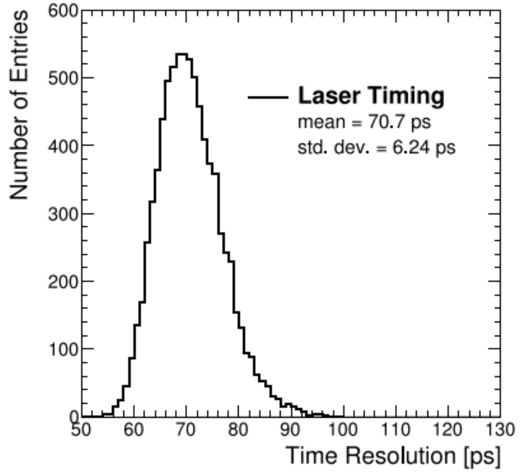

Planacom 85013-501 MCP, gain $\sim 10^6$.
Readout with Philips 715 CFD + LeCroy 2248 TDC
Laser test $\sigma_{TTS} = \sqrt{(32^2 - \sigma^2_{Laser} - \sigma^2_{Electronics})} \sim 27$ ps.

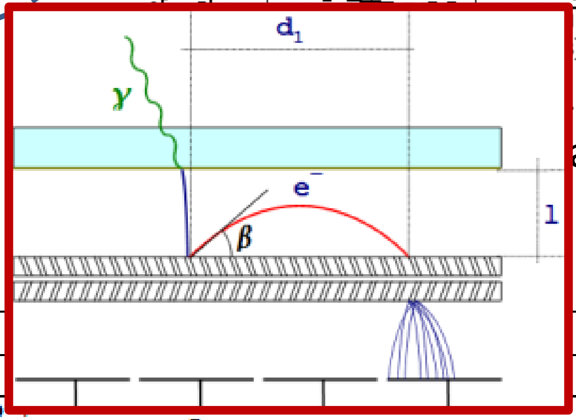

6, multichannel 4x4, gain $2\text{x}10^5$
ampler + FPGA SoC reco code

Beam test	-	-	[illegible]	[7,8,9]
Laser test	-	-	[illegible]	[21, 22]
PANDA Barrel test	10 MHz/cm^2 * (laser)	~20 C/cm2	-	[15, 16, 17]
Panda Endcap	~1 MHz/cm^2 ** (photons)	-	-	[38]
TORCH test	-	3-4 C/cm^2 *	~90 ps/photon *	[37]
TORCH	10-40 MHz/cm^2 ** (photons)	5 C/cm2 **	~70 ps/photon **	[34, 35, 36, 37]
Belle-II	<4MHz/MCP *** (photons)	-	80-120 ps/photon***	[32]

Va'vra 2020 J. Phys.: Conf. Ser. 1498 012013

MIP resolution

UNIVERSITÀ DI SIENA 1240

INFN

Two back-to-back Photek 240 MCPs:
- 6 microns MCP hole sizes
- Fused silica window: 8 mm
- Single pixel
- MCP Gain ~10^6
- DRS4 waveform digitizer
- Electronics resolution: 2.0 ps
- Npe ~ 80
- Total anode charge: 8x10^7

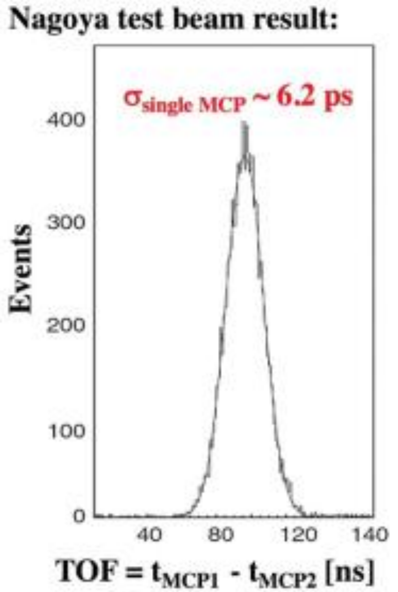

K. Inami et al., NIMA560(2006)303

Two Hamamatsu R3809U-59-11 MCPs:
- 6 microns MCP hole sizes
- Fused silica radiator:10+3 mm
- Single pixel
- MCP Gain ~2x10^6
- SPC-134, Becker & Hickl GmbH
- Electronics resolution: 4.1 ps
- Npe ~ 70
- Total anode charge: 1.4x10^8

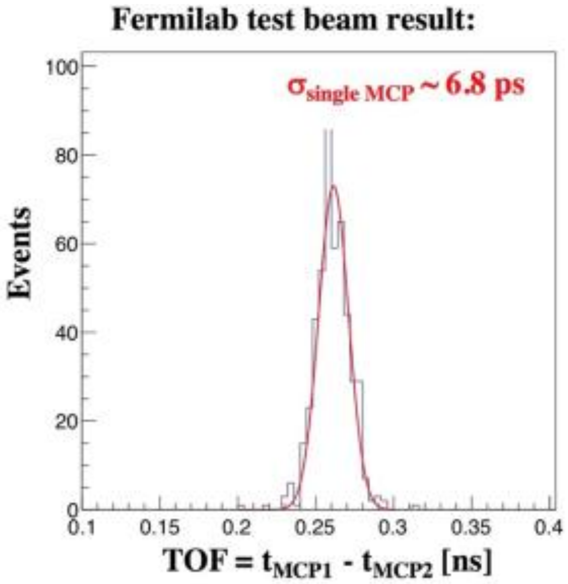

A. Ronzhin et al., NIMA795 (2015)288

Two Hamamatsu R3809U-50 MCPs:
- 6 microns MCP hole sizes
- Fused silica radiator: 3.2 mm
- Single pixel
- MCP Gain ~ 8x10^4
- 20 GSa/s scope + CFD algorithm
- Electronics resolution: 2.2 ps
- Npe ~ 44
- Total anode charge: 3-4x10^6

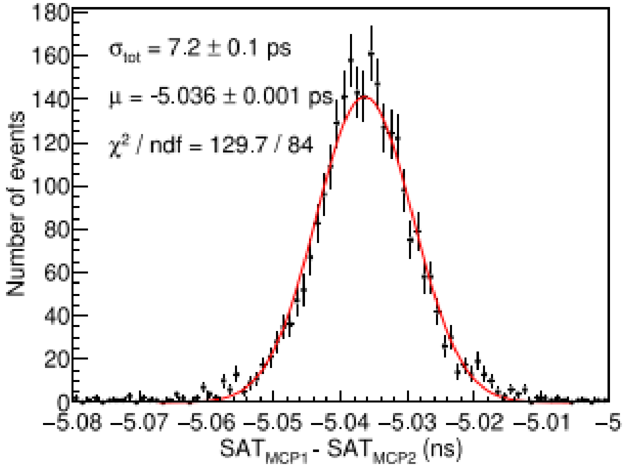

L. Sohl et al., Elba conf., 2018

ION feedback - Aging

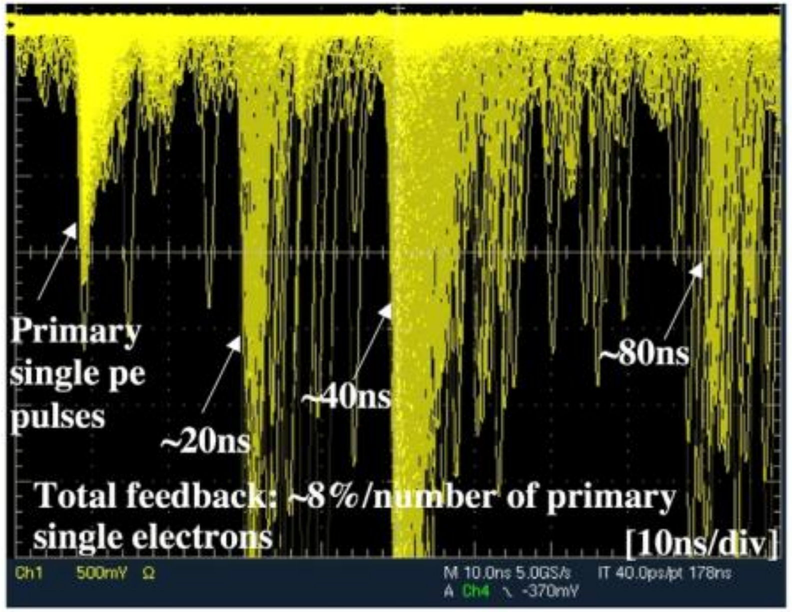

NIMA 876 (2017) 185–193

$1\ \mathrm{C/cm^2}\ @\ 10^6$ gain

$10^{13}\ \mathrm{pe/cm^2}$

$10^{11-12}\ \mathrm{MIP/cm^2}$!!

many application requires rad. hardnes up to $10^{15}\ \mathrm{p/cm^2}$

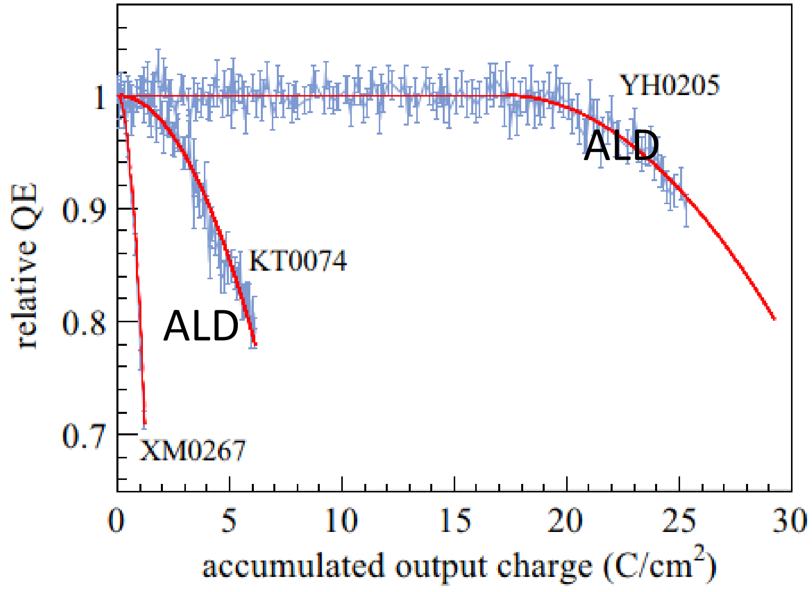

Nuclear Instruments and Methods in Physics Research A 876 (2017) 93–95

Ions from material outgassing damage the photocathode:

- Aluminum foil to reduce bombardment on photocathode (reduce photocathode efficiency)
- Atomic Layer Deposition (ALD) coating of MCP to reduce degas and enhance SEE (Secondary electron emission)
- Life extended from 1 to 10-20C/cm2

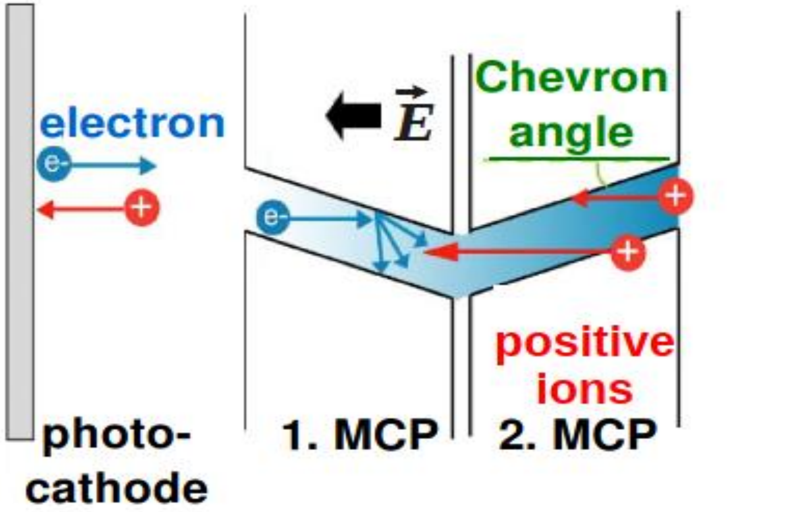

Atlas Forward Proton timing detector

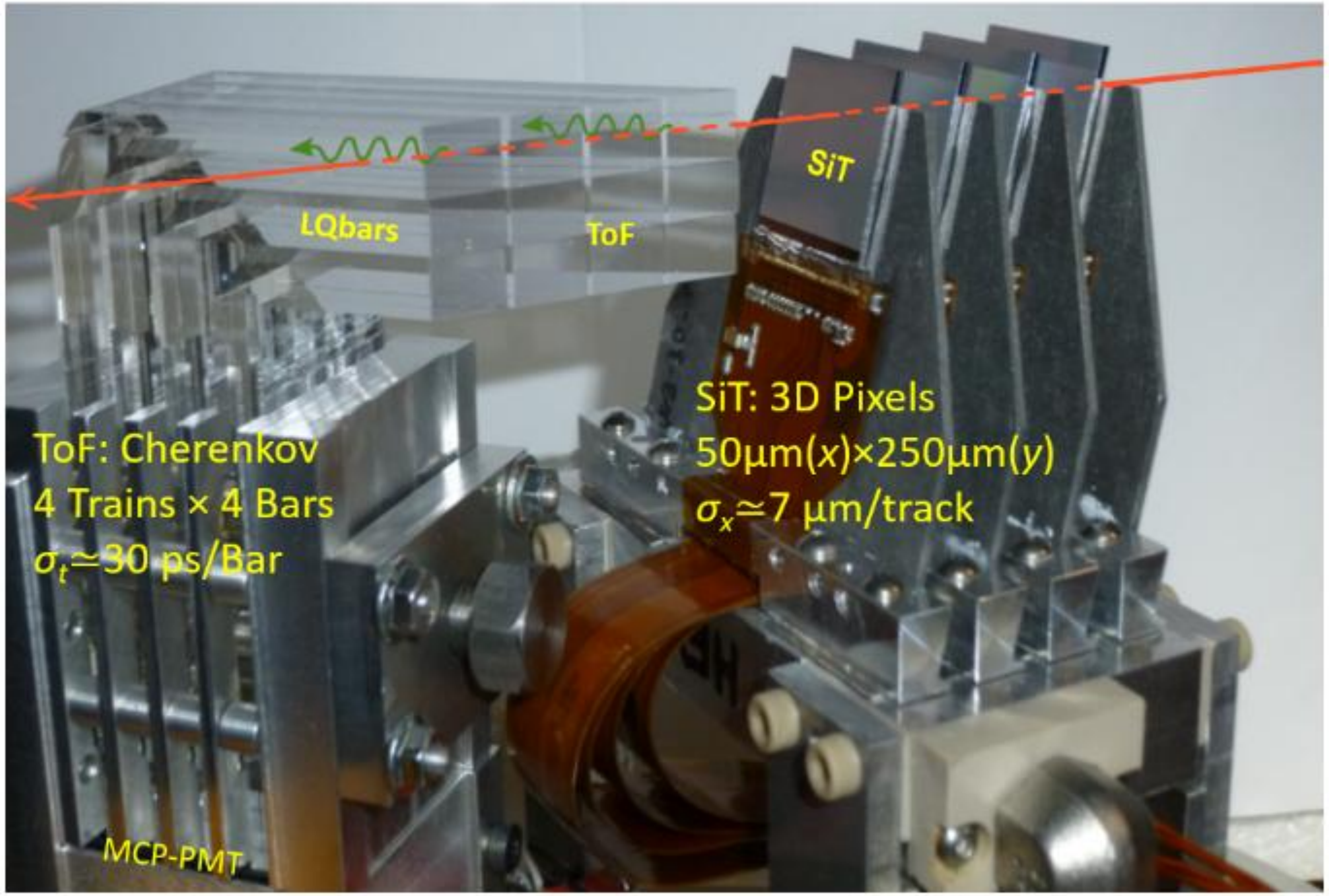

T. Sýkora , *JINST* 15 (2020) C10004

Resolution ~30ps/bar in test beam (full electronic chain, 180 GeV μ/π beam at CERN SPS)

MCP operated @ gain 1-2x10^4
Used in LHC in 2017 RUN2, very harsh environment

Several issue:

- MCP failure due to radiation
- MCP failure due to vacuum operation
- Channel Cross talk (common MCP issue)
- Light spread between bars

Not used in 2018, upgrade ongoing for Run3

miniPLANACON®

https://www.photonis.com/uploads/datasheet/pd/Mini-PLANACON-4x4-datasheet.pdf

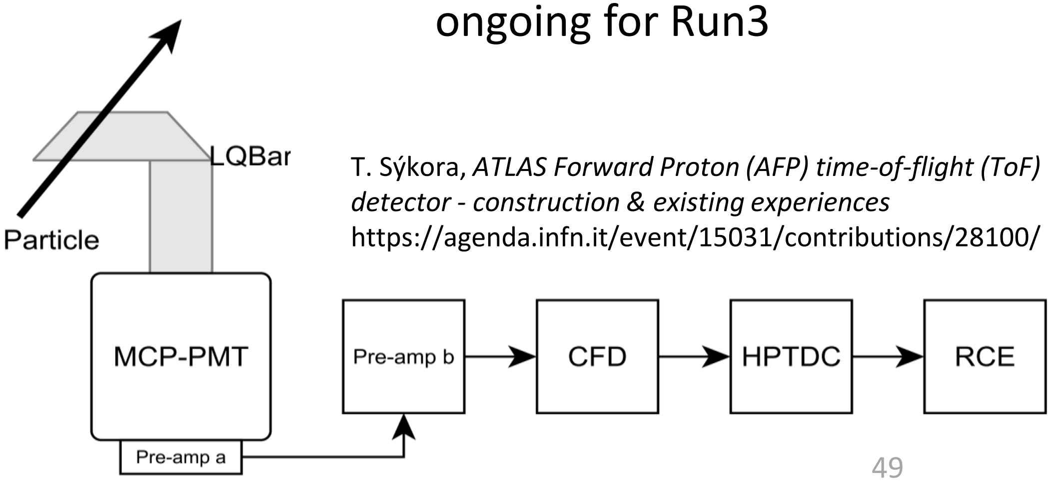

T. Sýkora, *ATLAS Forward Proton (AFP) time-of-flight (ToF) detector - construction & existing experiences*
https://agenda.infn.it/event/15031/contributions/28100/

Atlas Forward Proton timing detector

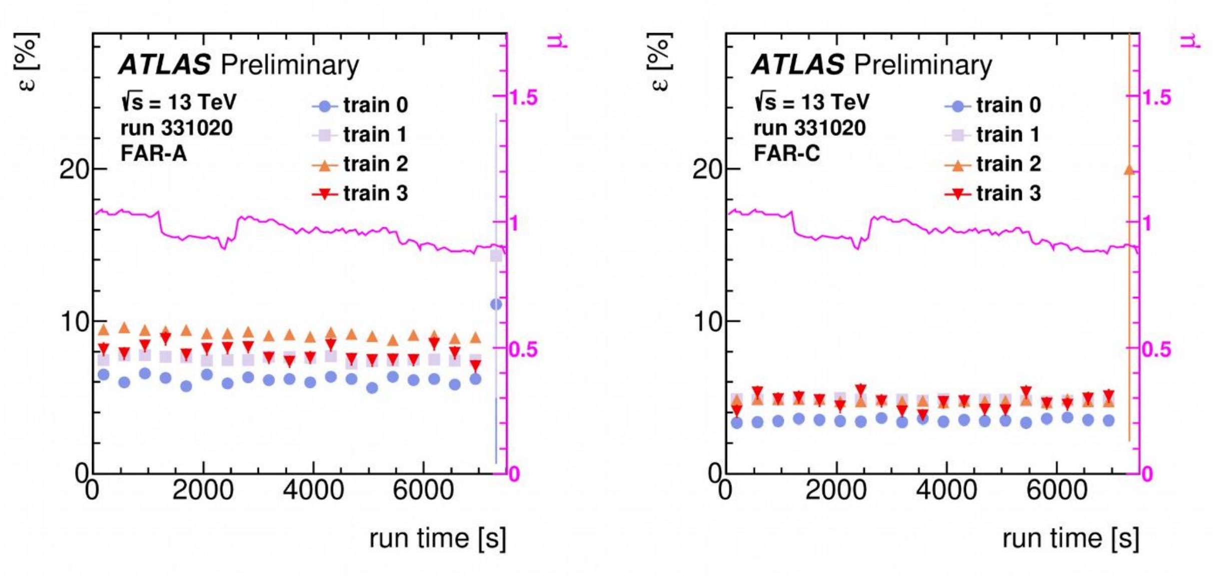

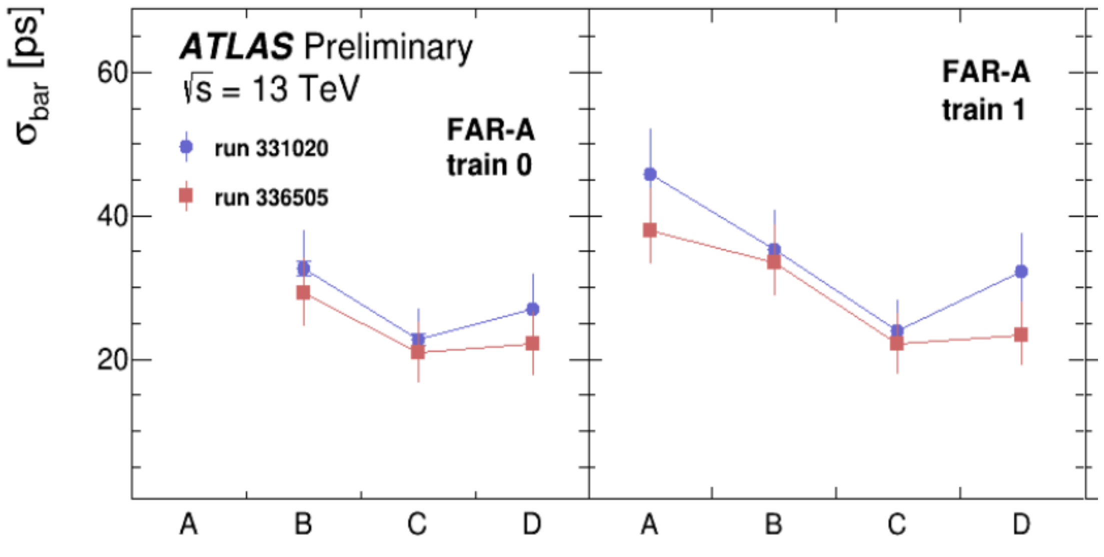

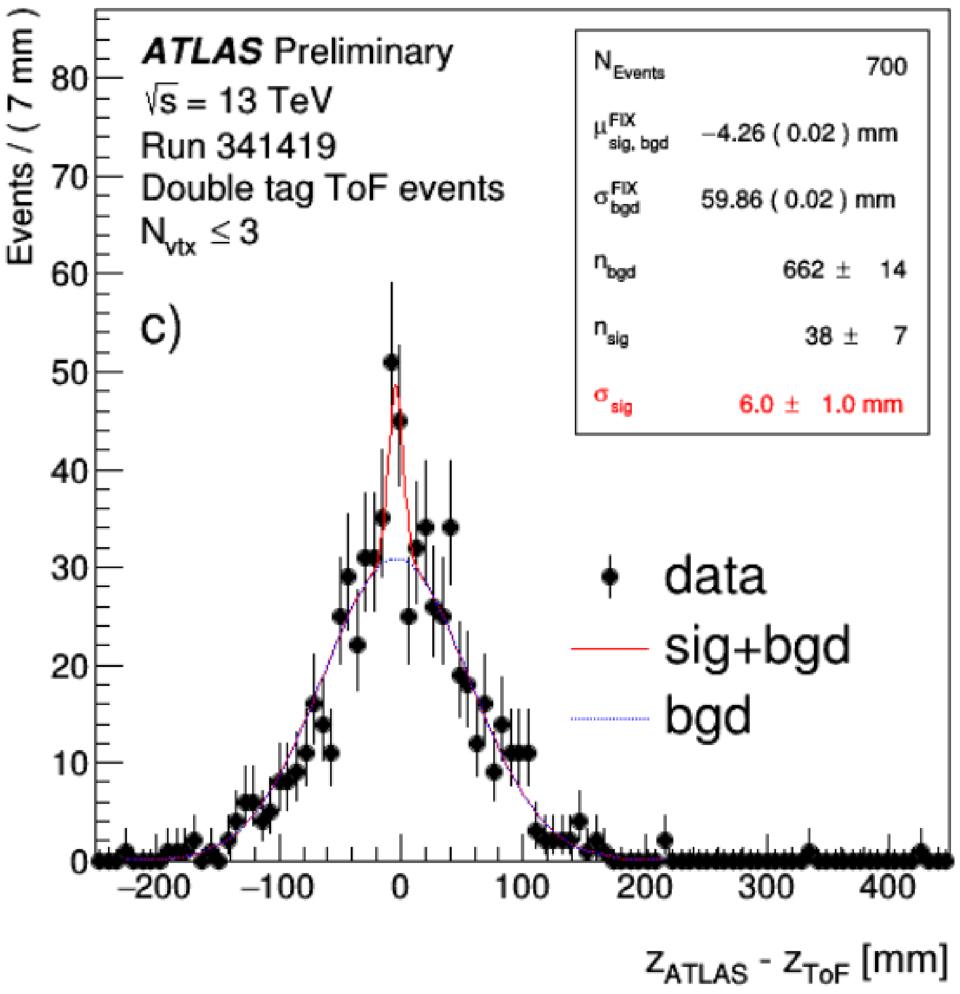

Source: https://twiki.cern.ch/twiki/pub/AtlasPublic/ForwardDetPublicResults/tof_vtx.pdf

TORCH

Resolution is quoted for a single photon!

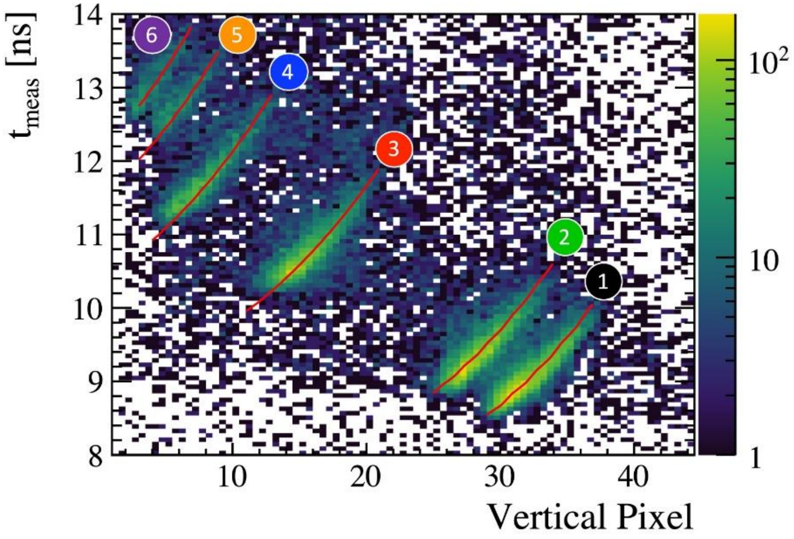

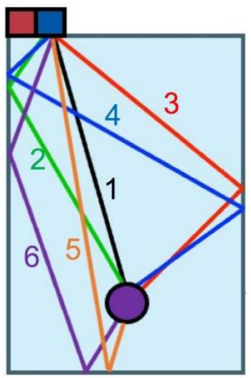

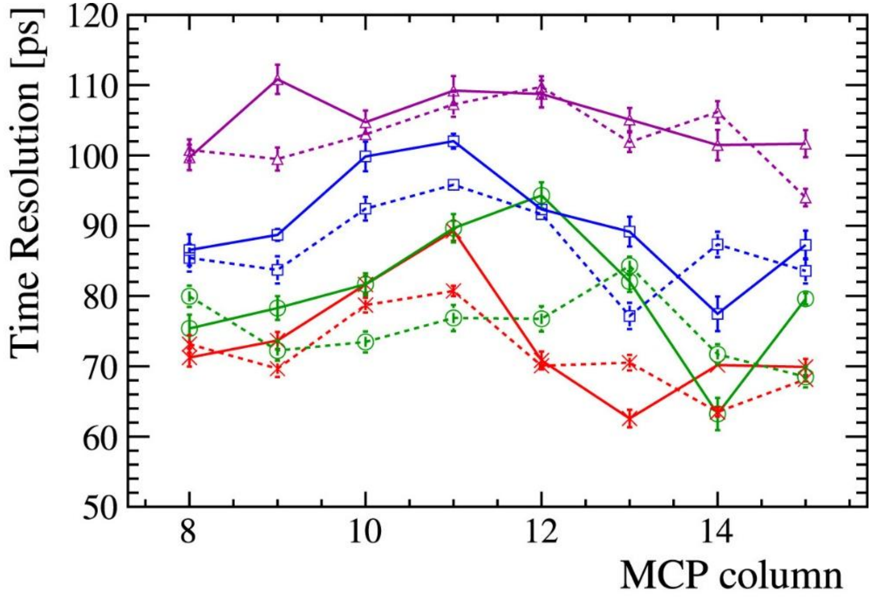

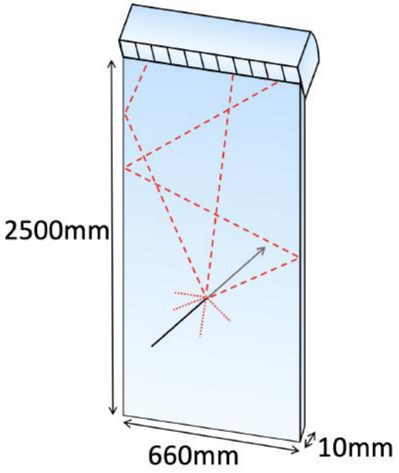

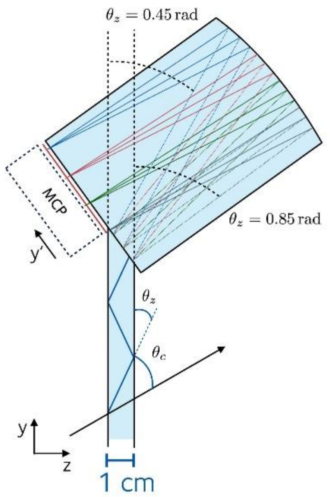

NIMA1050(2023)168181

PoSEPS-HEP2019 (2020) 140

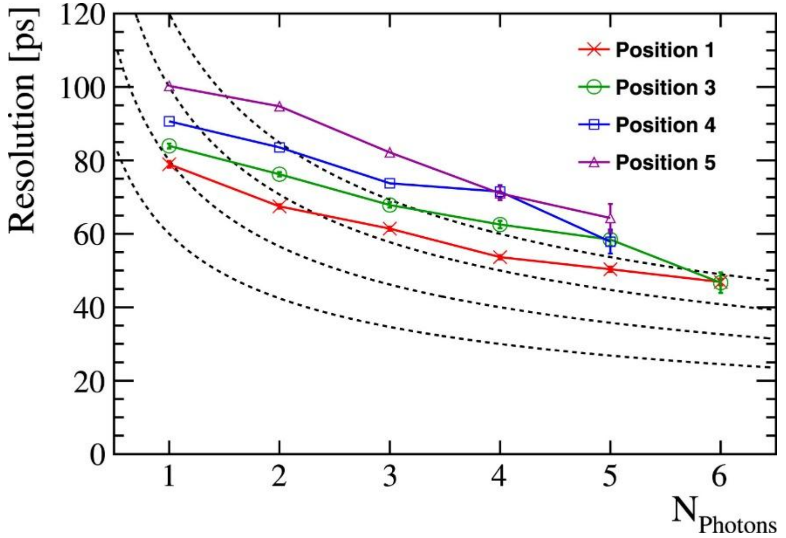

SiPM

SiPM

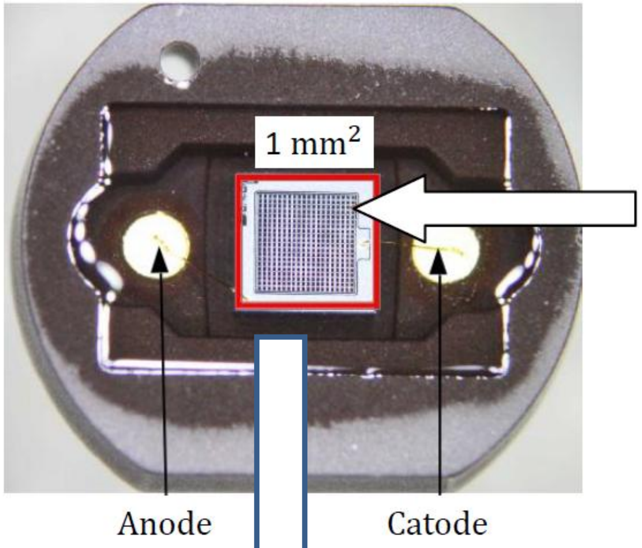

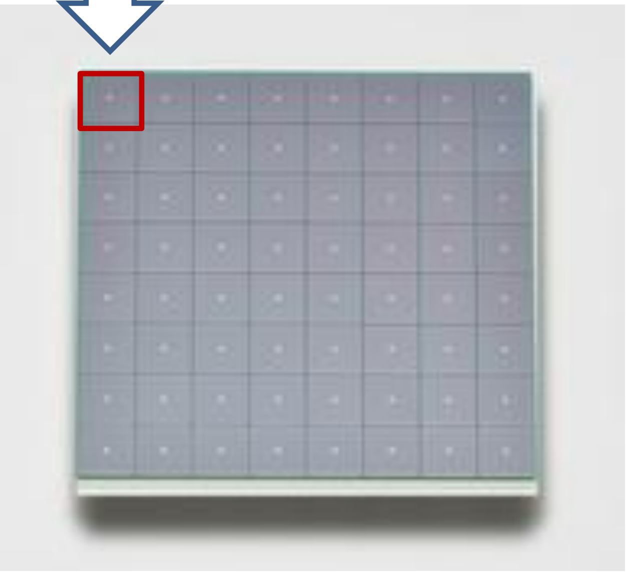

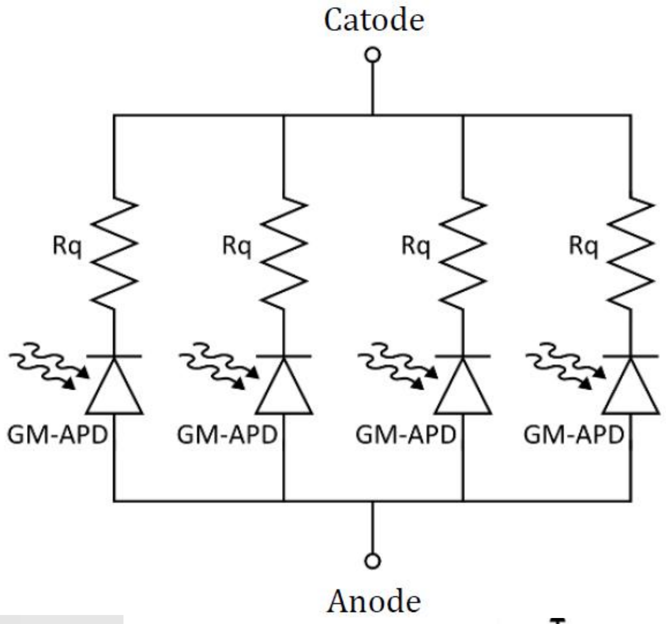

- Multiple Geiger-Mode Avalanche photodiodes (GM-APDs) with common output
- R_q integrated in each cell to provide avalanche dumping
- Each cell behaves like a digital sensor

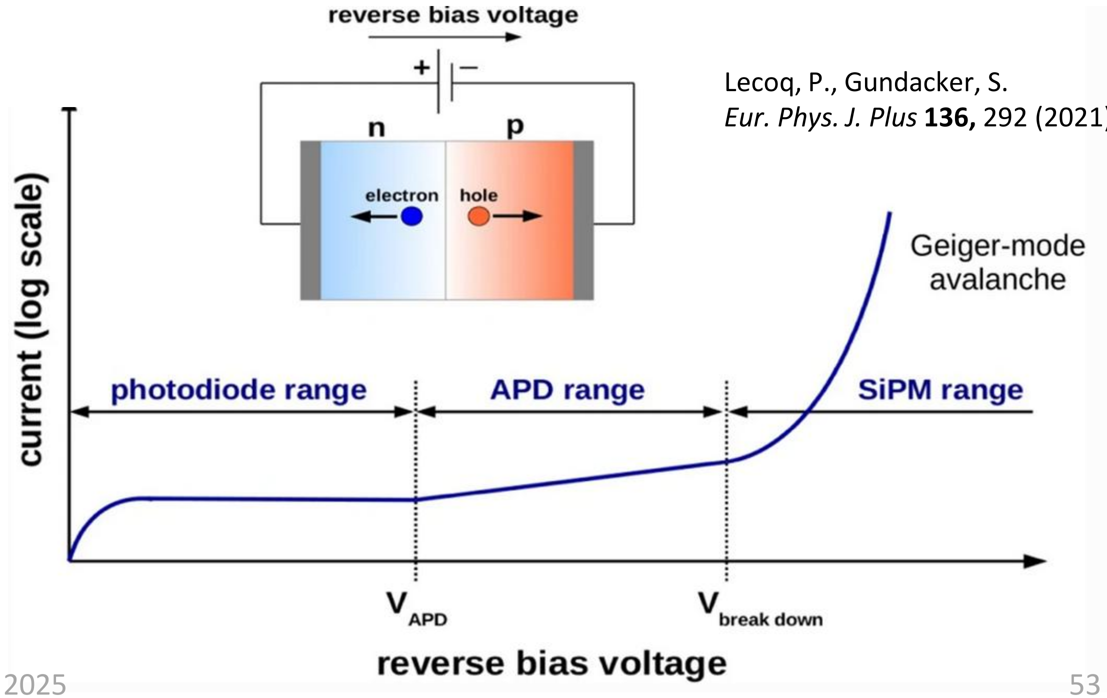

Lecoq, P., Gundacker, S.
Eur. Phys. J. Plus **136,** 292 (2021).

SiPM structure

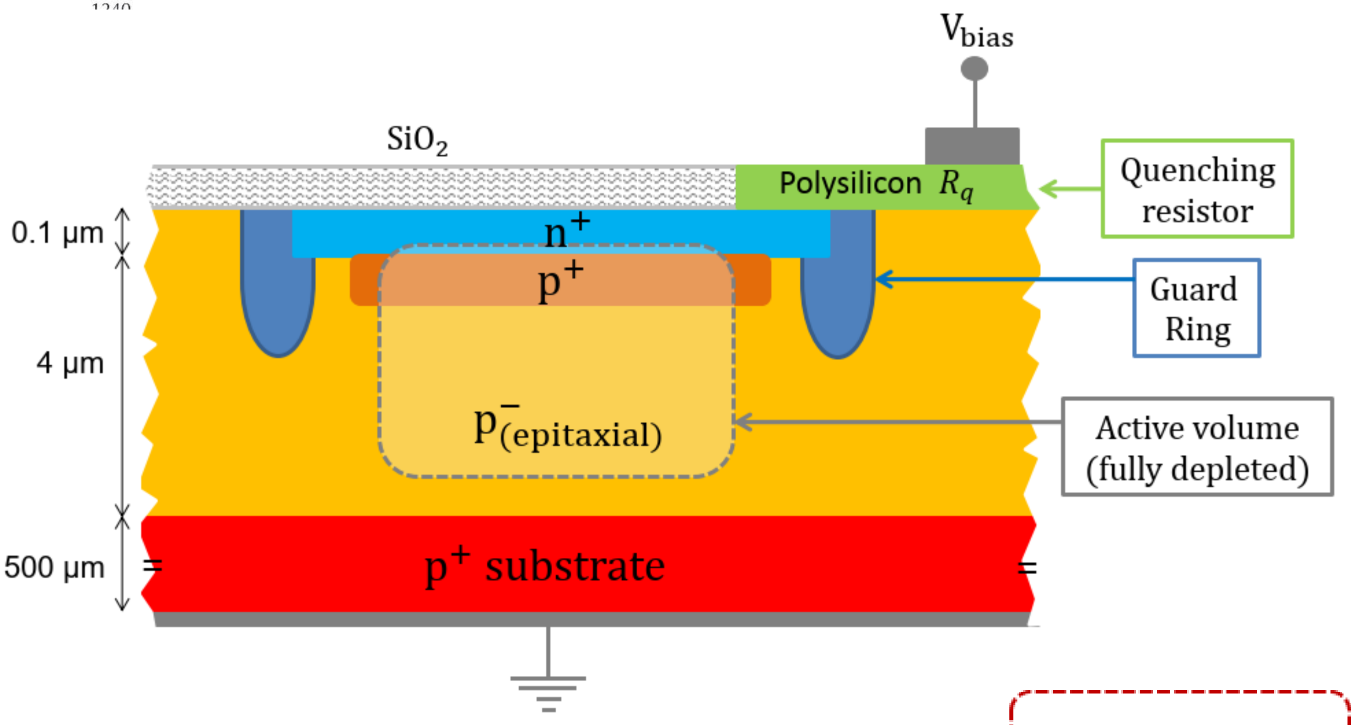

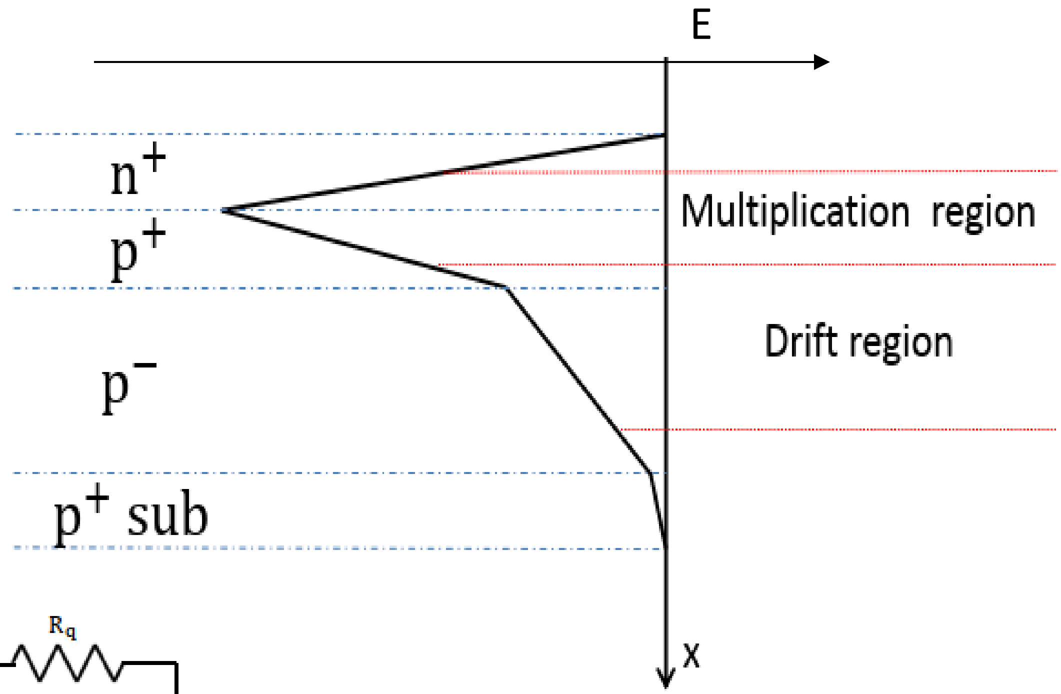

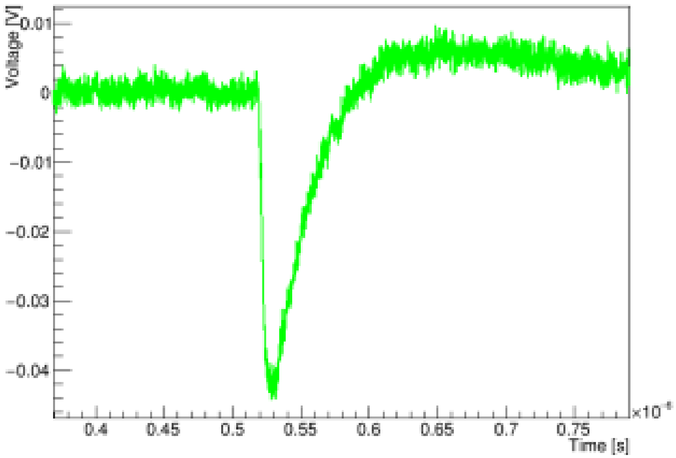

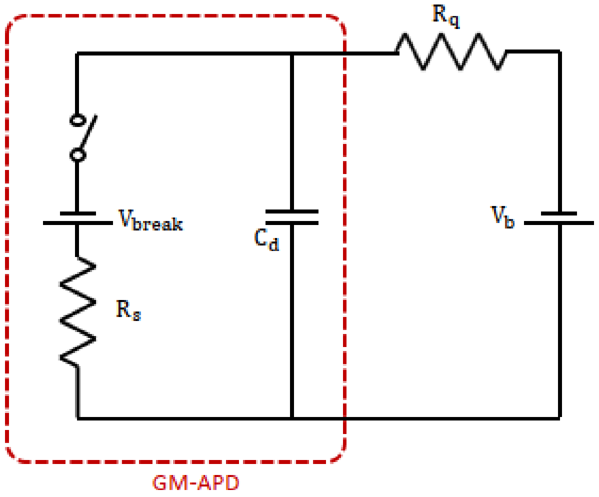

Main source of timing uncertainty given by the photon conversion point and consequent drift path. Reduction of active volume generate inefficiency in photon detection.

SiPM signal

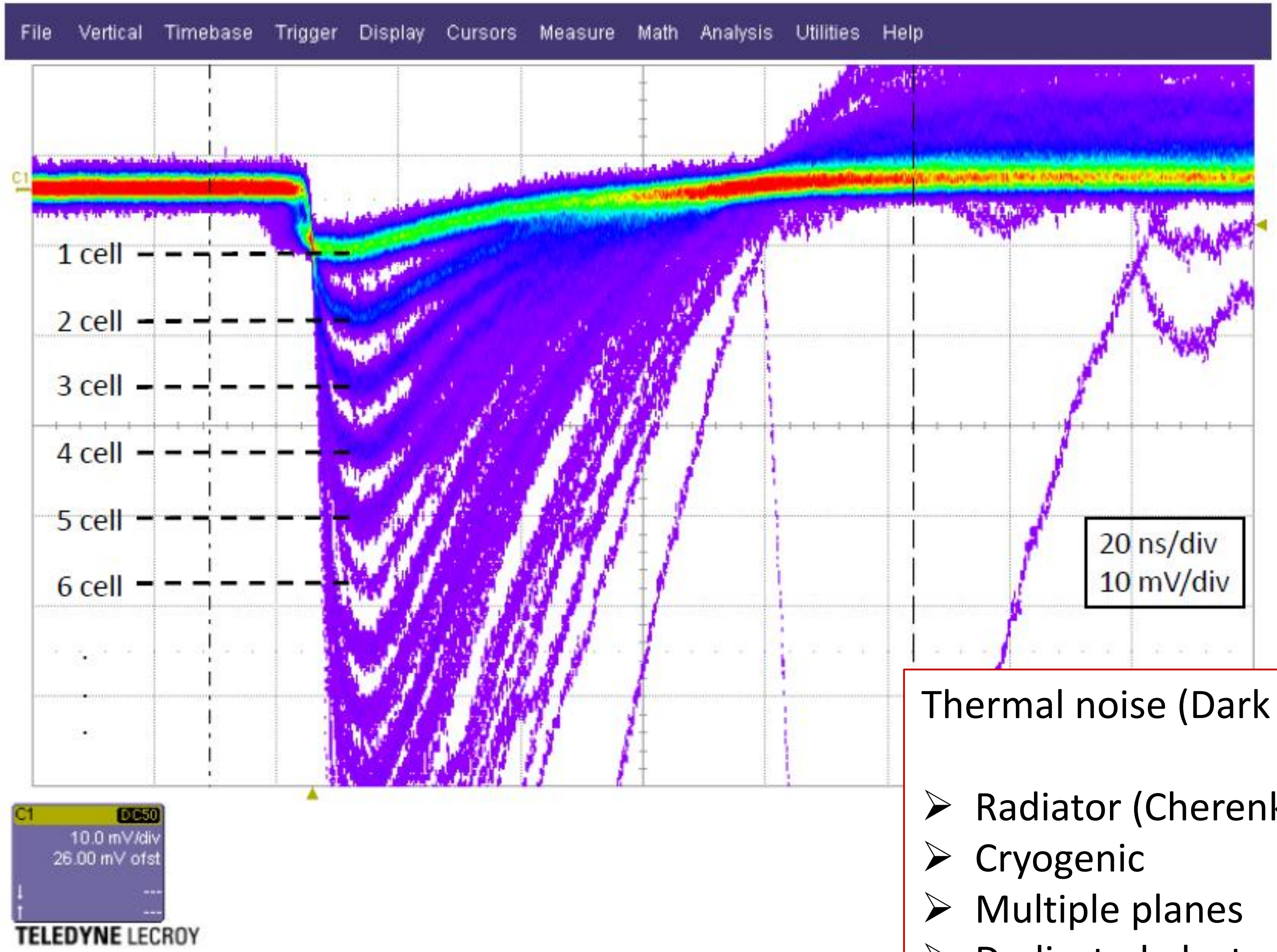

- Quantization of the signal
- Fast leading, slow trailing edge

- DCR can reach Mhz/channel at room temperature

The avalanche can be started by a thermally generated electron

Thermal noise (Dark Count) identical to MIP signal:

- Radiator (Cherenkov/scintillator)
- Cryogenic
- Multiple planes
- Dedicated electronics

SIPM signal: characterization

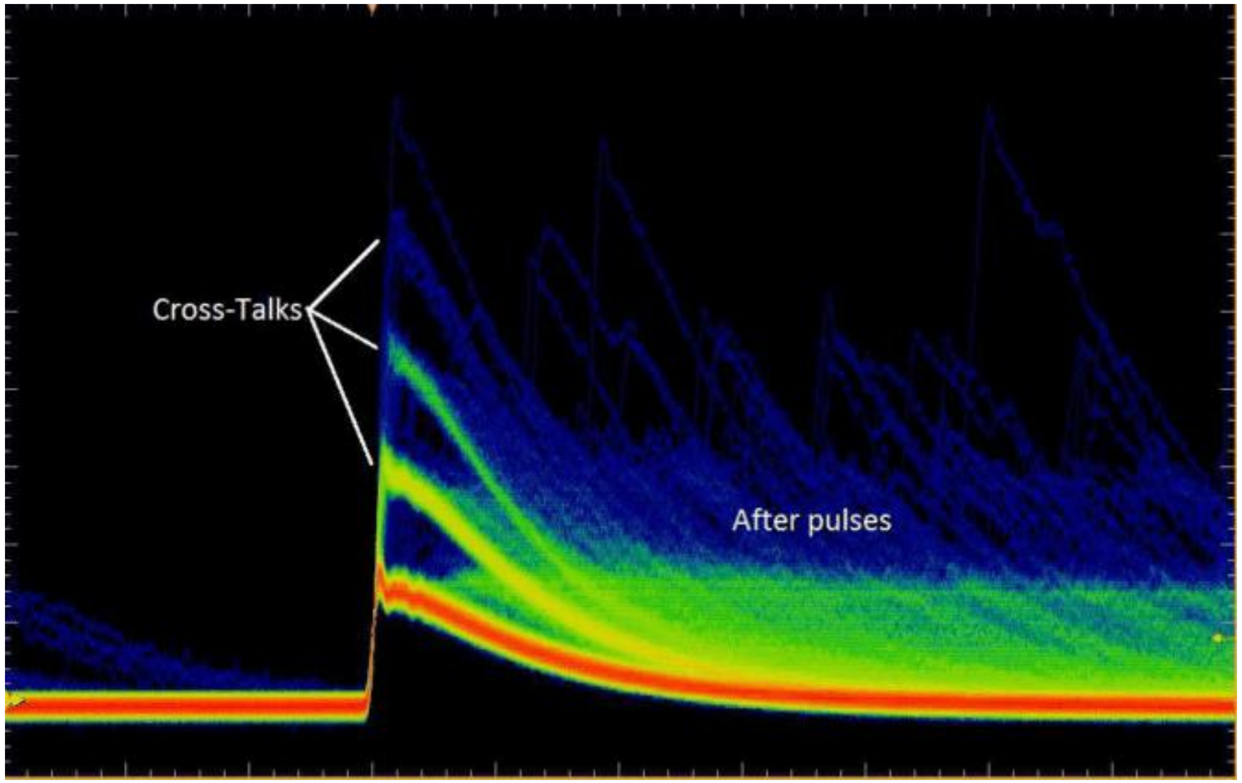

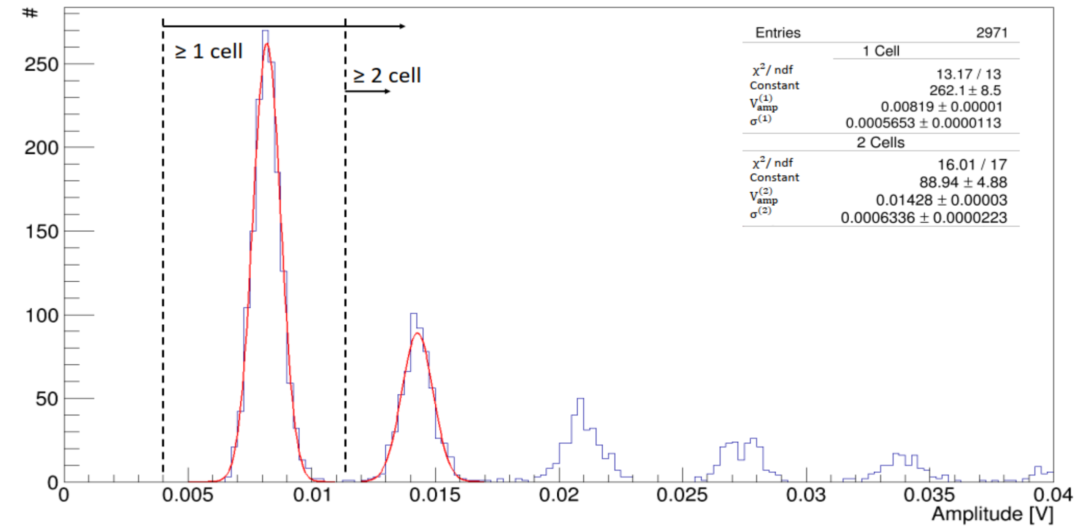

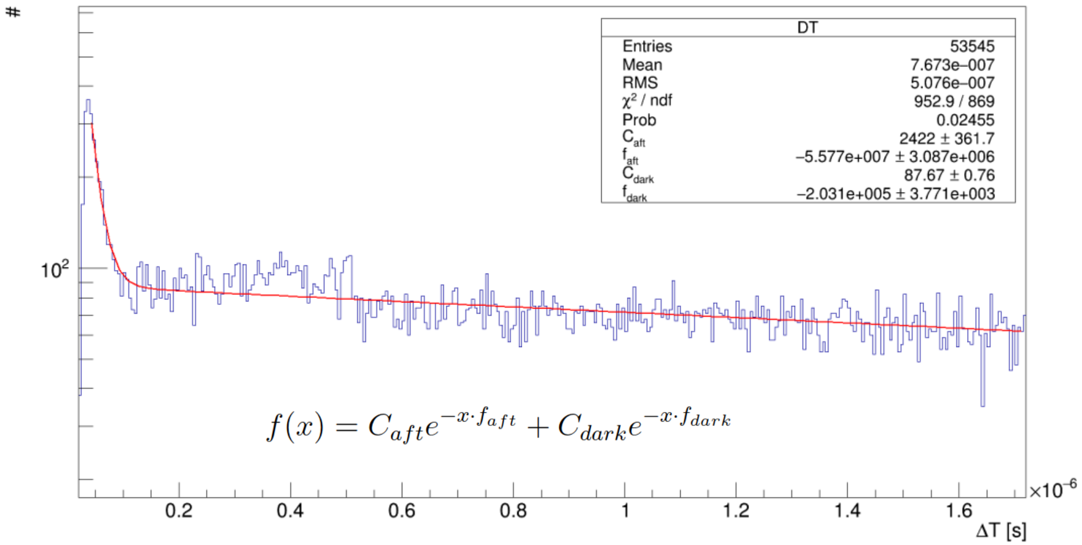

Amplitude distribution:
- Gain
- Resolution
- SNR
- Crosstalk probability

Time distribution:
- Dark count rate
- Afterpulse rate

SiPM timing detector

NIMA, Volume 623, Issue 3, 2010, Pages 931-941

Several combination of SiPM and MCP tested at Fermilab with 120 GeV proton (laser for the TTS)

Detector 1: Hamamatsu MPPC (3 x 3 mm2) SiPM with a
Matched Cherenkov radiator (fused silica) 30mm length
Detector 2 (reference): MCP-PMT240 Photek, 40um pores,
TTS 33ps, MIP resolution 7.7ps

Note the angle w.r.t. the beam

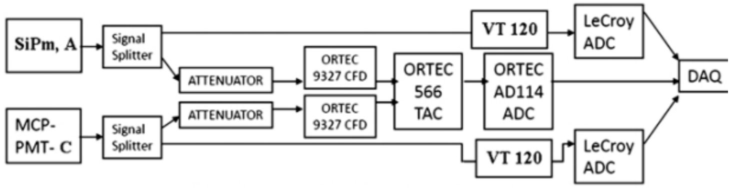

Readout: vintage but effective

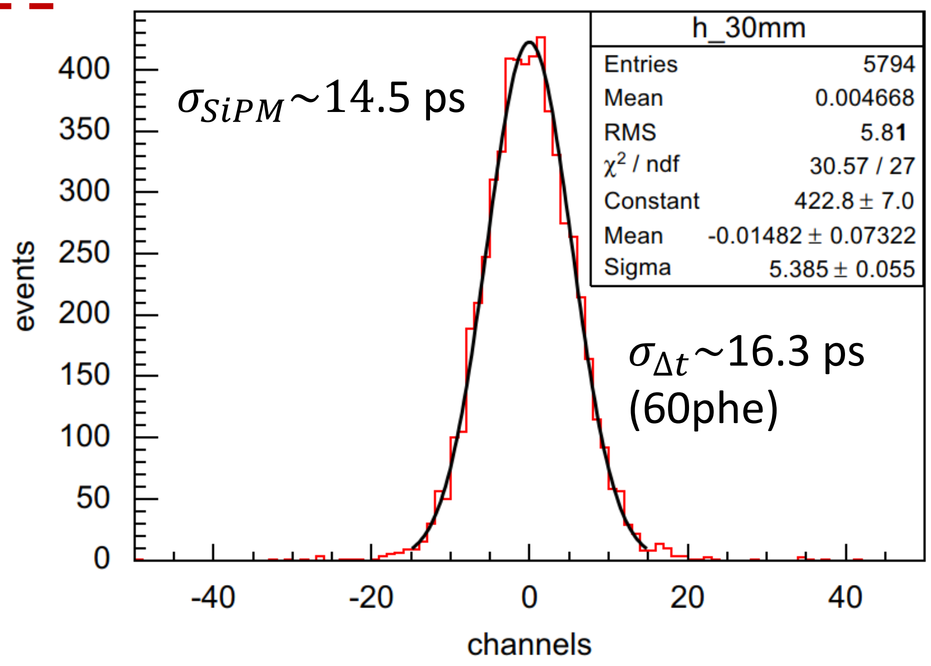

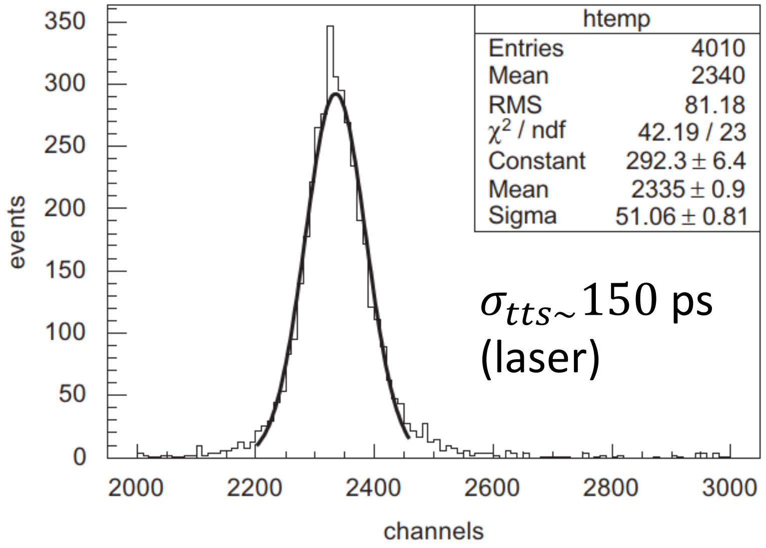

Precise and slow: CMS MTD-BTL

CMS MTD Barrel Timing Layer is a good example on how a precise timing detector do no need to be fast

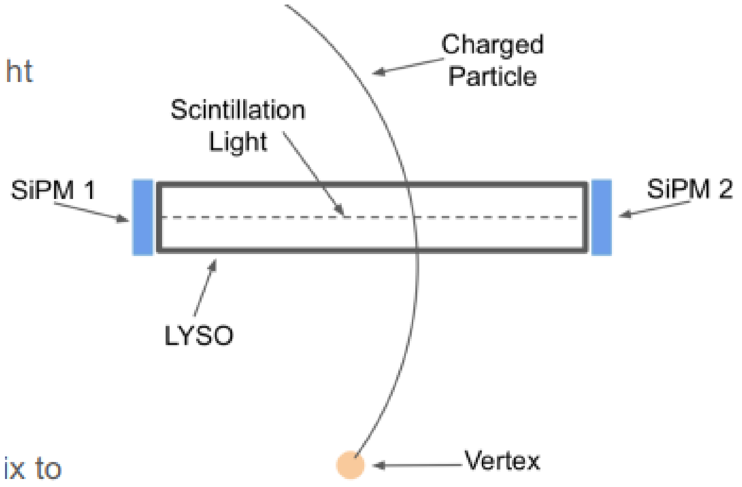

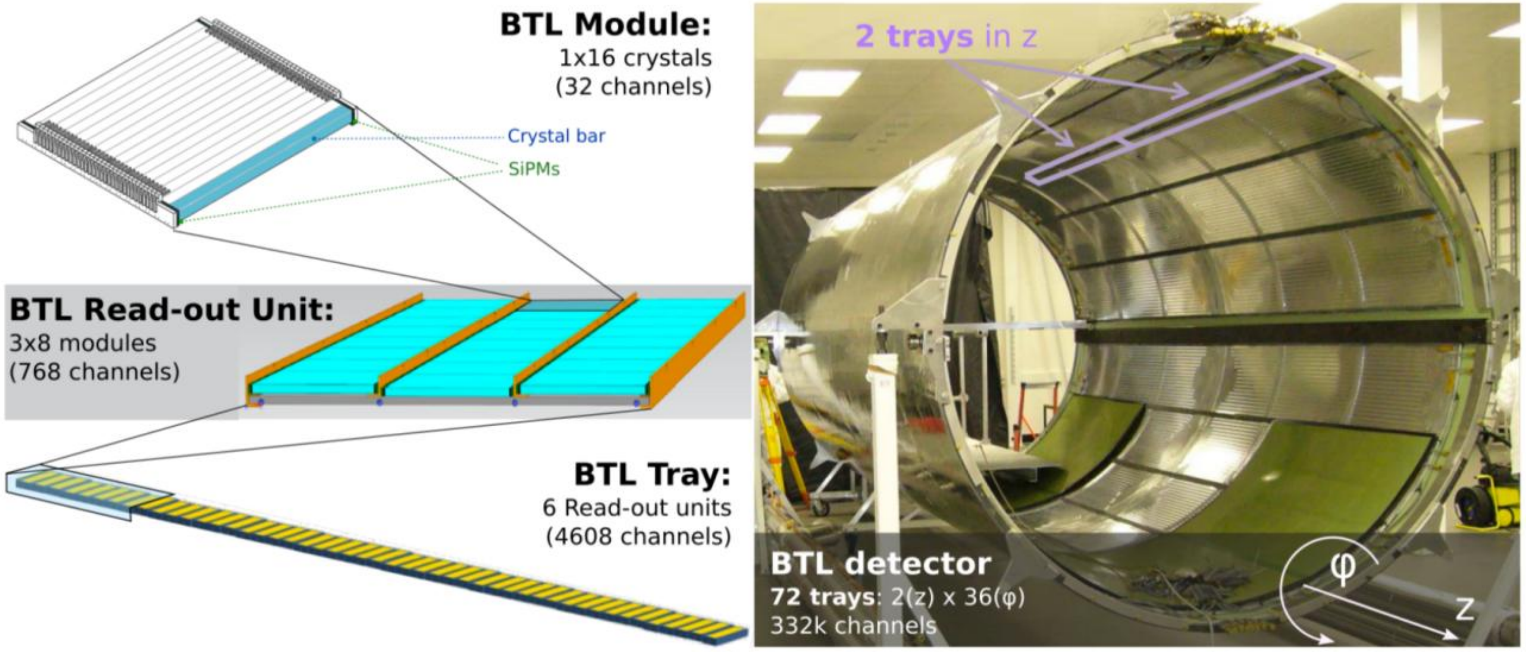

Each sensor made of a 3x3x57 mm3 LYSO:Ce crystal bars with two 3x3 mm2 SiPMs glued at each end

Common geometry:
You can make use of all the light, while avoiding light reflection at scintillator end.

UNIVERSITÀ DI SIENA 1240

Precise and slow: CMS MTD-BTL

LYSO crystals activated with cerium (LYSO:Ce) as scintillator:

- Excellent radiation tolerance
- High density -> expected 4.2MeV/MIP
- Elevated light yeld (~40K photon/MeV)
- Slow decay time ~40ns and signal peaking time ~20ns

Silicon Photomultipliers as photo sensors:

- Compact, fast (TTS 100 ps), insensitive to magnetic fields
- SiPM cell size: 15 µm, balance between radiation tolerance and photon detection efficiency
- Good (20-40%) Photon Detection Efficiency
- Gain: 1.5 – 4×10^5

Expected huge and slow signals

↓

timing is given by the arrival of the first photoelectrons (20-100 p.e.)– 2 per mille of the signal matters

Timing given by the signal start
Strategy applied also in TOF-PET, where scintillators must be used to detect gamma photons.

Similar approach for timing in calorimetry
Signal of tens of ns generated by showers

Radiation damage

Generally, for solid state detectors: Charge multiplication = Radiation damage multiplication

For SiPM the gain will drop and DCR will explode

Integrated luminosity (fb-1)	Number of p.e.	SiPM gain	DCR (GHz)
0	9500	3.8×10^5	0
500	9000	2.9×10^5	20
1000	8000	2.5×10^5	30
2000	7000	1.9×10^5	45
Run 4 -> 3000	6000	1.5×10^5	55

BTL SiPM parameter evolution

Under development electronics to filter DCR (Chip TOFHIR) for BTL

SiPM lifetime:

- Usually die very soon ($\sim 10^{13} neq/cm^2$)
- Both photocathode and silicon damaged

Lifetime extension:

- Run at low temperature
- Place far from particle beam
- Annealing procedure

Note that radiation damage in SiPM ≠ ion feedback aging in MCP. The second happen also if MCP is not directly hit by particles!

Diamond (2D/3D)

Diamond detectors

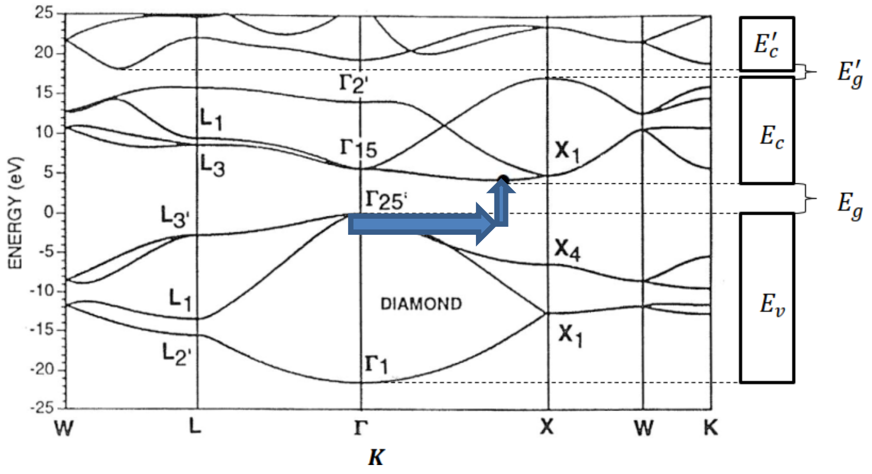

Diamond is an isolator from the bandgap perspective, but band structure is like indirect semi-conductor

W.r.t. silicon:

- Higher e/h mobility -> faster signal
- Larger band-gap -> No need to remove free carriers
- Higher energy to create e/h but similar density -> smaller signal
- Very high resistivity and breakdown field -> can operate with intense field
- Higher displacement energy (for single crystals) -> more rad. hard

		Silicon	Diamond
E_g	Band-gap (eV)	1.12	5.47 (7.5 eV direct)
E_b	Breakdown field (V/cm)	$3 \cdot 10^5$	10^7
ρ_{el}	Resistivity (Ω cm)	$2.3 \cdot 10^5$	$> 10^{15}$
ρ	Density (g/cm^3)	2.33	3.52
$E_{e/h}$	Energy to create e/h pair (eV)	3.6	13
E_{MIP}	Most probable energy released by MIP (MeV/cm)	3.21	4.69
$E_{e/h}$	Most probable number of e/h pair created by MIP (N/μm)	89	36
μ_e	Electron mobility (cm^2/V s)	1,350	4,551 [16]
μ_h	Holes mobility (cm^2/V s)	480	2,750 [16]
v_e	e saturation velocity (cm/s)	$\sim 10^7$	$\sim 2.6\, 10^7$ [16]
v_h	h saturation velocity (cm/s)	$\sim 7.5 \cdot 10^6$	$\sim 1.6\, 10^7$ [16]
ϵ_r	Relative permittivity	11.9	5.7
T_d	Displacement threshold energy (eV)	36 [18]	37.5–47.6 [17]

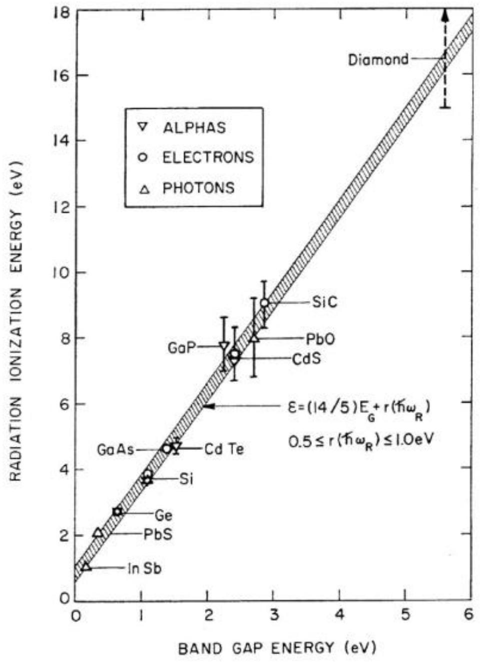

No need for cooling!!!

CVD diamond

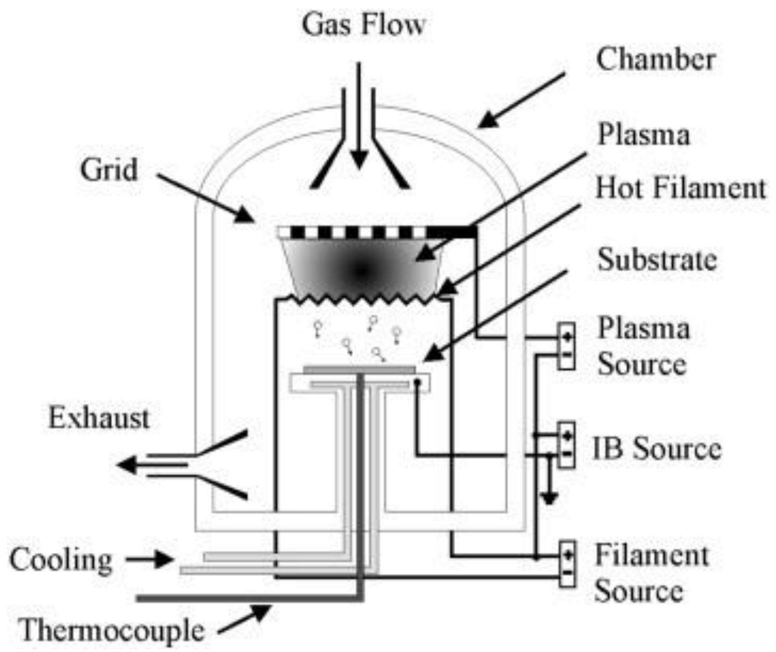

Diamond and Related Materials, Volume 20, Issue 9, October 2011, Pages 1287-1301

- ➢ Methane and H in low pressure reactor cavity
- ➢ Plasma through microwave or hot filament
- ➢ Carbon created through the reaction

$$CH_x + H \to CH_{x-1} + H_2.$$

- ➢ Nucleation on the substrate
- ➢ Crystal growth

Diamond Type	Thickness (μm)	Area (mm^2)	*ccd* (μm)
Sample 1 pCVD	516	10×10	230/227
Sample 2 pCVD	510	10×10	218/228
Sample 3 pCVD	511	10×10	227/241
Sample 4 scCVD	466	5×5	466/466

Bani L. et al. J.PhysD. (2019) 52:465103

CCD (Charge Collection Distance): distance made by charges before recombination

Poly-crystalline diamond can be made larger, but CCD significantly lower (~10 μm/h)

To create single crystal better to use another single crystal as substrate

Key role of atomic H:
- ➢ Carbon formation
- ➢ Removal of residual H from carbon
- ➢ Effective in graphite removal

Metallization/graphitization

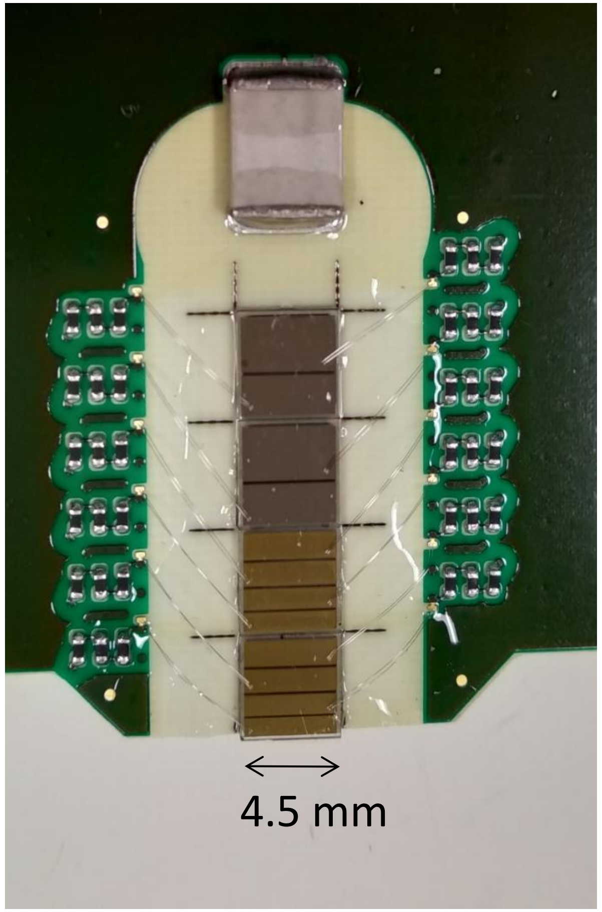

- Two possible way to create (ohmic) contacts on the diamond:
- Metallization
- Laser graphitization

Metallization can be done applying a mask on the crystal and making a vapor deposition of some metal (Cr-50 nm + Au-150 or 100 nm Ti-W alloy for example).

After deposition of a metallic layer the crystal can be annealed so that certain metal (Cr or Ti) will react with the diamond and form carbides resulting in a final ohmic contact

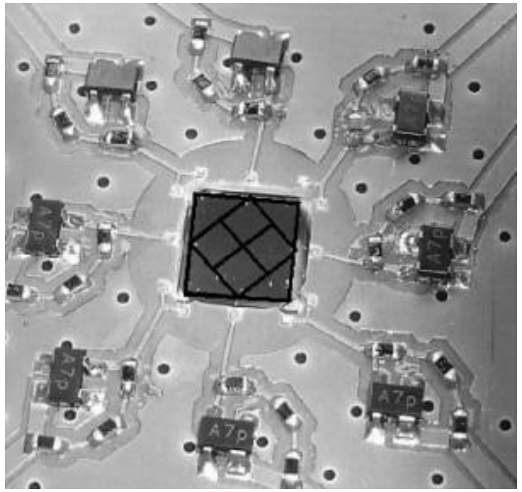

Main characteristics:

- Wide pads can be created. Difficult to create small pad (< 100x100 μm^2)
- All geometries available
- Minimum separation between pads $\sim$ 50 μm
- Precision limited by the mask quality and the deposition process. 10 μm on the border at best.
- Can be removed (not always easy)!
- Very low and constant electrode resistance

Metallization/graphitization

Very hard to control graphite depth

- ➢ Two possible way to create (ohmic) contacts on the diamond:
- ➢ Metallization
- ➢ Laser graphitization

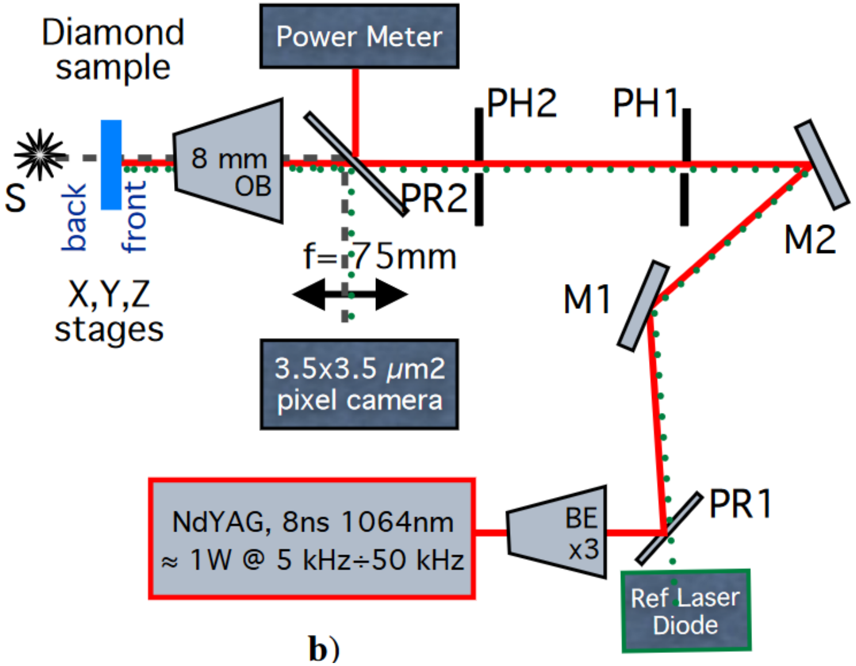

b)

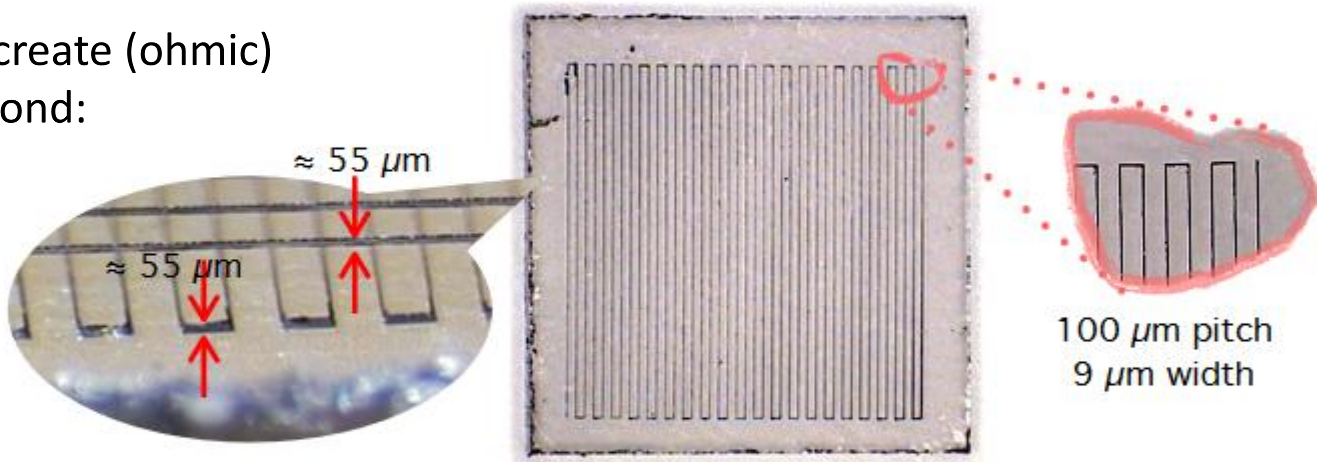

Parrini G. et Al., *Pos*. (2011) RD11:17

Main characteristics:

- ➢ Suitable for thin electrodes
- ➢ All geometries available
- ➢ Can be removed by mechanical polishing
- ➢ Resistivity of electrode may vary a lot
- ➢ Graphitization reduce the thickness of the diamond

Nb. Both processes can be made in few laboratories across the world. Actually only 2-3 can made high precision metallization!

UNIVERSITÀ DI SIENA 1240

INFN

Pads and electric field

Current is induced on the electrode by moving charges (Ramo Theorem):

$$I(t) = q\nabla\Phi_w \frac{d}{dt}\mathbf{r}(t) = -q\mathbf{E}_w v(t)$$

The weighting field $\mathbf{E}_w(\boldsymbol{x})$ represents the static electric field in the detector volume in case all electrodes are grounded, and a delta potential V is applied to the electrode in question

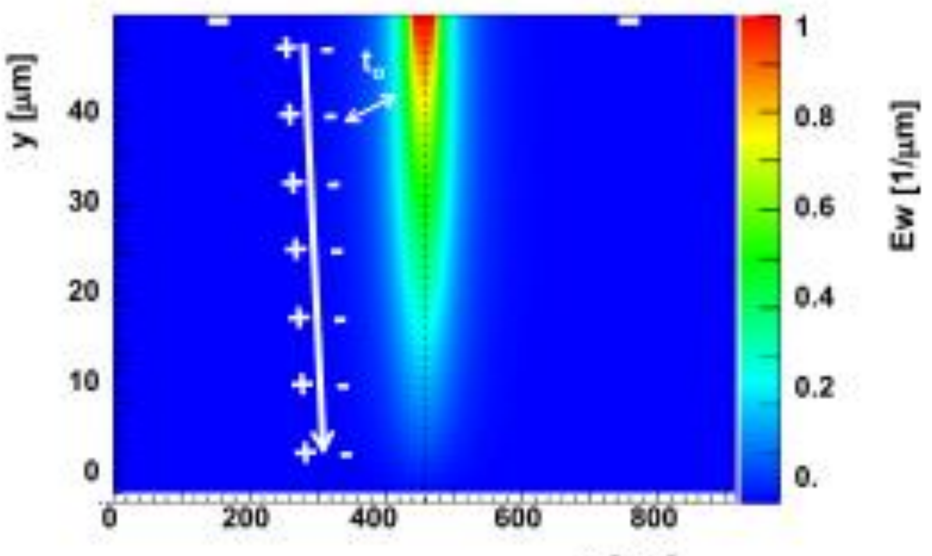

Hartmut F-W Sadrozinski et al 2018 Rep. Prog. Phys. 81 026101

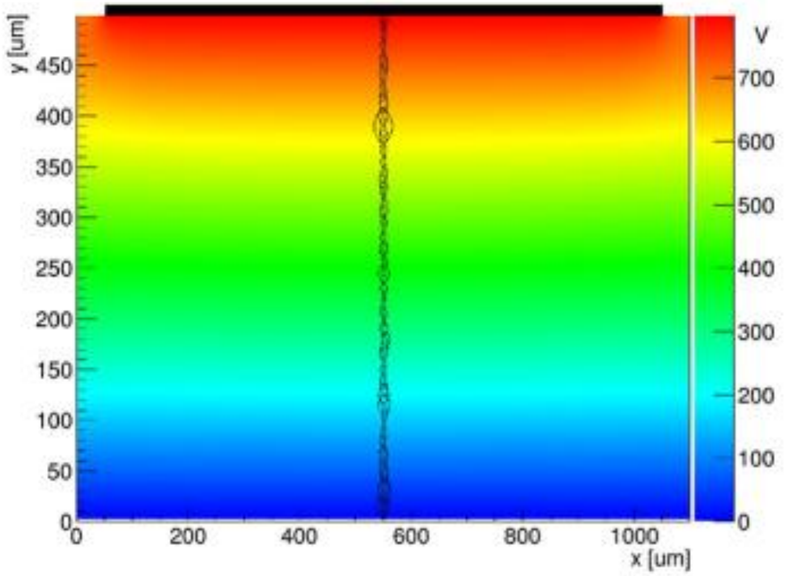

Valid for diamond and silicon

Large, thin pad favored for the field perspective but keep capacitance under control!!

Non uniform weighting field causes an additional drift time from the interaction point to the electrode.

Electrode should cover the full pad area -> metallization
Still border effect and local non-uniformities due to the generated charge are present, affecting the shape of the final signal

Saturation velocity

$$v_{d,e} = \frac{e\tau_{R,e}(T)}{m^*}\mathbf{E} = \mu_e\mathbf{E}$$

μ_e:
- Constant for $E < 10^3$ V/cm
- $\propto 1/\sqrt{E}$ for 10^3 V/cm $< E < 10^4$ V/cm
- $\propto 1/E$ for $E > 10^4$ V/cm

$$\mathbf{v}_d(\mathbf{E}) = \frac{\mu\mathbf{E}}{1 + \frac{\mu\mathbf{E}}{v_{sat}}} \qquad v_{sat} = \sqrt{\frac{8E_{opt}}{3\pi m^*}tanh\left(\frac{E_{opt}}{2k_BT}\right)}$$

Saturation due to collision with optical phonons (E_{opt}~160 meV in diamond)

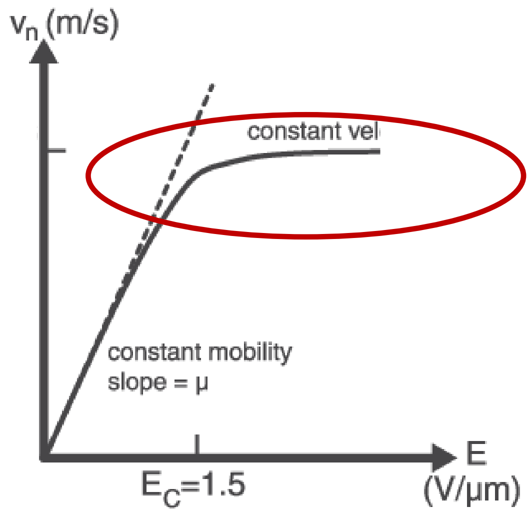

For diamond we can achieve full saturation for electric field ~1 – 2 V/μm, far from the breakdown field (~ 10^3V/μm).

For silicon, the gap is much closer (breakdown at ~50 V/μm, other destructive phenomena @ 11 V/μm) and further reduced by irradiation.

E.Bossini, https://cds.cern.ch/record/2227688/files/CERN-THESIS-2016-137.pdf

Signal shape

UNIVERSITÀ DI SIENA 1240

E.Bossini, https://cds.cern.ch/record/2227688/files/CERN-THESIS-2016-137.pdf

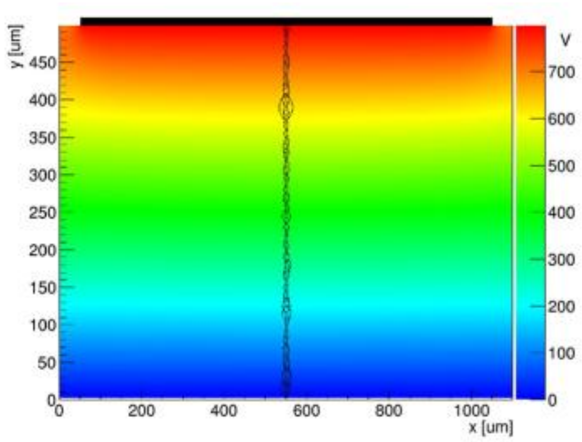

$$I(t) = q\nabla\Phi_w \frac{d}{dt}\mathbf{r}(t) = -q\mathbf{E}_w v(t)$$

Parallel plate geometry

$$E_w = -\frac{d\Phi_w}{dx} = -1/d$$

Current generated by a single charge:

$$i(t) = qv_d(x,t)/d$$

For a constant uniform electric field

$$I(t) = q\Big((N_e(t)v_{d,e}) + (N_h(t)v_{d,h})\Big)/d$$

At $t = 0 \rightarrow I(0) \propto N_{e,h}(0)v_{de,h}/d$

But $N_{e,h}(0) = \frac{dE}{d\xi}\frac{\rho \cdot d}{W_{eh}} \Rightarrow I(0) \propto \frac{dE}{d\xi}\frac{\rho \cdot v_{de,h}}{W_{eh}}$

The peak current of the detector does not depend on the thickness!

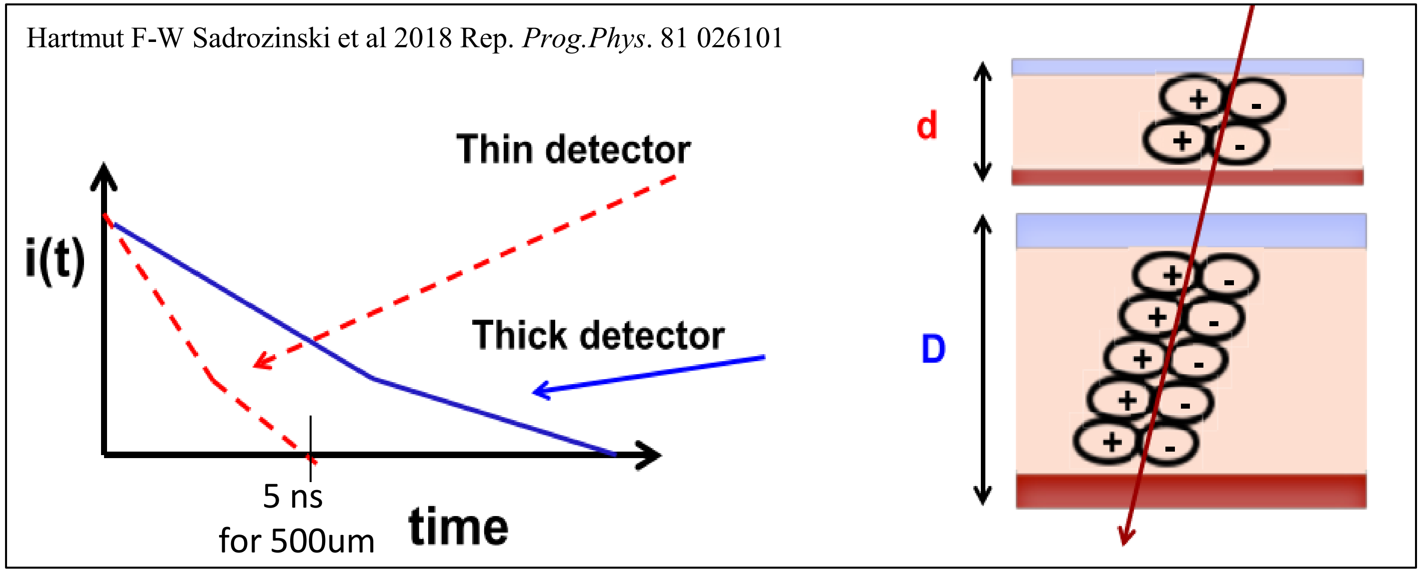

Hartmut F-W Sadrozinski et al 2018 Rep. *Prog.Phys*. 81 026101

Note that if I add any capacitance, the integration of the signal will generate differences in the peak amplitude

Diamond signal

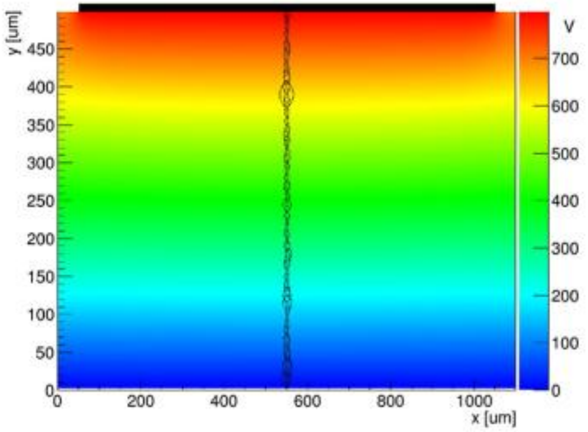

Signal from a single crystal CVD diamond 500 μm thickness, polarized with 800V (1.6 V/μm), 10 pF capacitance

Signal ripple due to local landau fluctuation in the released charge

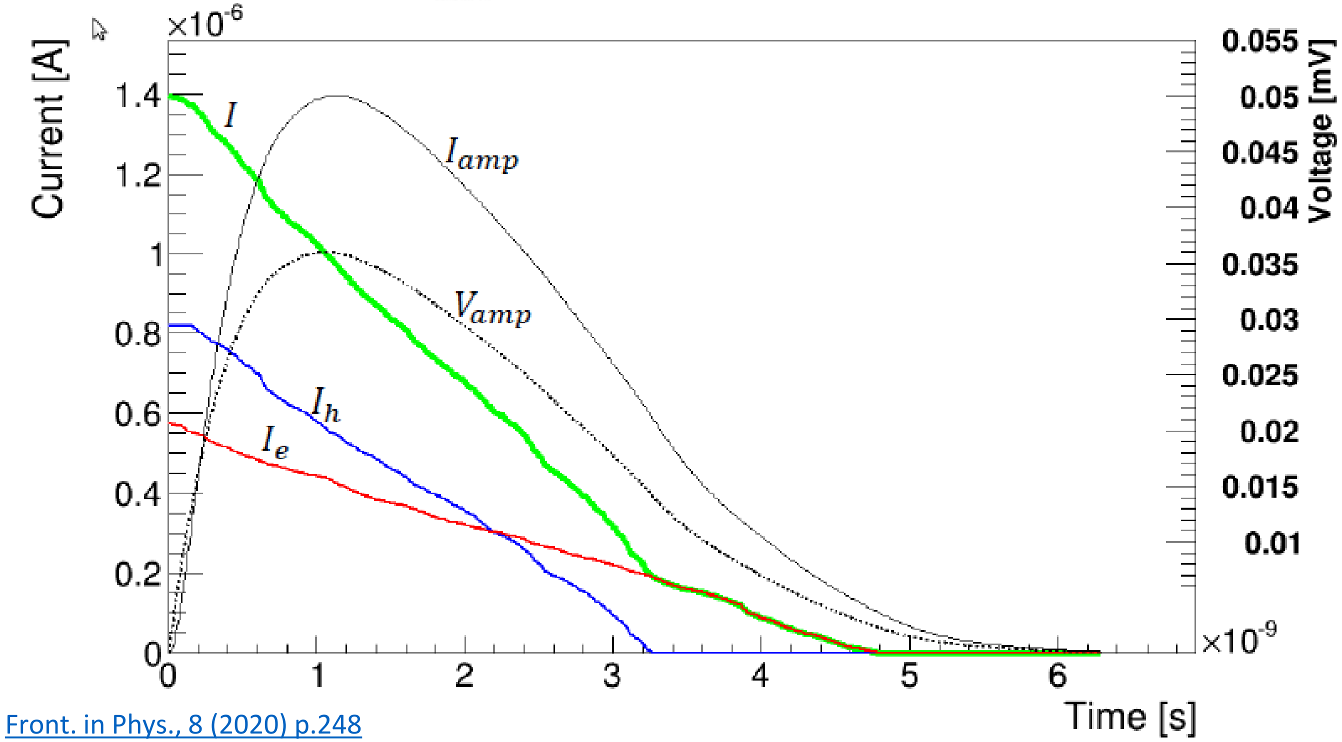

[Front. in Phys., 8 (2020) p.248](#)

Main signal characteristics:

- Fast intrinsic rise time (few ps)
- Very low noise (<nA) → Noise dominated by pre-amp input stage
- Intrinsic SNR above 1000!
- Low signal ~ 1 fC/MIP
- Electron/hole mobility nearly equal
- Signal duration few ns

Fast current amplifiers have a noise $\sim \mathrm{nV}/\sqrt{Hz}$
With a BW above 1 GHZ we get a SNR ~1

Better SNR with charge amplifier (integrate the charge) but will spoil timing performance

Need for special dedicated amplifier! Note that if a final BW < 10 GHz will however generate an integration and favor ticker sensors!

Diamond detector: performance

Signal characteristics (after amplification):
Rise time ~ 1.4 ns
Signal-to-noise ratio (SNR) ~ 30-40
Amplitude ~ 300-700 mV

Tested with 5.6 GeV electrons @Desy anc
180 GeV μ/π beam at CERN SPS

Sensor readout performed with oscilloscope or SAMPIC sampler, offline CFD 30%.

Sensor	Pad area [mm^2]	σ_t	Ampl. [V]	Rise Time [ns]	SNR
StripA	$0.7 \cdot 4.2$	80	0.74	1.48	30
StripB	$0.83 \cdot 4.2$	85	0.70	1.51	31
StripC	$1.02 \cdot 4.2$	87	0.70	1.48	30
StripD	$1.34 \cdot 4.2$	102	0.62	1.49	28
PRN	$4.2 \cdot 4.2$	108	0.39	1.56	18

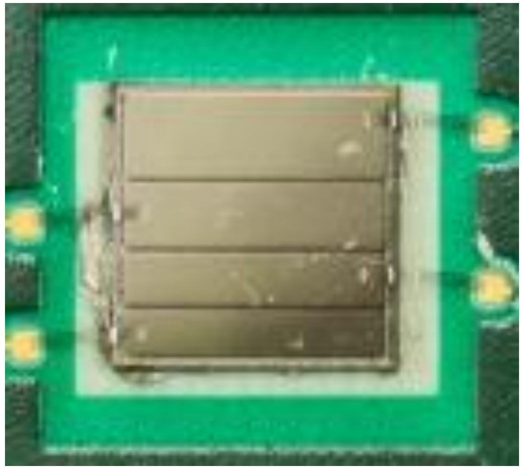

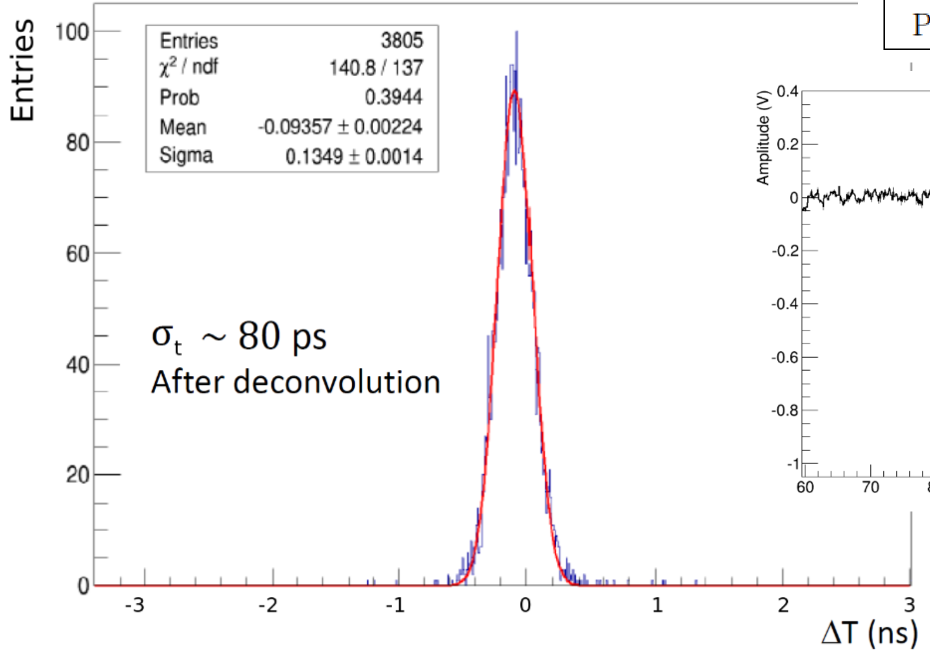

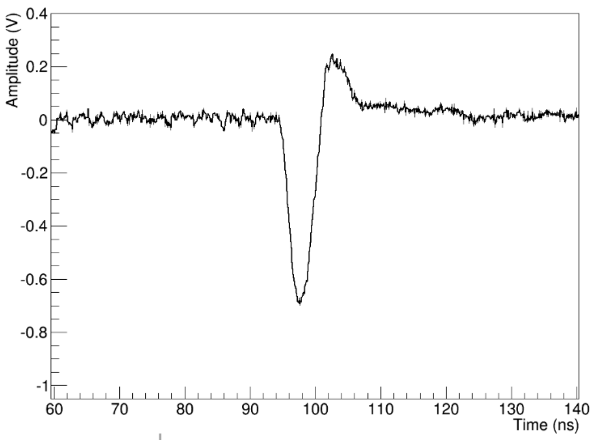

Time difference distribution between small strip and full pad

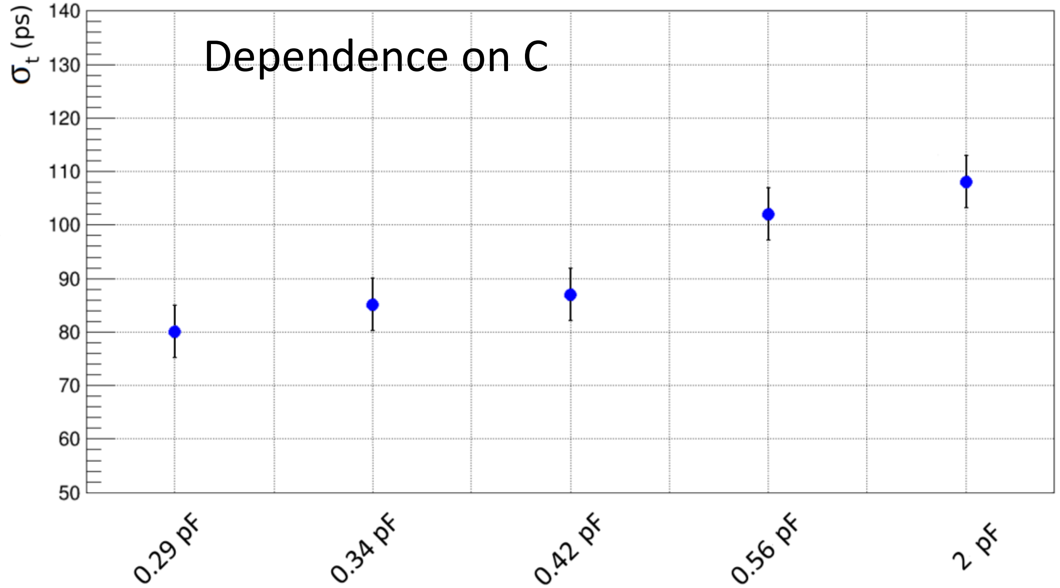

Time resolution w.r.t. pad capacity (∝ pad size, 2pF = 4.2x4.2 mm2)

[JINST 12 (2017) no.03, P03007]

Double Diamond

JINST 12 (2017) no.03, P03026

Sensor readout performed with oscilloscope.

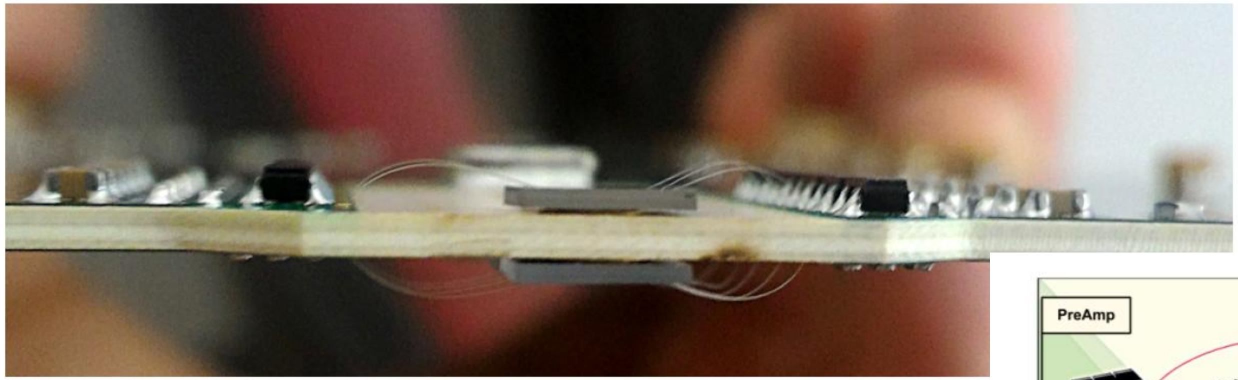

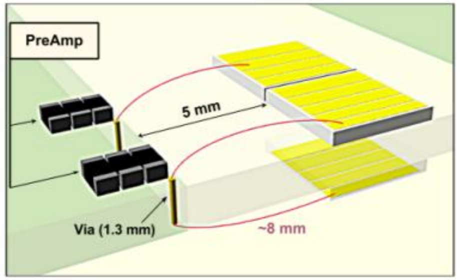

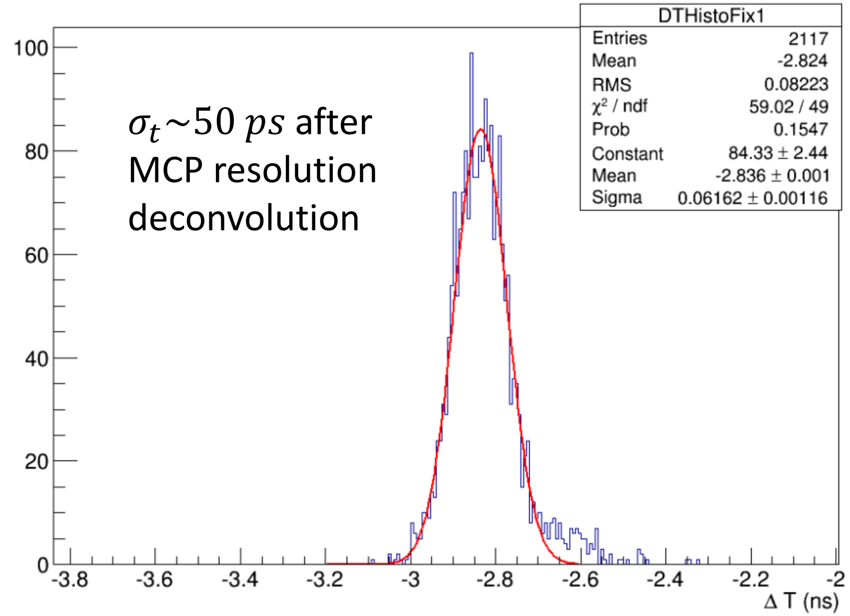

Time difference distribution between DD and reference MCP ($\sigma_{t,MCP} \sim 40\ ps$)

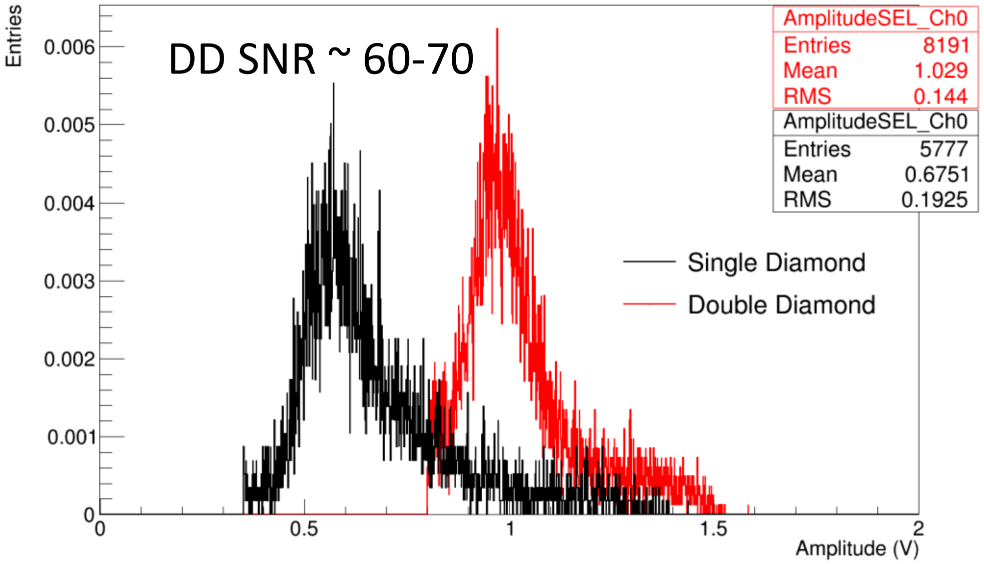

Signal amplitude comparison between DD and SD

Signal from corresponding pads is connected to the same amplification channel:

- Higher signal amplitude
- Same noise (pre-amp dominated) and rise time (defined by shaper)
- Higher sensor capacitance
- Need a very precise alignment

Better time resolution (factor ~1.7) w.r.t SD

Radiation hardness

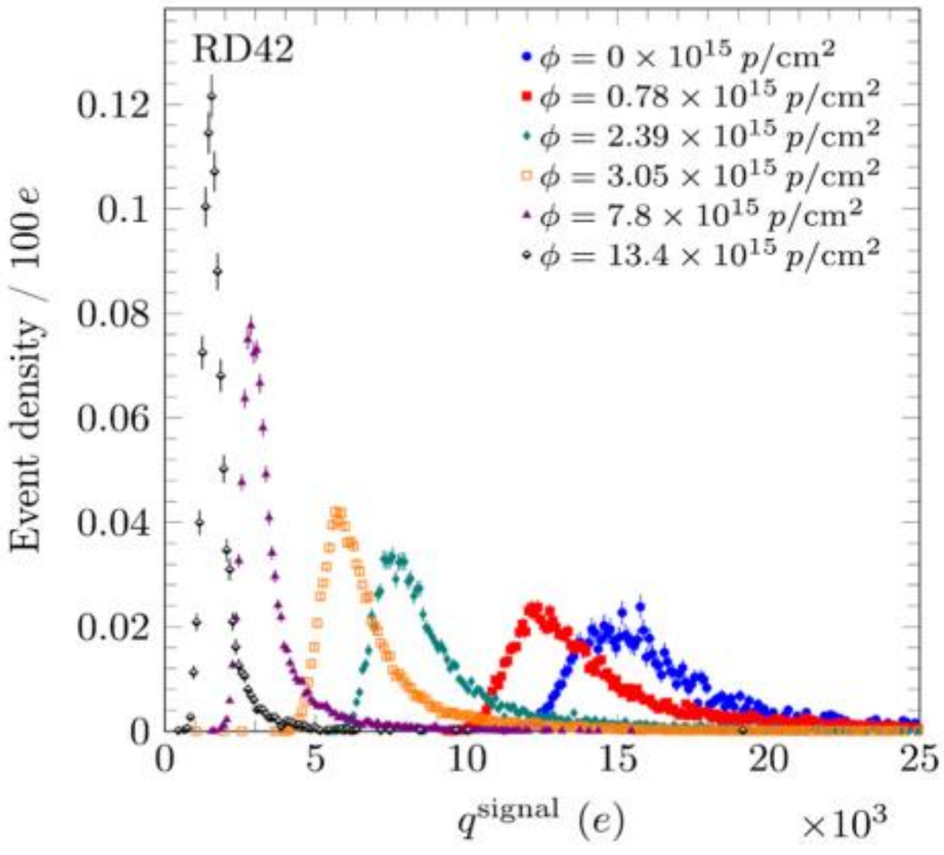

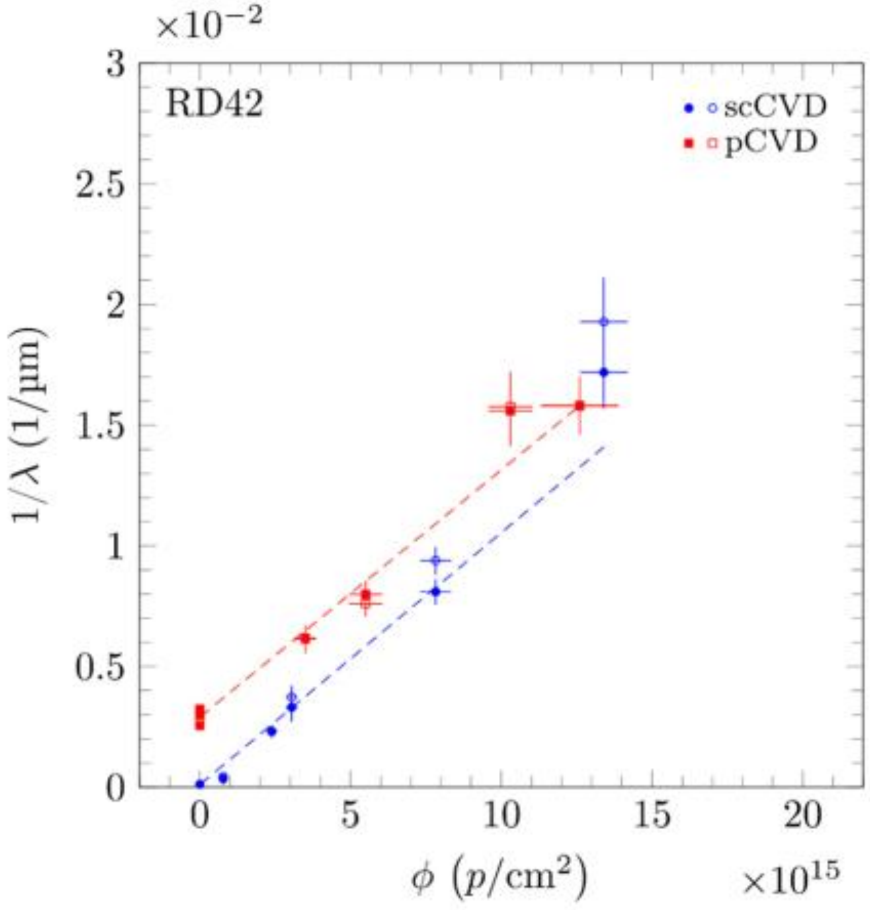

Bäni L, Alexopoulos A, Artuso M, Bachmair F, Bartosik M, Beck H, et al. A study of the radiation tolerance of poly-crystalline and single-crystalline CVD diamond to 800 MeV and 24 GeV protons. *J Phys D.* (2019) **52**:465103. doi: 10.1088/1361-6463/ab37c6

Can still operate after $\sim 10^{16} \mathrm{p/cm^2}$(!!!) with 20% signal amplitude.
$\sim$ no degradation up to $10^{15} \mathrm{p/cm^2}$

3D diamond

3D detector possible through columnar graphitization by laser

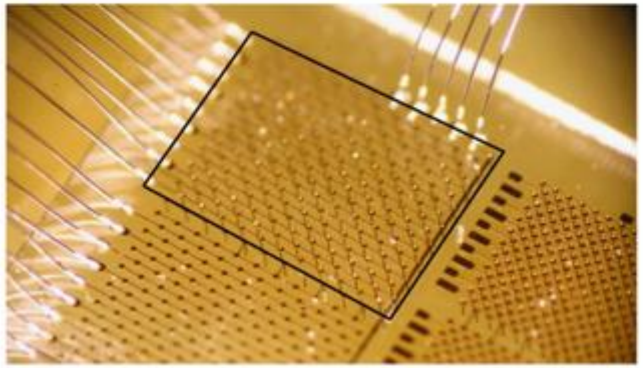

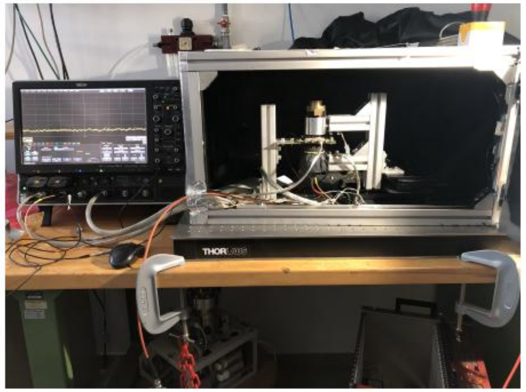

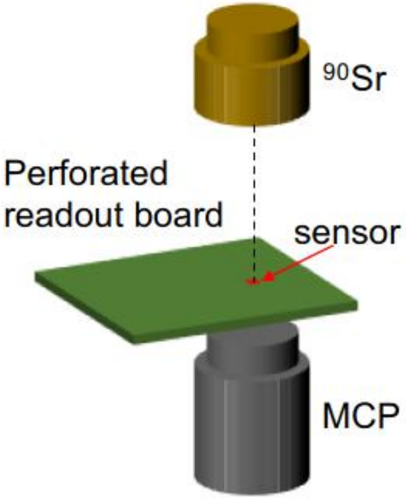

- Electrodes can be closer, reducing the problem of CCD for polycrystalline
- High spatial resolution (4D tracking)

- Integration with readout electronics challenging
- Poor timing (but improving):
  - Non uniform field
  - Electrode resistance variation

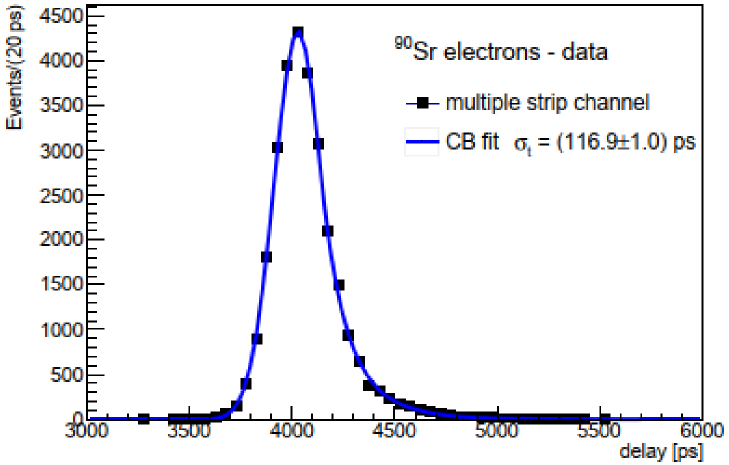

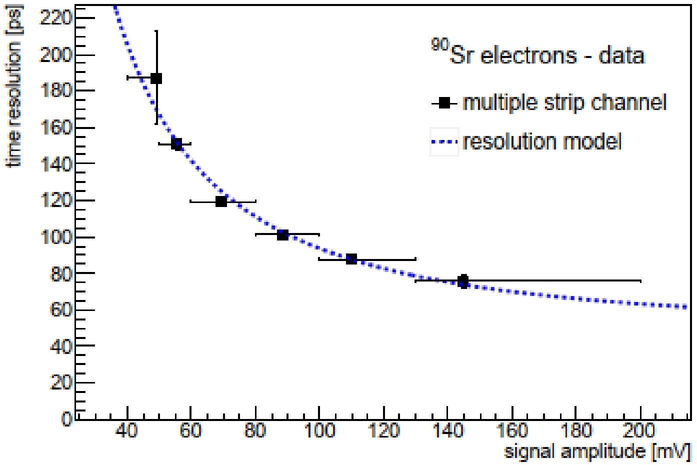

Anderlini, L. et Al, *Instruments* 2021,5,39

Recent results @SPS (L. Anderlini, FAST 2023 workshop) demonstrated a time resolution 0f ~82 ps can be reached on MIP.

First test of integration with readout ASICS successful.

LGAD

Low Gain Avalanche Detector

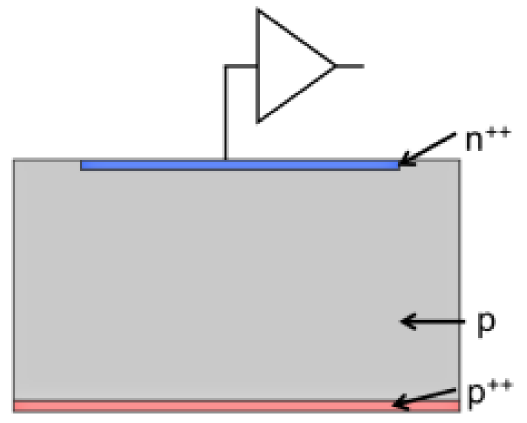

Traditional silicon detector

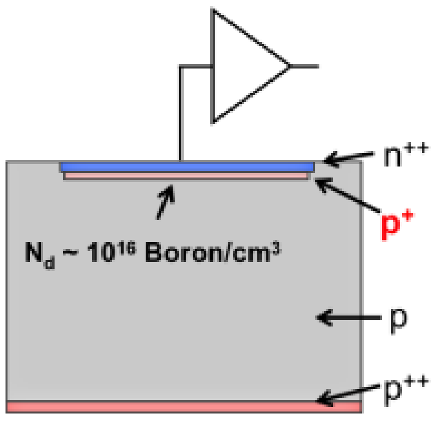

Low gain avalanche detectors

M. Berretti et al. 2017 *JINST* 12 P03024

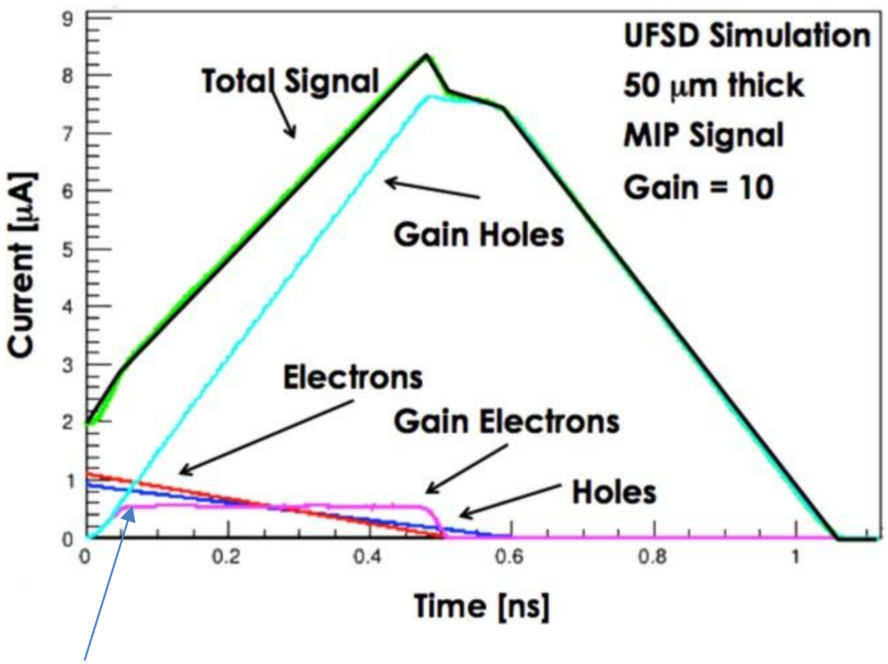

The current induced by primary charges is identical to the case of the diamond (or to no-gain silicon detector)

The larger current is induced by the gain charges (holes in the above design) drifting towards the layer on the opposite side of the gain layer (p++).
Current induced by the gain charges of opposite sign reach a steady value.

Low Gain Avalanche Detector

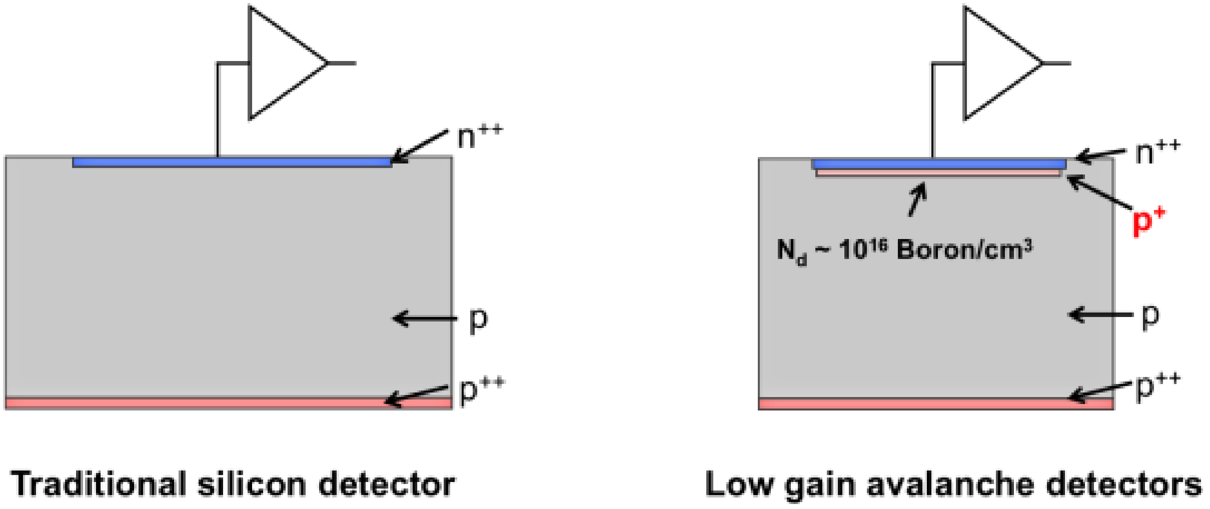

M. Berretti et al. 2017 *JINST* 12 P03024

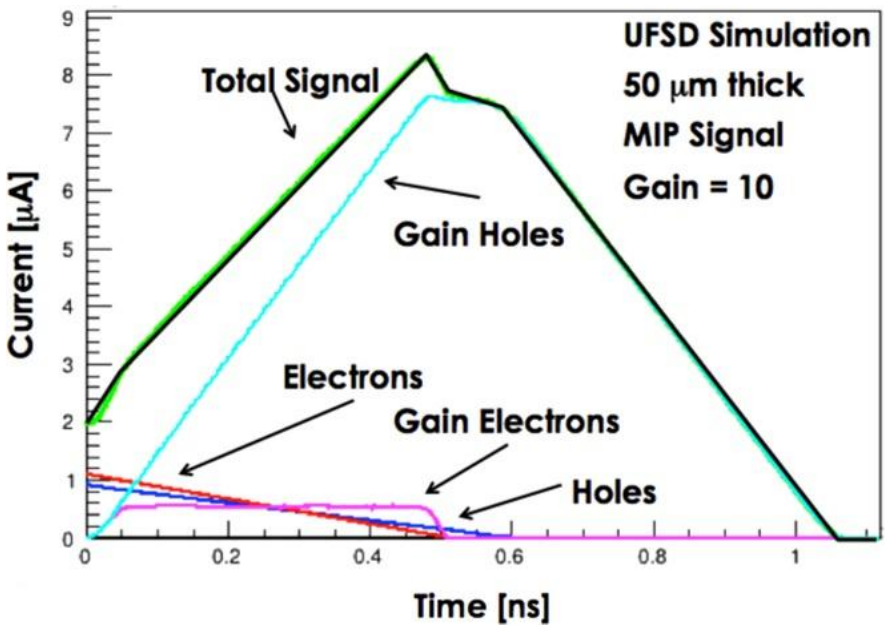

Electrons reaching the amplification region per unit time $n_{e-h} v_{sat} dt$

New charges generated per unit time $dN_{Gain} \propto n_{e-h} \left(v_{sat} dt\right) G$

$$di_{gain} = dN_{gain}\, qv \left(\frac{1}{d}\right) \propto \frac{G}{d} dt$$

$$I_{max} \propto N_{max} q \frac{1}{d} v_{sat} = \left(n_{e-h} dG\right) q \frac{1}{d} v_{sat} = n_{e-h} G q v_{sat}$$

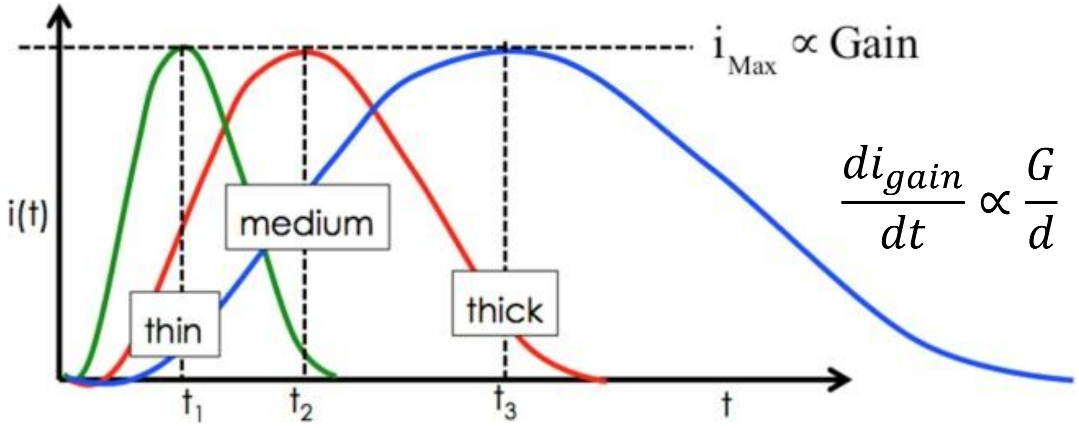

$$\frac{di_{gain}}{dt} \propto \frac{G}{d}$$

Hartmut F-W Sadrozinski et al 2018 Rep. Prog. Phys. 81 026101

Why limiting the gain?

Hartmut F-W Sadrozinski et al 2018 Rep. Prog. Phys. 81 026101

- Don't want to lose proportionality to released charge (SiPM like)
- Can't generate too intense fields. Only electrons should be amplified -> lower Gain
- At higher gain, the noise get dominate by the shot noise

$$i^2_{\mathrm{Shot}} = 2qI_{\mathrm{Det}} = 2q\left[I_{\mathrm{surface}} + \left(I_{\mathrm{Bulk}} + I_{\mathrm{Signal}}\right)G^2G^x\right]$$

$$G^x = Gk + \left(2 - \frac{1}{G}\right)(1-k)$$

- One of the effect of radiation is the increase of the bulk current

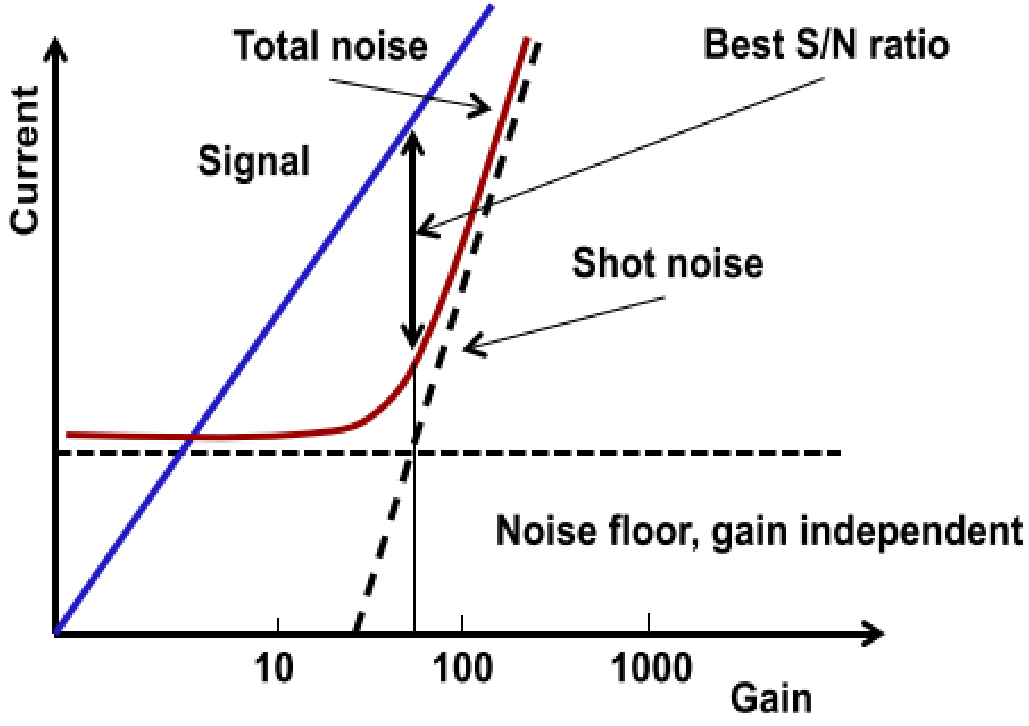

Usual gain ~10-50

Also thickness to be taken under control (parasitic capacitance!), minimum d ~30-50 μm

Performance(1)

Surface [mm^2]	Capacitance [pF]	HV [V]	Time precision [ps]
1.8	3.1	180	32
2.2	4.4	180	33
3.0	6.0	180	38
7.0	14	180	57
14	28	180	102
2.2	4.4	140	49
2.2	4.4	160	41
2.2	4.4	180	33

- Tested @ CERN SPS (180 GeV 180 GeV μ/π beam)
- Biasing voltage 180V
- Thickness 50 μm
- Readout with oscilloscope (2GHz, 20 GSa/s) + offline CFD 30%
- Reference: MCP (40ps res. on MIP)

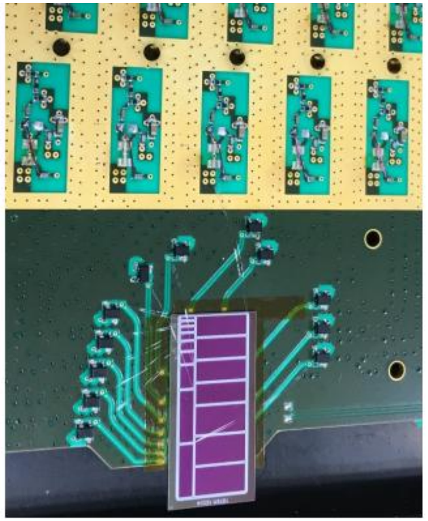

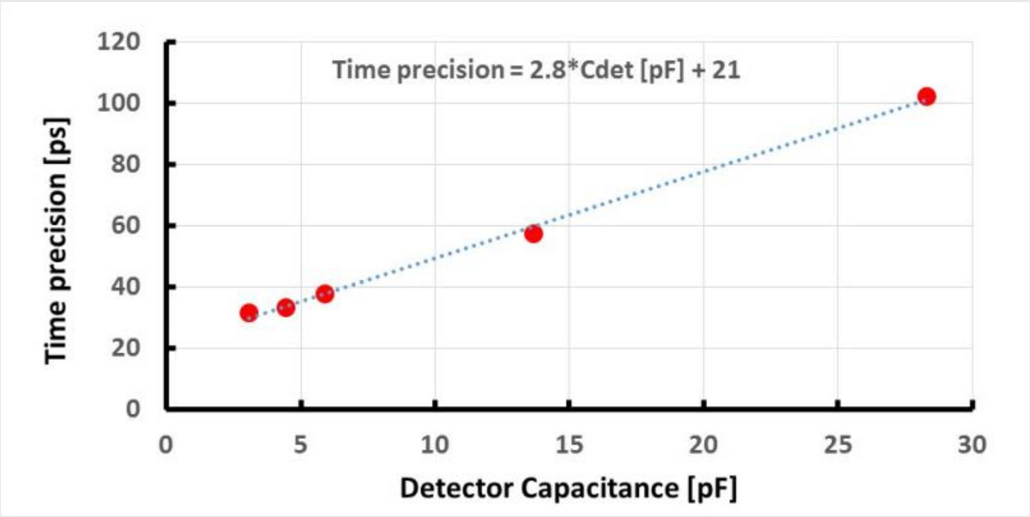

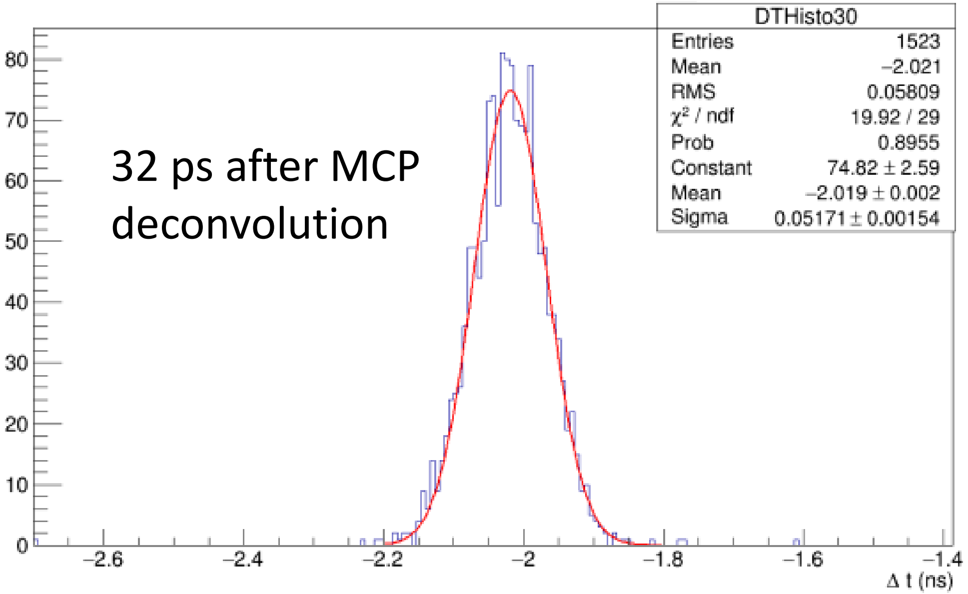

M. Berretti et al. 2017 *JINST* 12 P03024

Performance (3)

Latest R&D for the ALICE experiments: test on thin double-LGAD (same concept of double diamond)

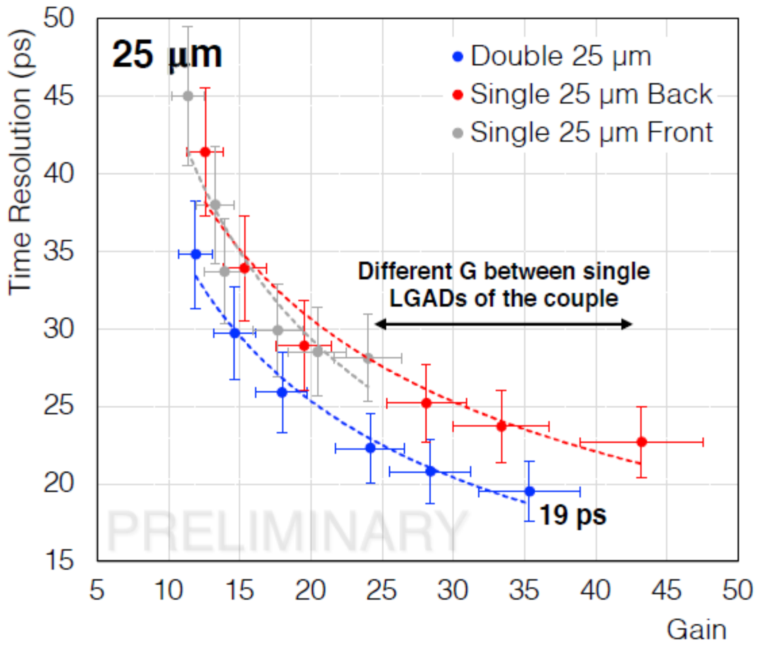

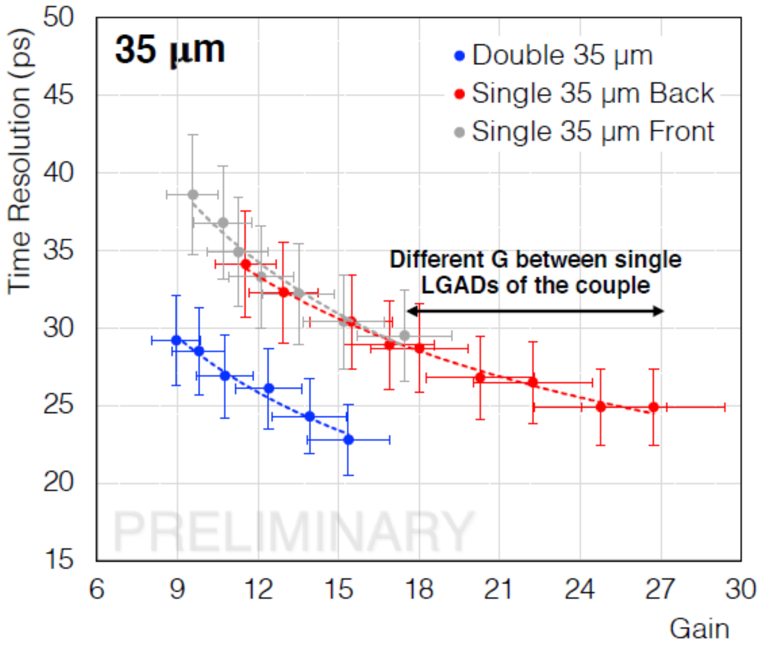

S. Strazzi, FAST 2023 Workshop

Pad area of 1 mm^2

- Tested @ CERN PS (10 GeV $\mu/\pi\,/p$ beam)
- Biasing voltage 170-240V
- Amplification with dedicated hybrid board amplifier
- Readout with oscilloscope (4GHz, 20 GSa/s) + offline CFD
- Reference: similar sensors

For LGAD the gain is not as much as for diamond(~15 & 24%) -> non negligible contribution of the detector to the noise!!
~no improvement from 35 to 25 µm (due to parasitic capacitance?)

Radiation damage

Radiation induces a reduction of the dopant concentration, reducing the effective gain of the sensor.

➡ Performance recovery by changing the biasing voltage.

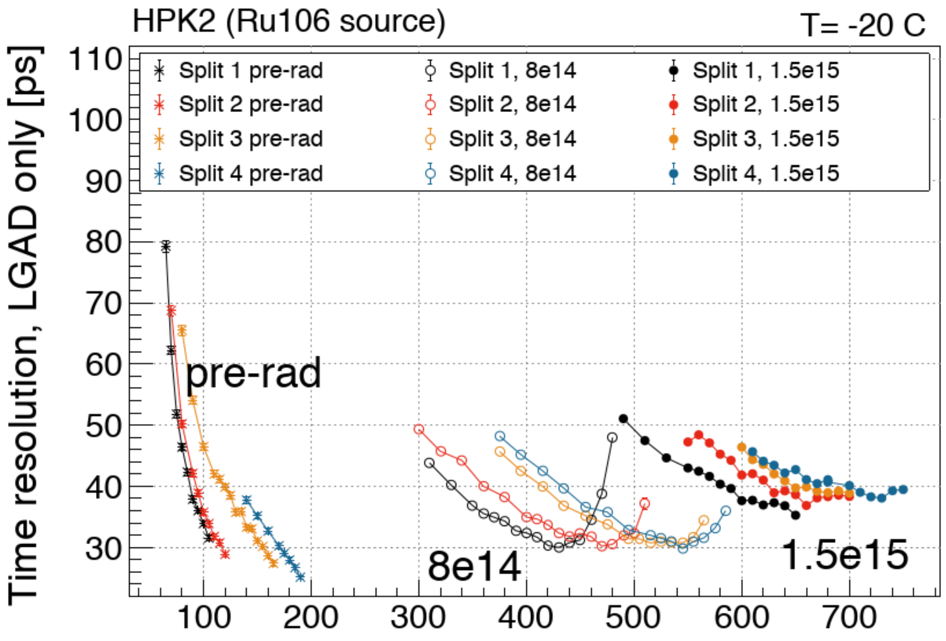

R. Heller, 38th RD50 Workshop (2021)

They represent the choice for large scale timing system in several experiment.
But radiation hardness still a concern.

Doping material can affect the radiation hardness. Boron+Carbon best choice in recent test

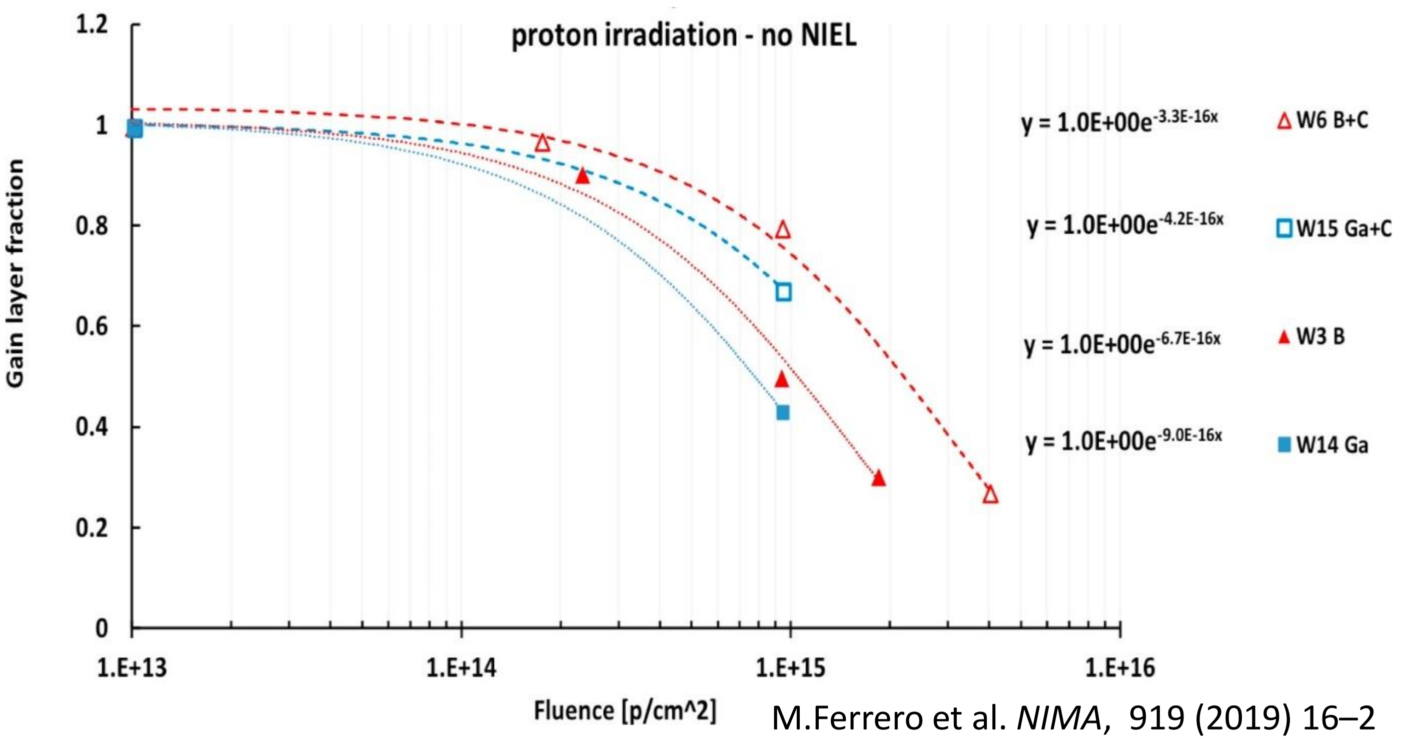

M.Ferrero et al. *NIMA*, 919 (2019) 16–2

Radiation damage: death

Recently observed highly ionizing particle catastrophic single event damages on irradiated LGAD.

For electric fields above 11 V/µm, thin silicon sensors undergo fatal death once exposed to particle beams → Single-Event Burnout

Exact reason under investigation

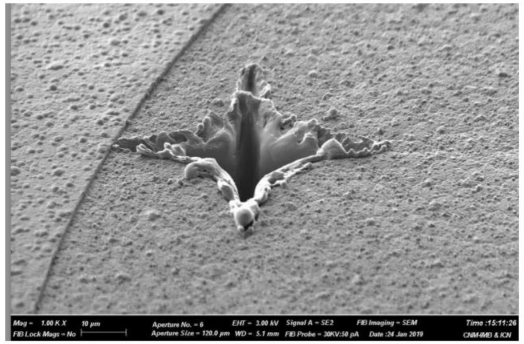

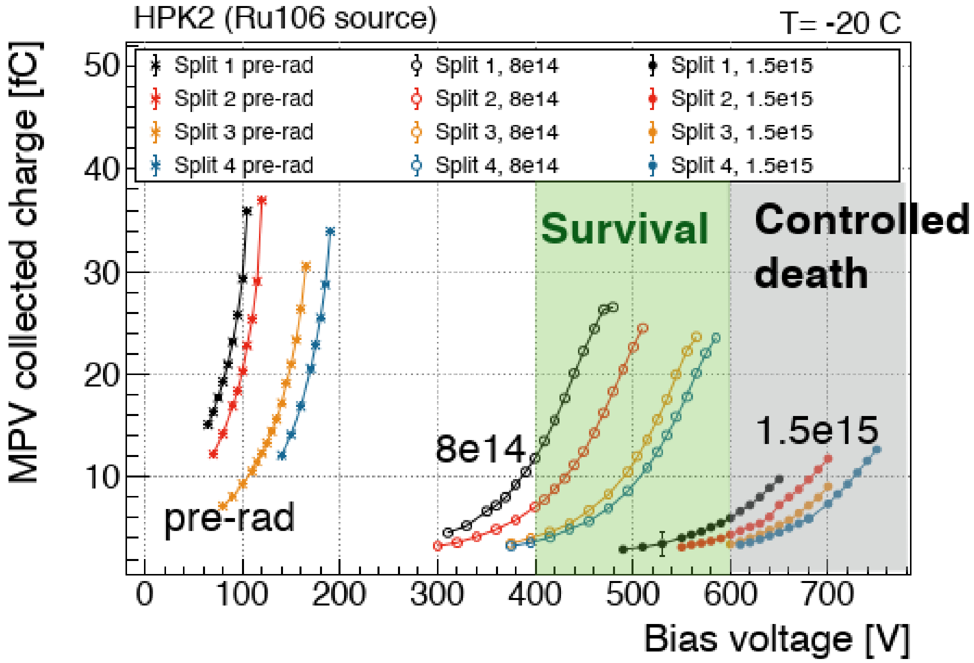

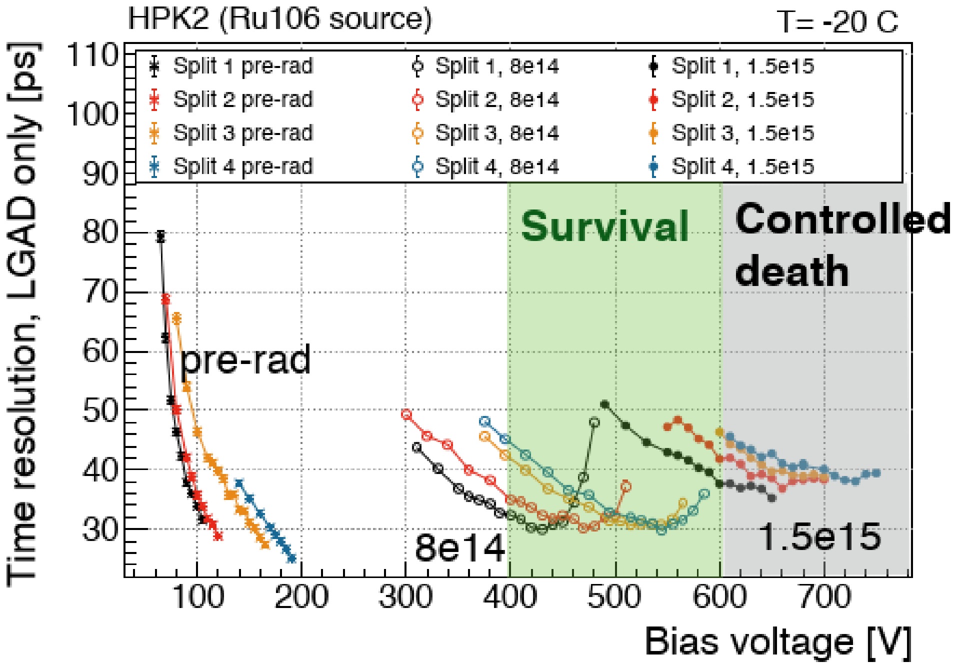

R. Heller, 38th RD50 Workshop (2021)

SILICON (3D)

Silicon 3D

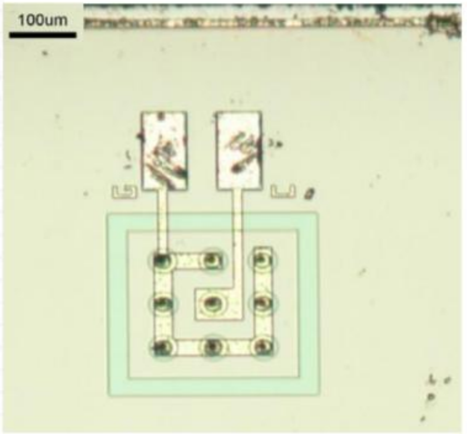

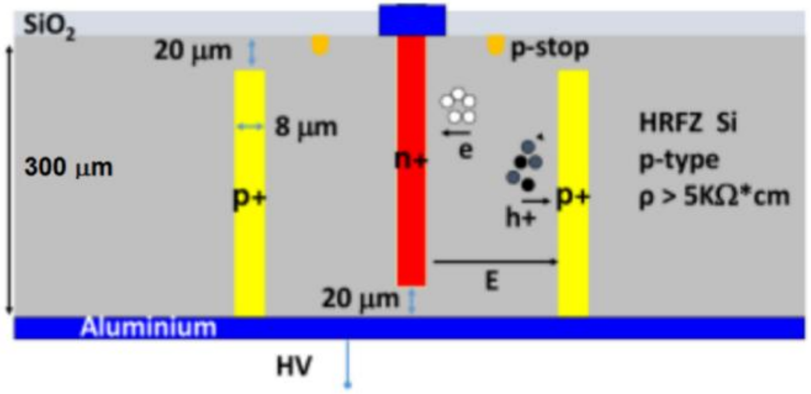

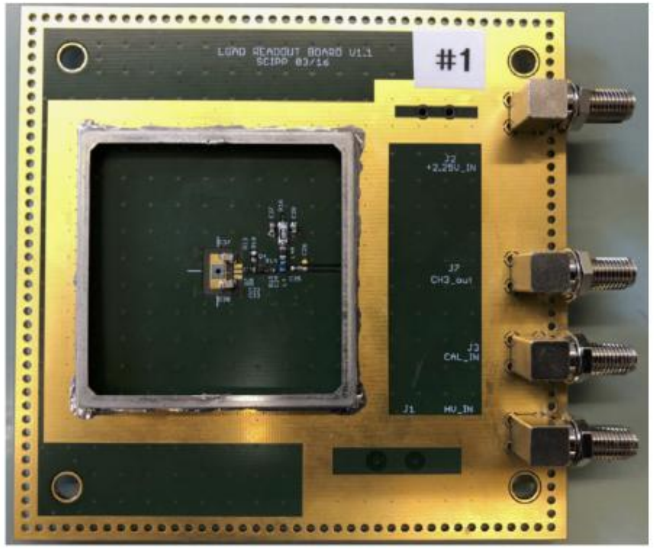

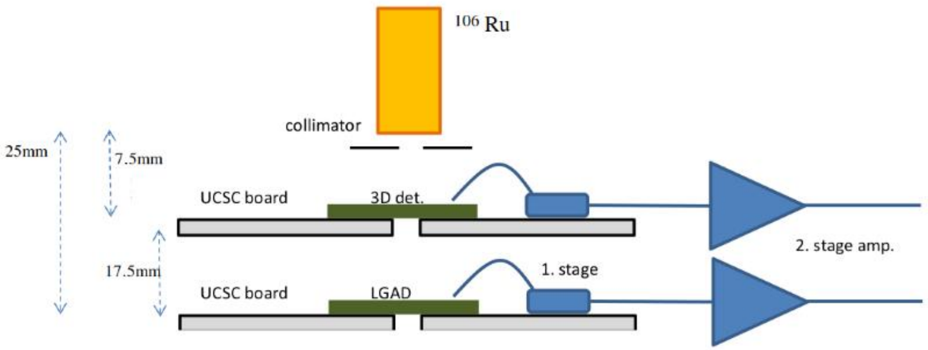

Recent study of 3D sensor timing performance before and after irradiation:

- Single cell 3D with dedicated amplifier
- Readout by scope + offline CFD
- Reference: LGAD with 30-35ps resolution
- Climatic chamber
- Tested with ^{106}Ru (few MeV electrons)

C.Betancourt et al, *Instruments* **2022**, *6*(1), 12

Silicon 3D

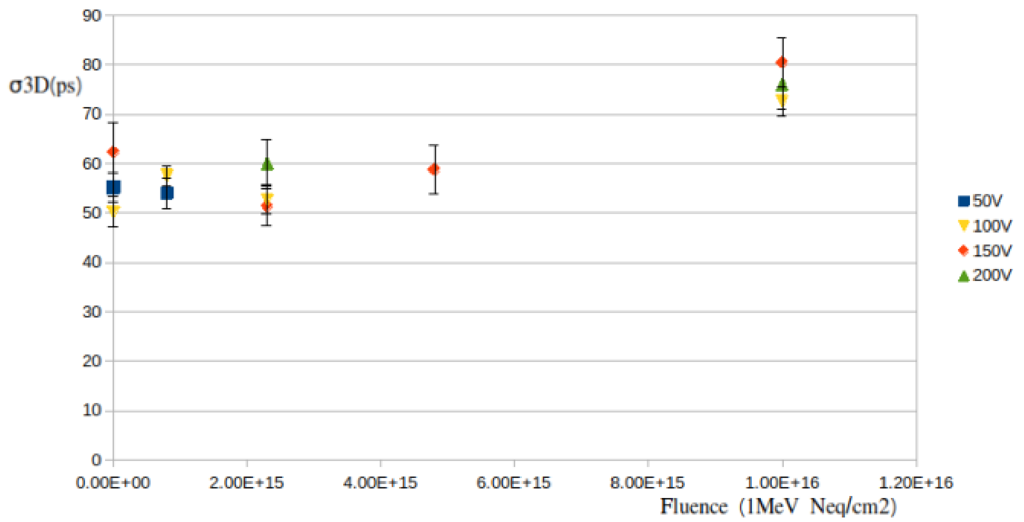

+20 ° C	σ_{3D} (ps)	σ_{wf} (ps)	σ_j (ps)
not irradiated	62 ± 6	55 ± 6	29 ± 5
2.3×10^{15} n_{eq}	51 ± 4	43 ± 3	28 ± 5
4.8×10^{15} n_{eq}	59 ± 5	53 ± 3	26 ± 5
1.0×10^{16} n_{eq}	80 ± 5	68 ± 2	22 ± 4
−20 °C	σ_{3D} (ps)	σ_{wf} (ps)	σ_j (ps)
not irradiated	52 ± 6	43 ± 6	29 ± 4
2.3×10^{15} n_{eq}	33 ± 2	24 ± 3	22 ± 5
4.8×10^{15} n_{eq}	47 ± 2	40 ± 3	26 ± 5
1.0×10^{16} n_{eq}	45 ± 2	40 ± 2	20 ± 4

C.Betancourt et al, *Instruments* **2022**, *6*(1), 12

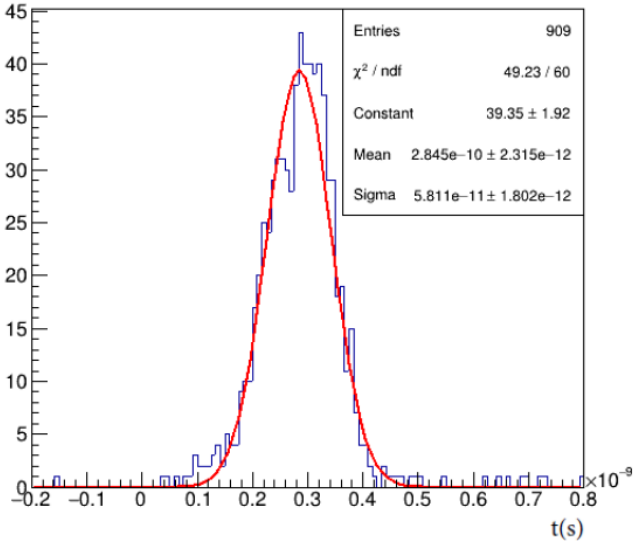

Distribution of ΔT in the configuration 3D-LGAD with the 3D detector irradiated at a fluence of $\sim 10^{16}$p/cm^2(!!!), at a temperature of −20 °C for a bias voltage of 150 V

Given the particular setup (1 sample, single channel, source), results quite far from LGAD, but radiation hardness very good!

Towards 3D for timing

What we like in 3D architecture:

- ✓ Radiation hardness
- ✓ Low bias voltage (depletion @ ~10V, velocity saturation @ ~100V)
- ✓ Mitigation of local landau fluctuation
- ✓ Very fast charge collection (< 500ps)
- ✓ Fine segmentation for 4D (cell of ~50x50 μm^2)

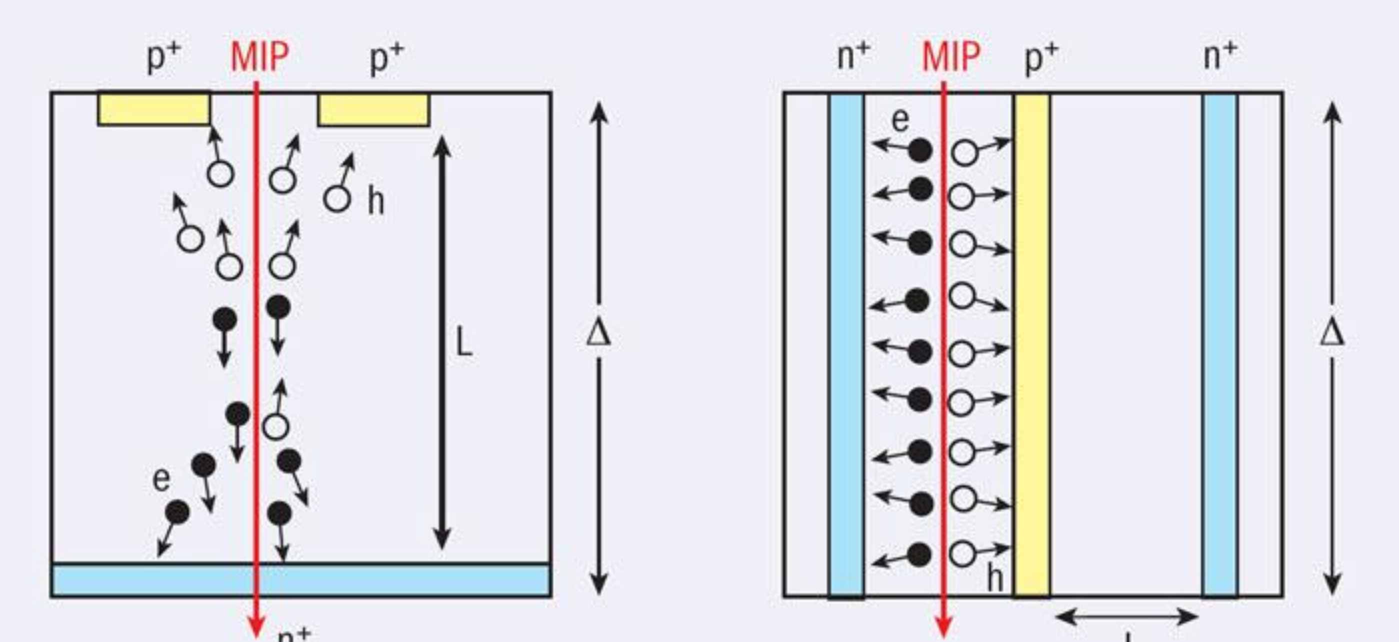

From CERN Courier

What we DON'T like in 3D architecture:

- ✓ Fabrication complexity and cost
- ✓ Inefficiency in the region of the electrode
- ✓ <u>Non uniform electric field</u>

→ Large effort to create a different architecture, compatible with the actual available production process

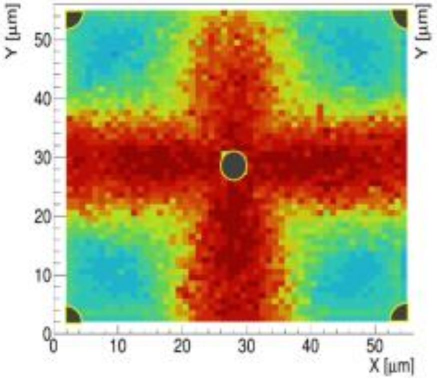

TimeSpot 3D timing sensor

Replace circular electrode with tranches: generation of a very uniform electric field

Drawback is the increase of insensitive area.
Can be mitigated using staggered double layer or putting the detector at some angle w.r.t. the beam.

With the geometry on the right:

- ➢ Charge collection time < 400 ps
- ➢ Full depletion @ ~20V
- ➢ Velocity saturation @ ~40V!

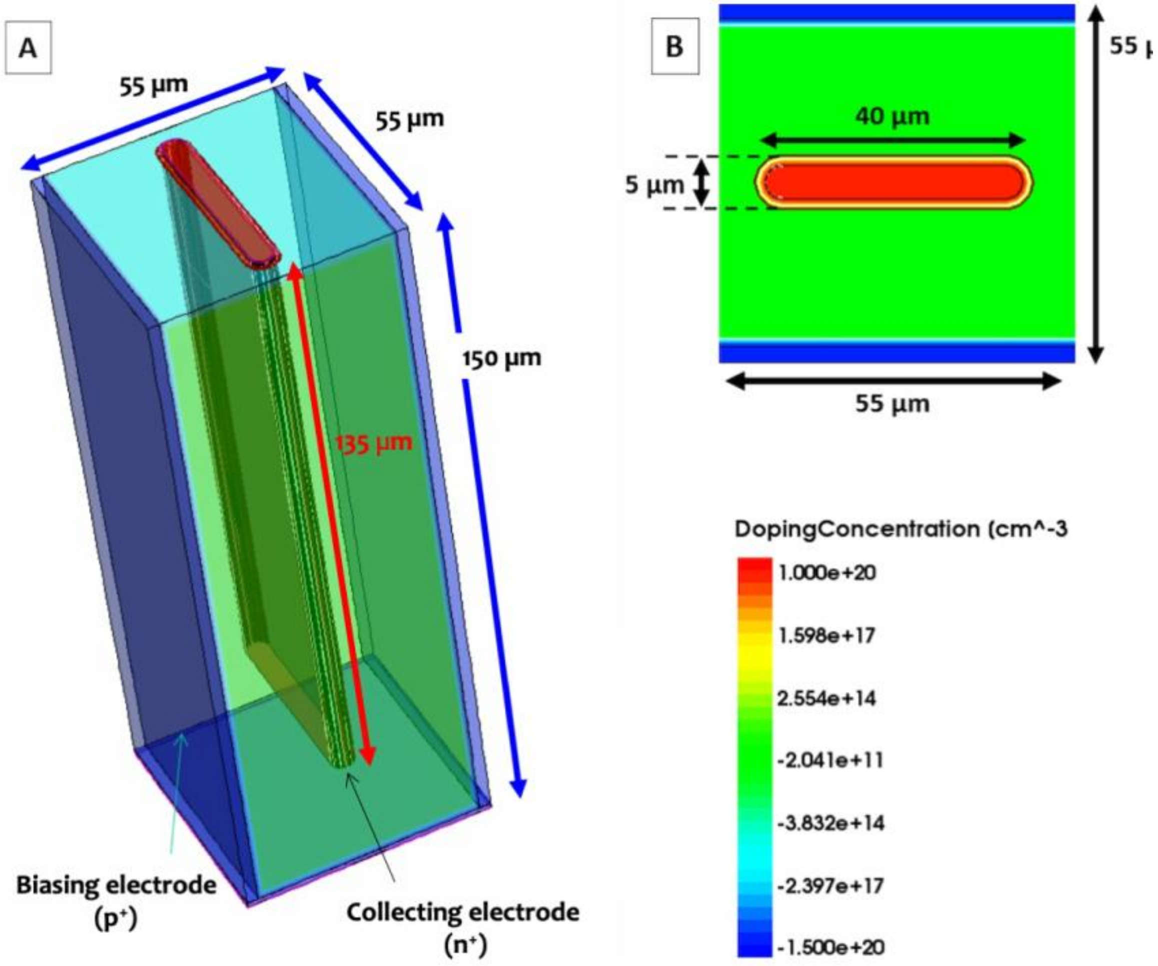

L. Anderlini *et al*, *JINST*, 15 (2020) P09029

Field simulation

L. Anderlini *et al*, *JINST*, 15 (2020) P09029

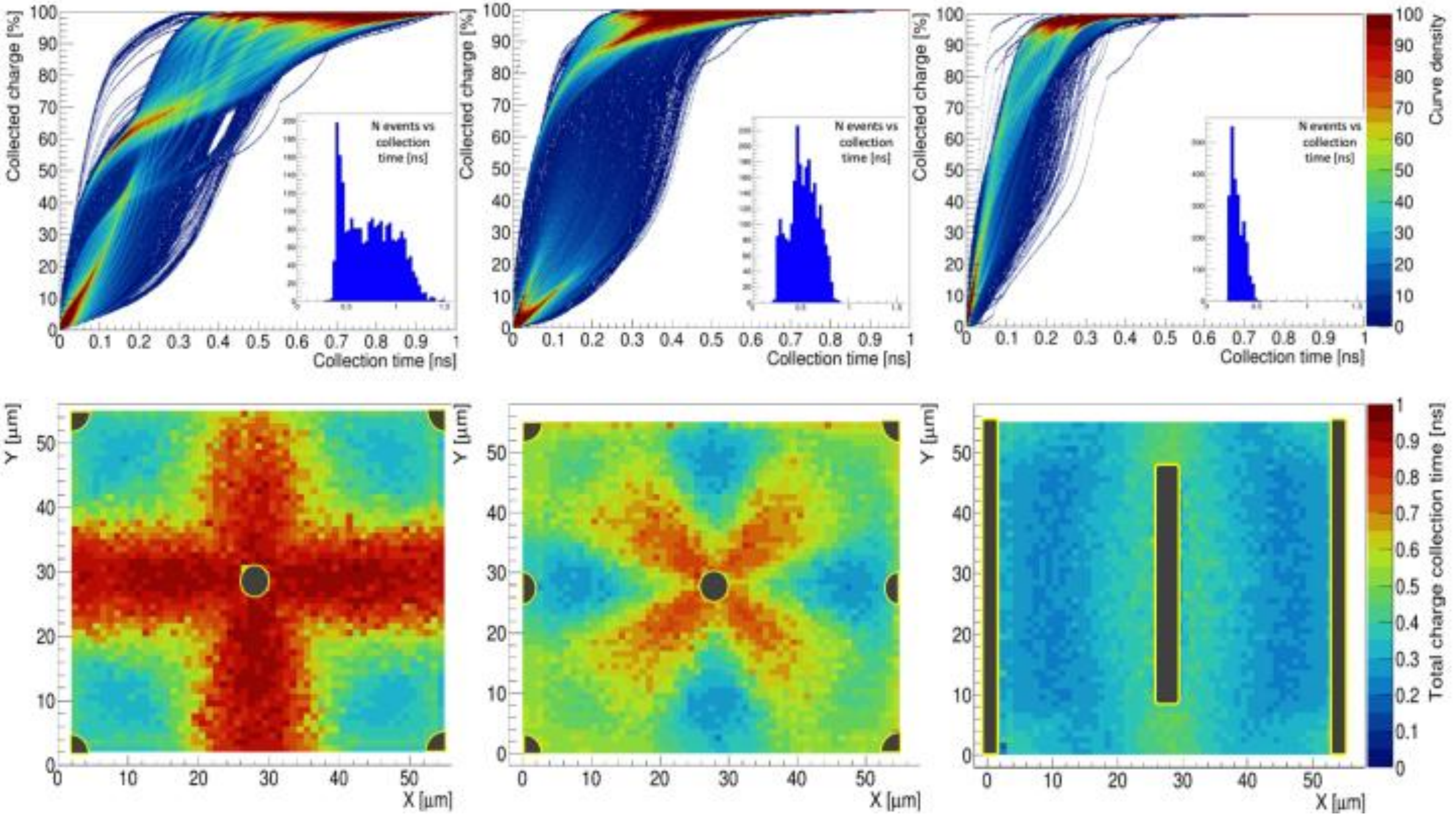

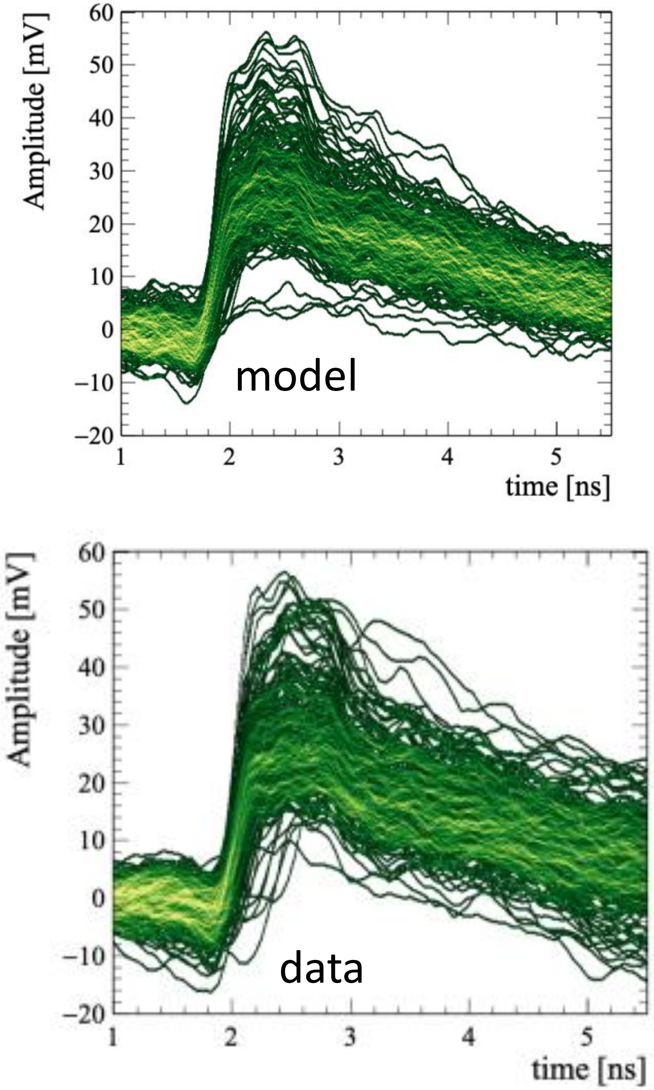

L. Brundu *et al*, arXiv:2106.08191v1

Performance

- Tested @ PSI πPM1 line (270 MeV π^+, 5-10% more w.r.t. MIP)
- Biasing voltage 50-150V
- Custom amplification + Readout oscilloscope (2GHz, 20 GSa/s)
- Different methods exploited to define T
- Reference: two MCP with Cherenkov radiator (12.5ps global resolution on MIP)
- Structure: double cell (one channel)

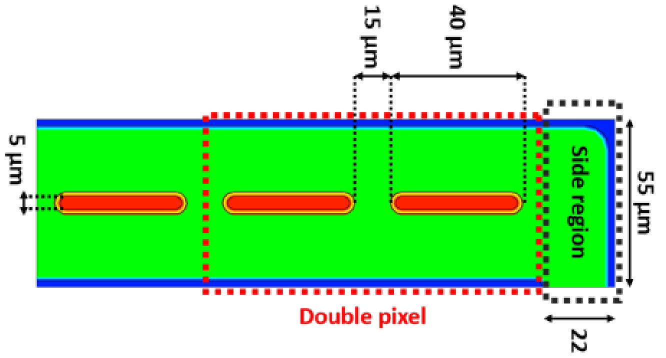

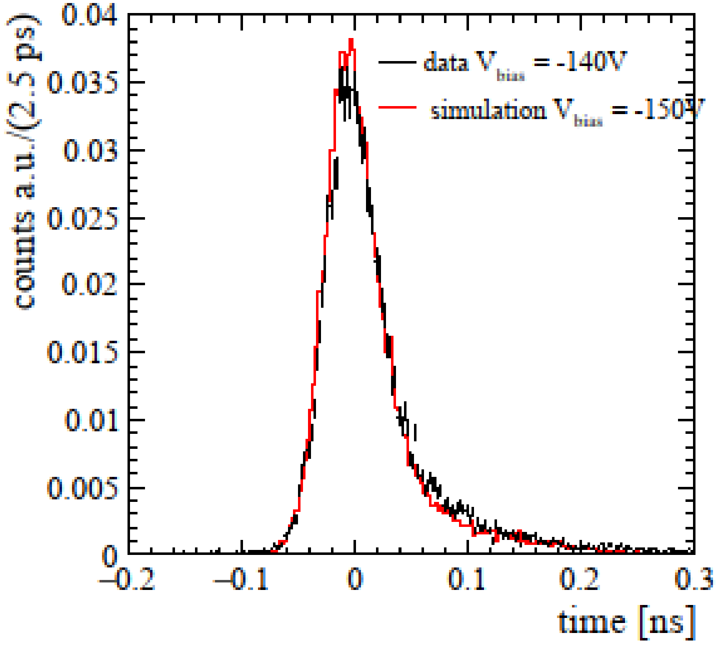

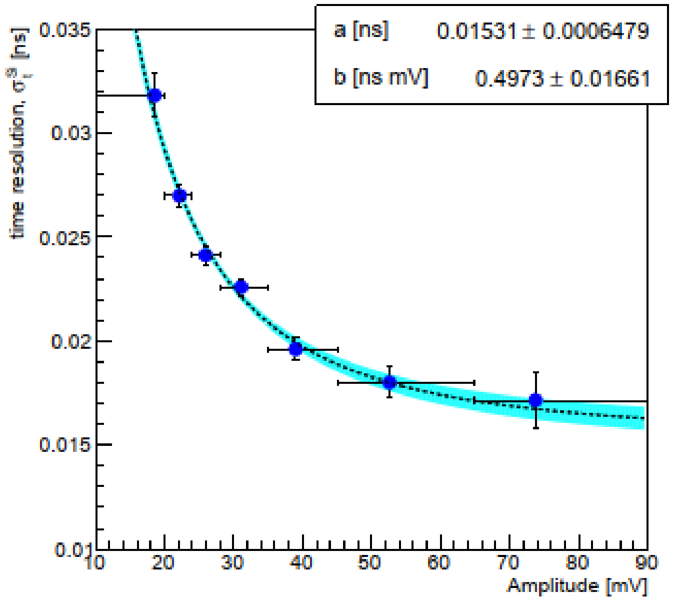

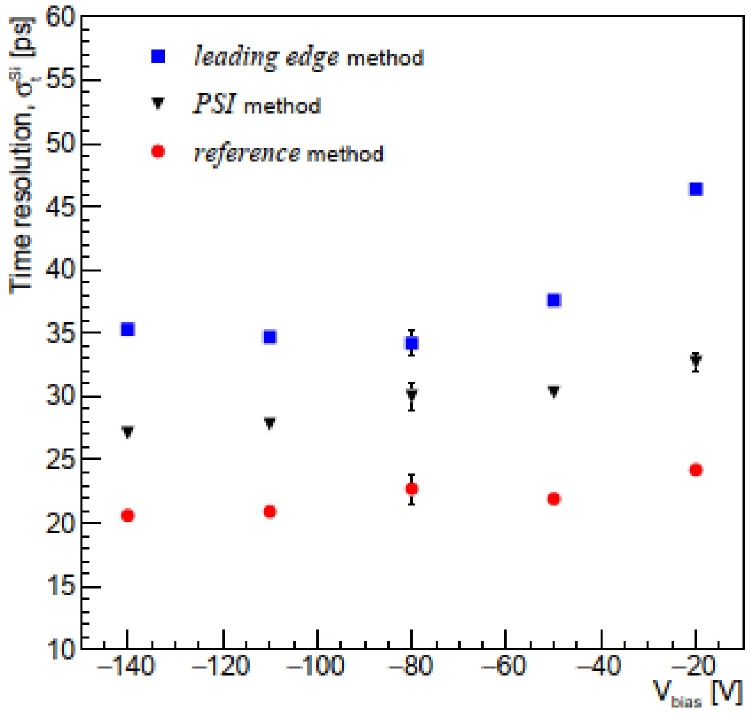

L. Anderlini *et al*, *JINST*, 15 (2020) P09029

Performance

- Tested @ PSI πPM1 line (270 MeV π^+, 5-10% more w.r.t. MIP)
- Biasing voltage 50-150V
- Custom amplification + Readout oscilloscope (2GHz, 20 GSa/s)
- Different methods exploited to define T
- Reference: two MCP with Cherenkov radiator (12.5ps global resolution on MIP)
- Structure: double cell (single channel)

setting	method								
	reference				*PSI*				*leading edge*
V_{bias} [V]	S/N	N [mV]	dV/dt [mV/ps]	σ_t^{Si} [ps]	S/N	N [mV]	dV/dt [mV/ps]	σ_t^{Si} [ps]	σ_t^{Si} [ps]
−20	12.2	2.22	0.097	24.2 ± 0.5	14.8	2.13	0.070	32.7 ± 0.7	46.4 ± 0.5
−50	13.0	2.24	0.114	21.9 ± 0.4	13.1	2.38	0.086	30.3 ± 0.4	37.6 ± 0.3
−80	13.3	2.26	0.121	22.7 ± 1.2	12.2	2.56	0.095	30.0 ± 1.1	34.2 ± 1.0
−110	13.6	2.26	0.125	20.9 ± 0.4	12.3	2.57	0.098	27.8 ± 0.4	34.7 ± 0.3
−140	13.9	2.25	0.128	20.6 ± 0.4	12.6	2.56	0.100	27.1 ± 0.4	35.3 ± 0.4

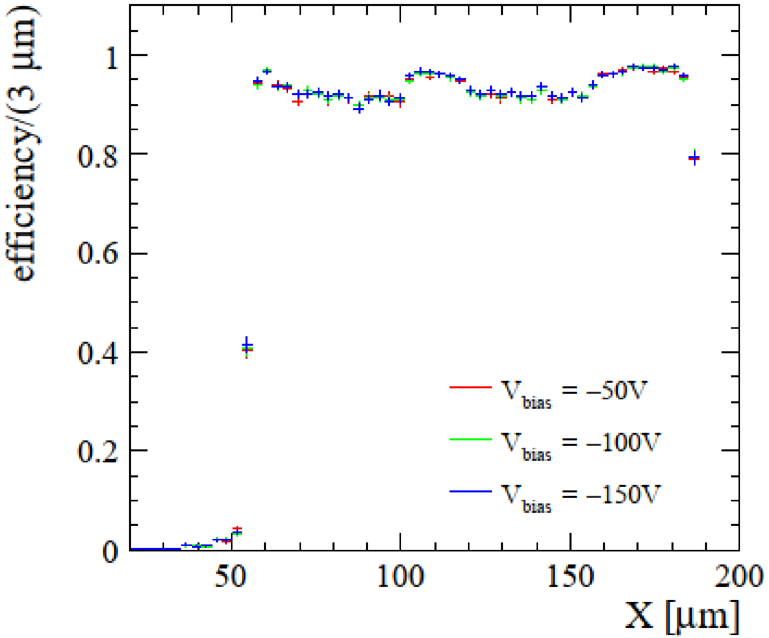

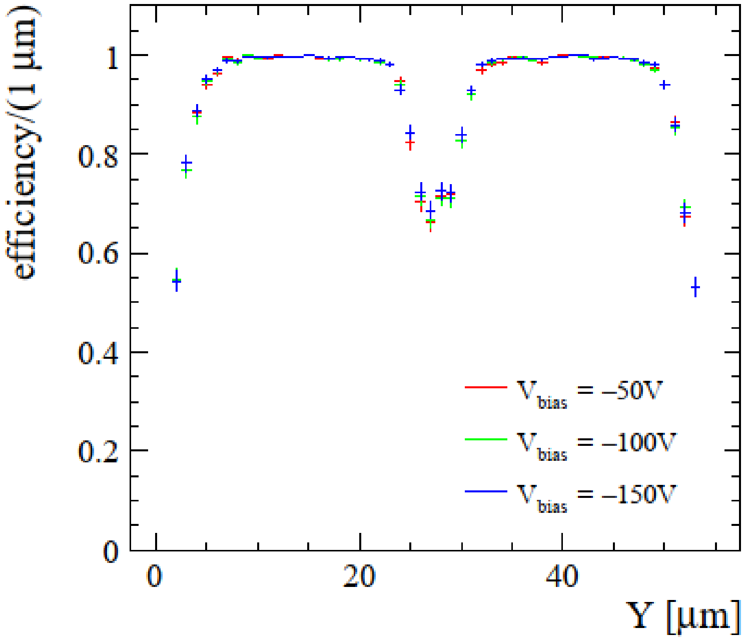

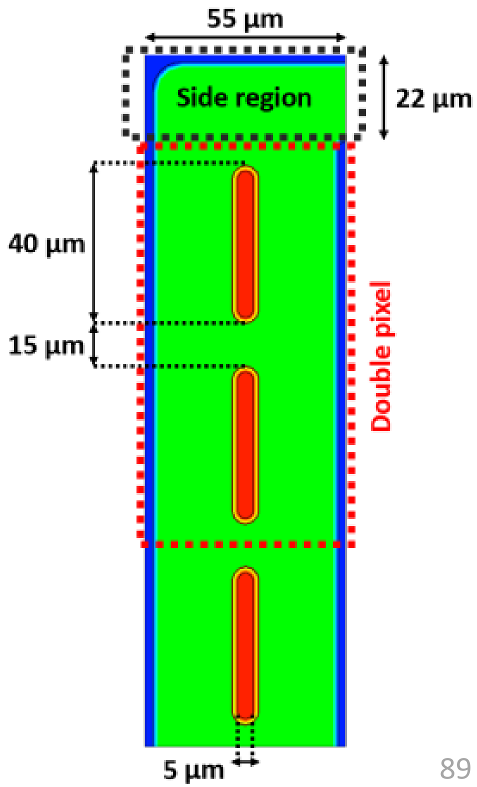

L. Anderlini *et al*, *JINST*, 15 (2020) P09029

CMOS MAPS

(Monolithic Active Pixel Sensors)

Optimization of CMOS

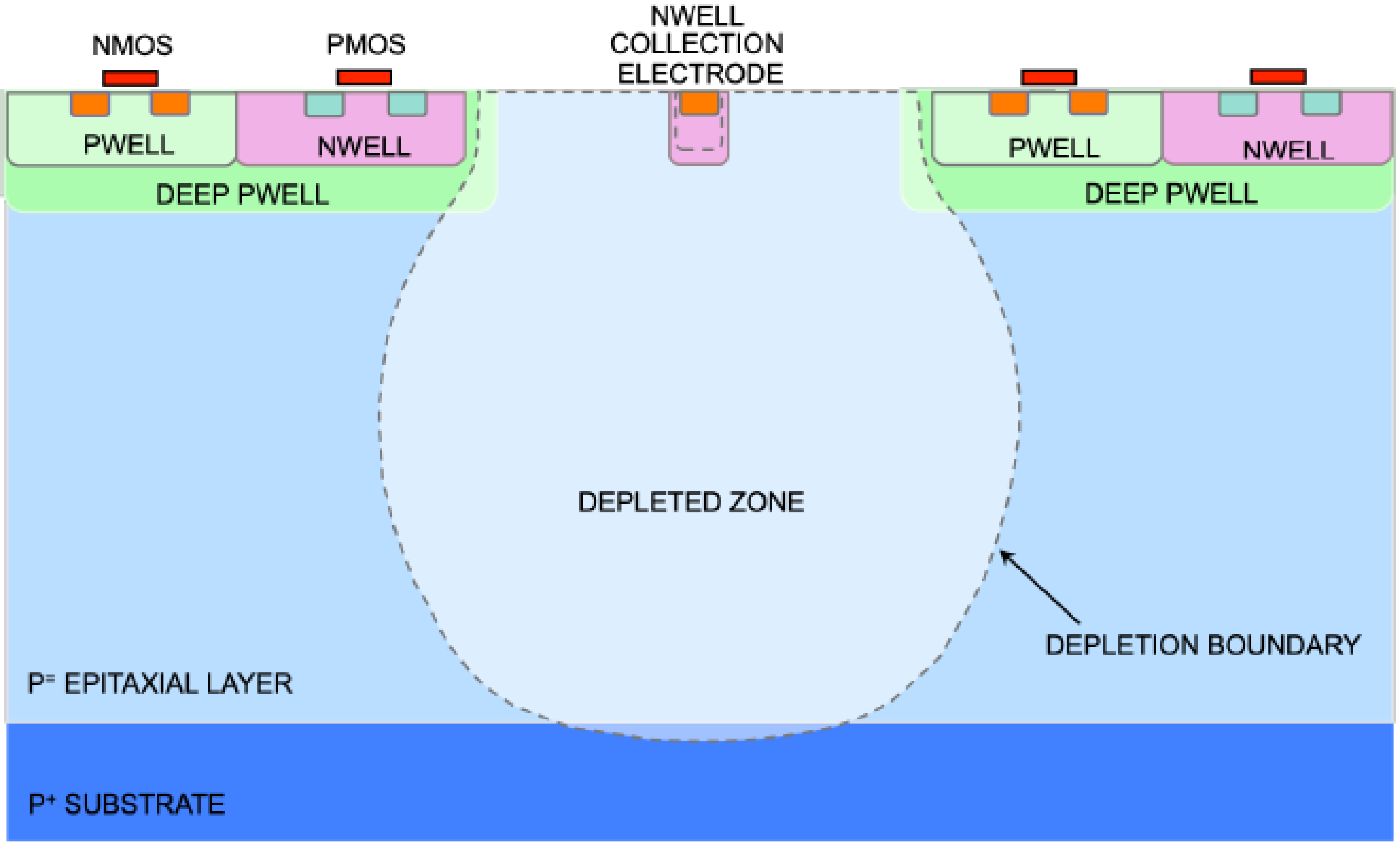

CMOS originally not suitable for timing due to the large variation in electric field and the long drift time of the charge.

Lots of improvement in the latest few years to make them more rad hard

MAPS CMOS sensor: Electronics and sensor on the same piece of silicon + standardized process

Optimization of CMOS

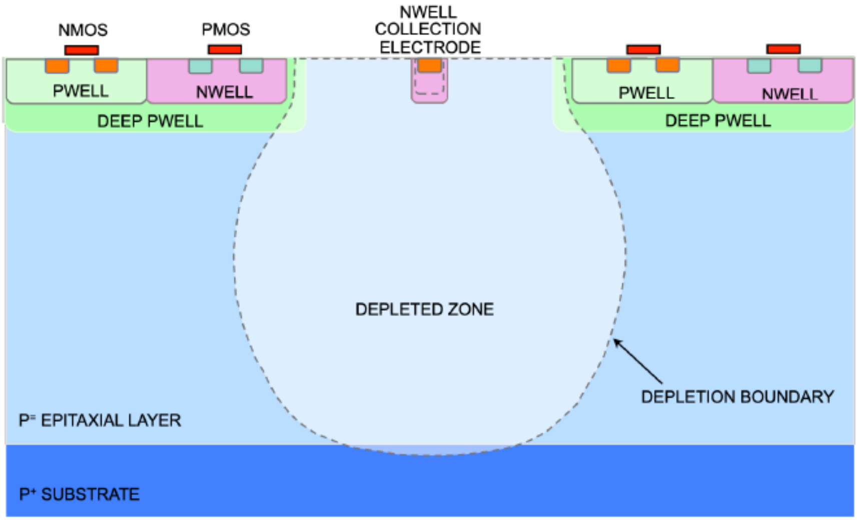

CMOS originally not suitable for timing due to the large variation in electric field and the long drift time of the charge.

Lots of improvement in the latest year to make them more rad hard

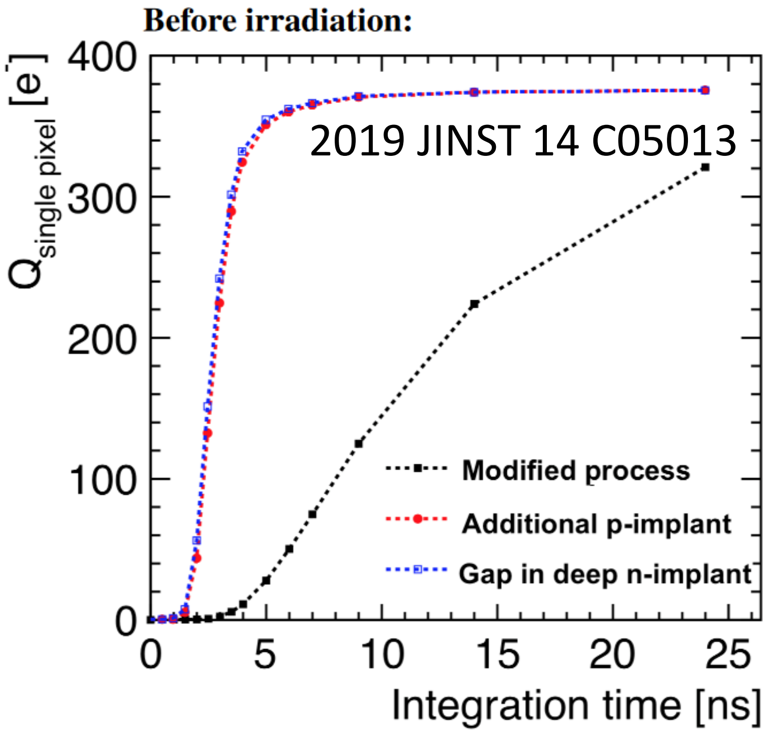

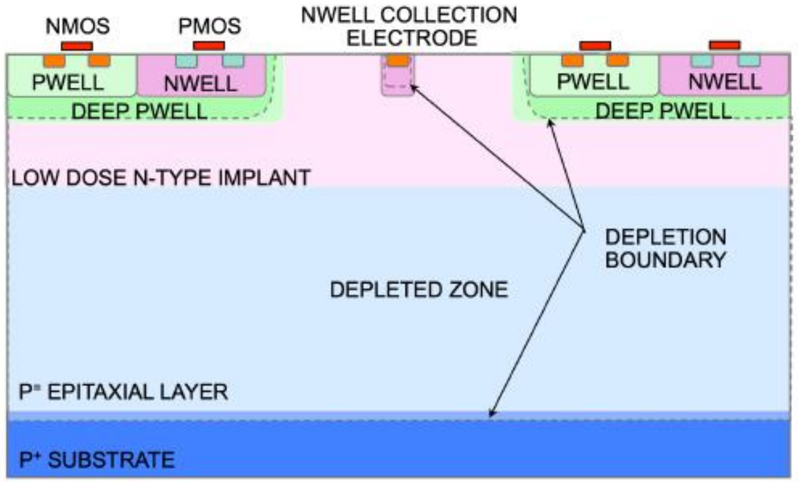

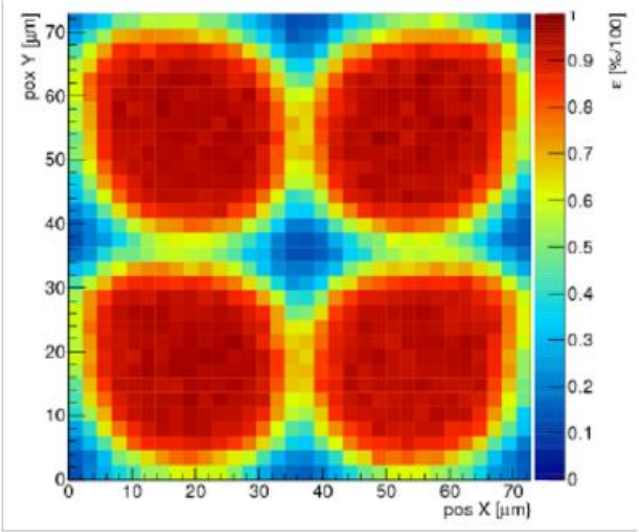

Still not efficient in the corner after an irradiation ~ 10^{15} $\mathrm{neq/cm^2}$

G. Aglieri Rinella et Al., PoS(Pixel2022)083

Timing performance (1)

G. Aglieri Rinella et Al., PoS(Pixel2022)083

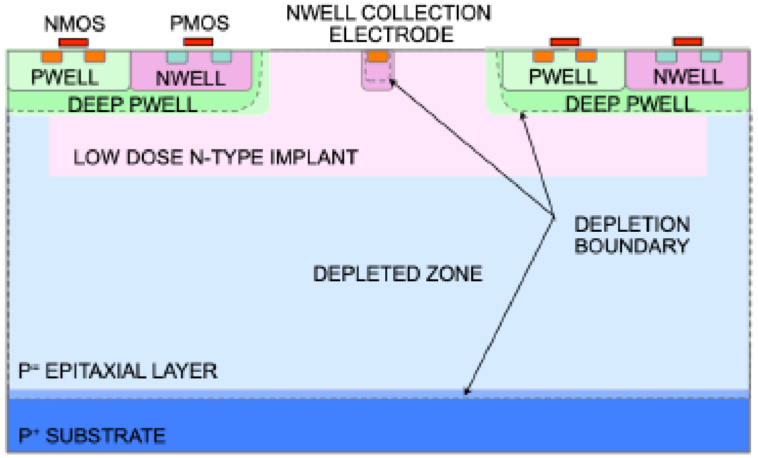

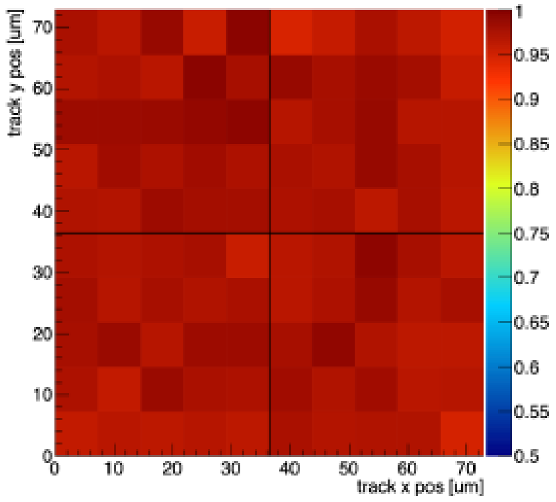

- SPS, 120 GeV
- only preamp integrated in the monolithic sensor,
- readout with oscilloscope,
- offline CFD 10%

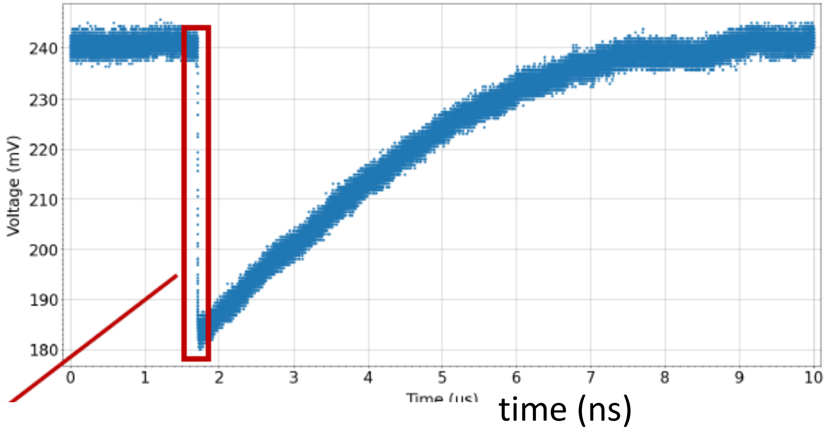

Fast rise time followed by long signal tail:
rate capability?

R. Russo, Fast 2023 Workshop

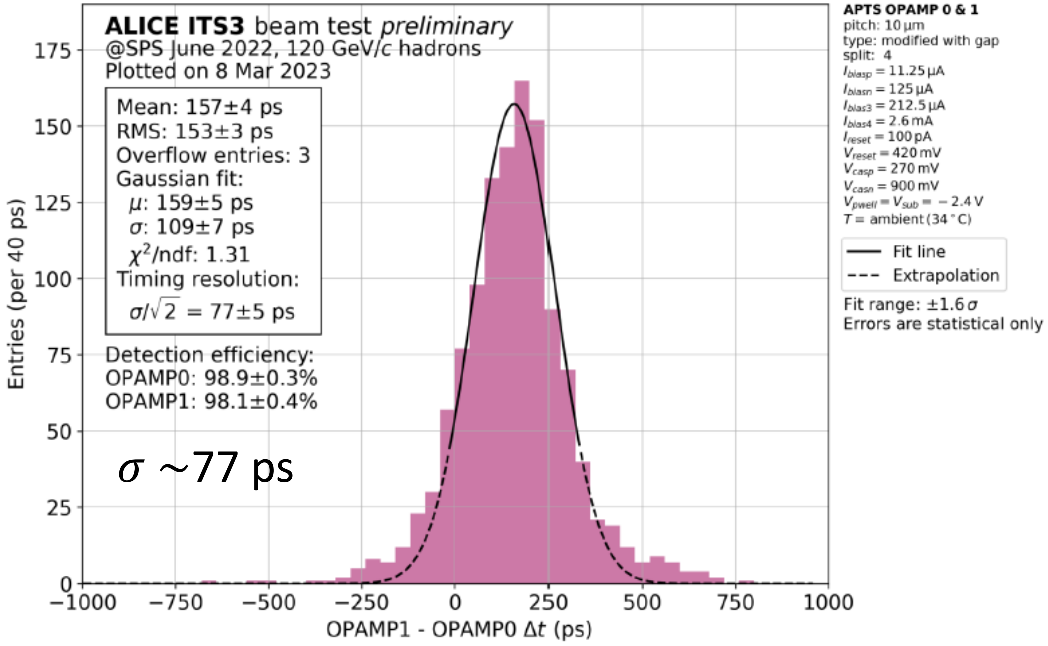

R. Russo, Fast 2023 Workshop

Timing performance (2)

MONOLITH Project - JINST 18 (2023) P03047

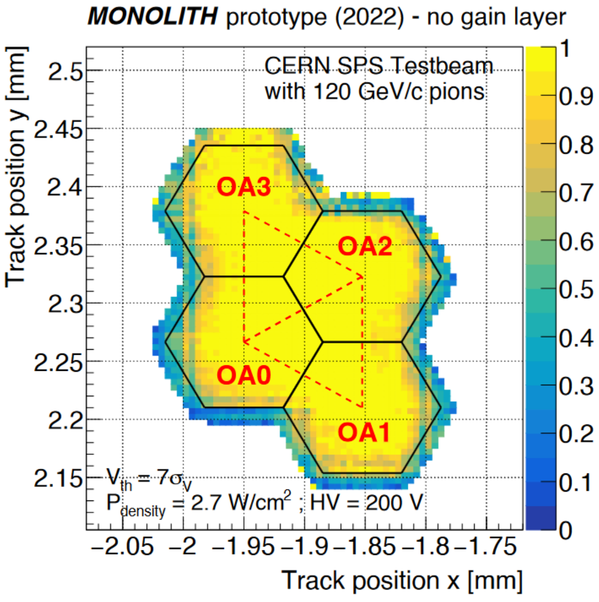

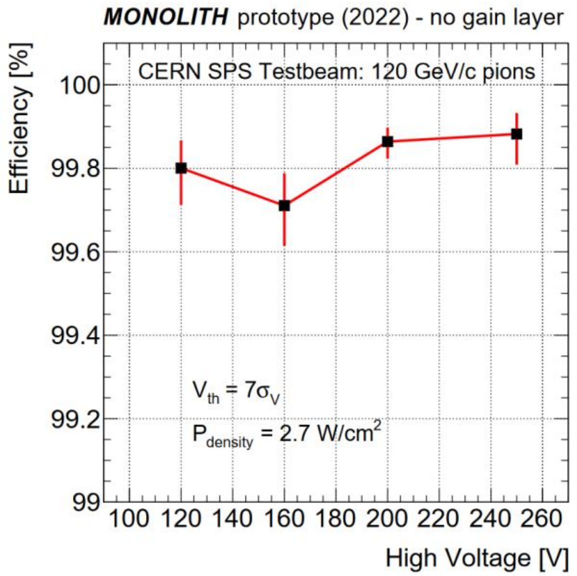

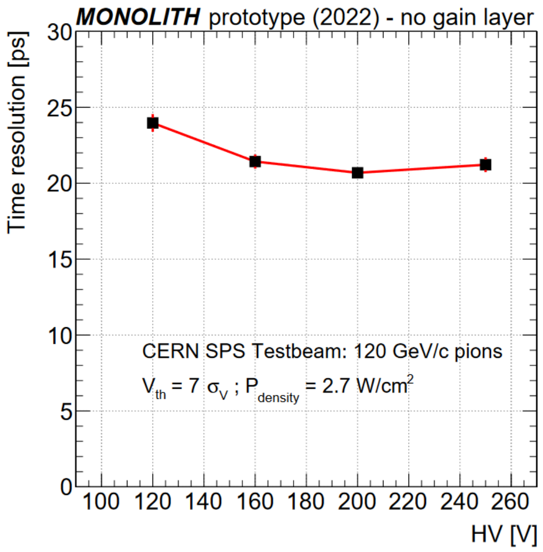

$$ENC_{series\ noise} \propto \sqrt{k_1 \frac{C_{tot}^2}{\beta} + k_2 R_b C_{tot}^2}$$

In custom SiGe BJT the doping can be adjusted to achieve:

- high current gain β
- reduced base resistance R

As for the diamonds, we are dealing with low charge -> need low noise amplification!

- SPS, 120 GeV
- **SiGe- BJT amplifier in common emitter configuration integrated in the monolithic sensor,**
- readout with oscilloscope,
- offline CFD
- 2 MCP as reference

GAS (MRPC/MICROMEGA)

RPC limitation

Innovative Detectors for Supercolliders

29 Sep 2003, 09:00 → 3 Oct 2003, 19:00 Europe/Zurich

Erice (Italy)

Nappi, E. / Seguinot, J.

- Time uncertainty generated by the position of the first cluster
- Very slow signal rise time (ion drift time ~5 cm/μs!, ~5 mm/ns for electrons)
- Severe rate limitation

Hard to improve:

- Large HV generate discharge
- Small gap generate inefficiency

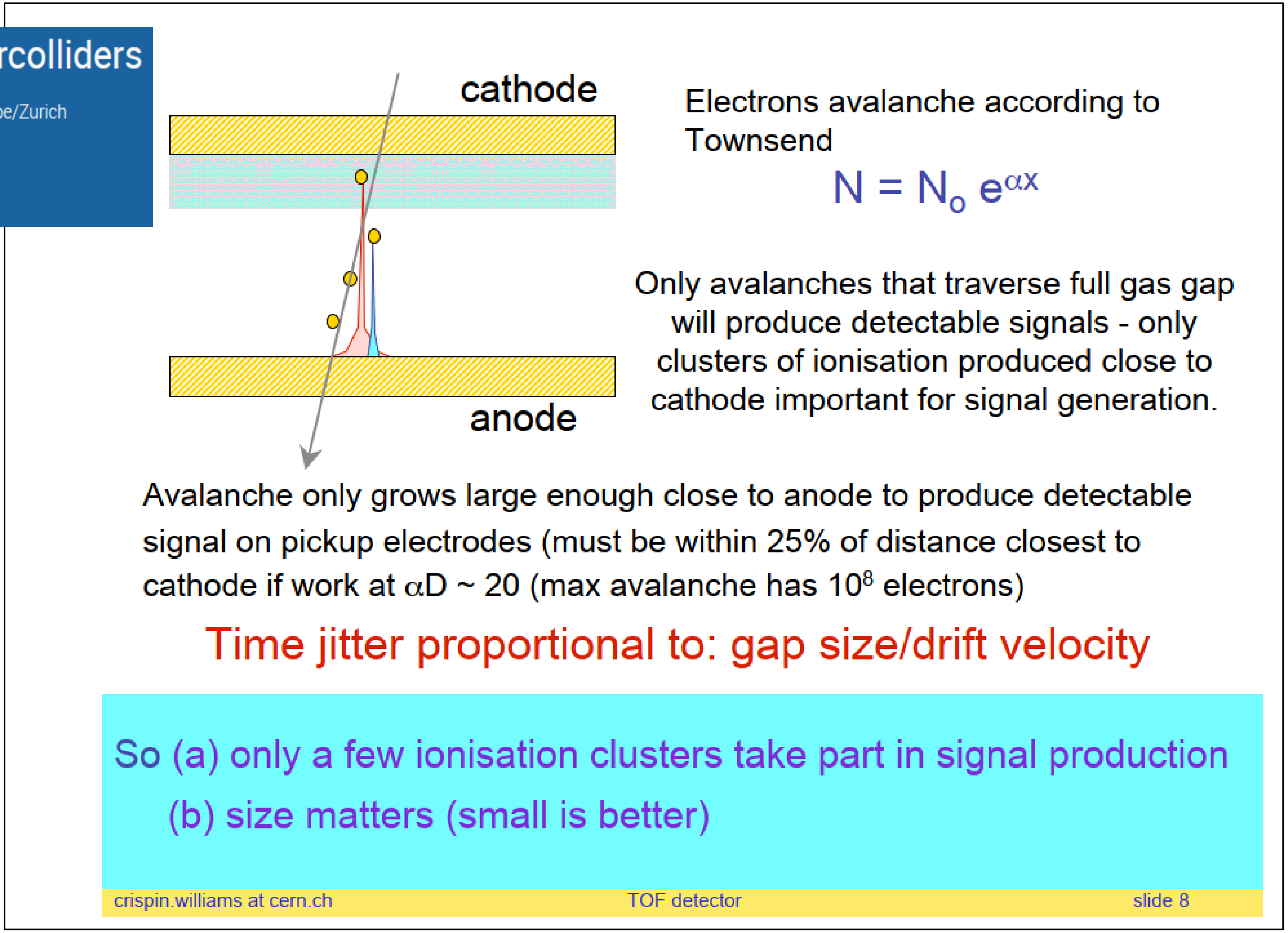

https://indico.cern.ch/event/415278/contributions/997124/attachments/848946/1183143/Williams.pdf

TIMING improvement

Gas detector at atmospheric pressure (Pestov at 12 atm) needs large gas gap to have high efficiency

Question: Can we increase gas gain such that avalanche produces detectable signal immediately?

(a) Need very high gas gain (immediate production of signal)

(b) Need way of stopping growth of avalanches (otherwise streamers/sparks will occur)

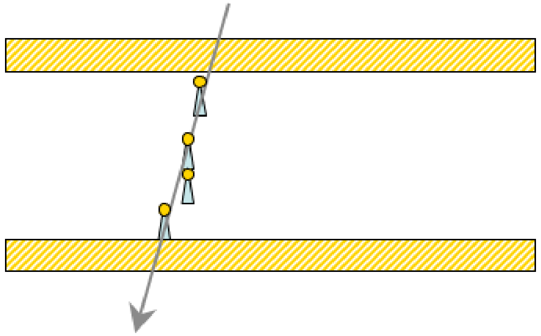

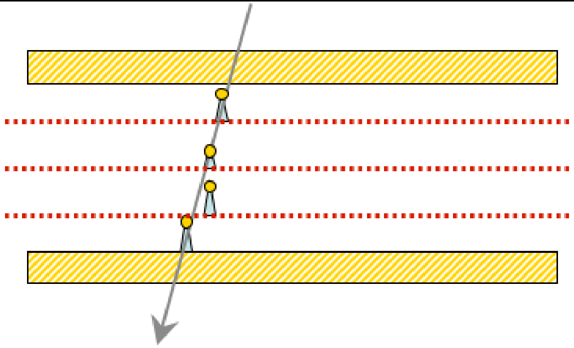

Answer: add boundaries that stop avalanche development. These boundaries must be invisible to the fast induced signal - external pickup electrodes sensitive to any of the avalanches

From this idea the Multigap Resistive Plate Chamber was born

crispin.williams at cern.ch TOF detector slide 10

https://indico.cern.ch/event/415278/contributions/997124/attachments/848946/1183143/Williams.pdf

MRPC

MULTIGAP RESISTIVE PLATE CHAMBER

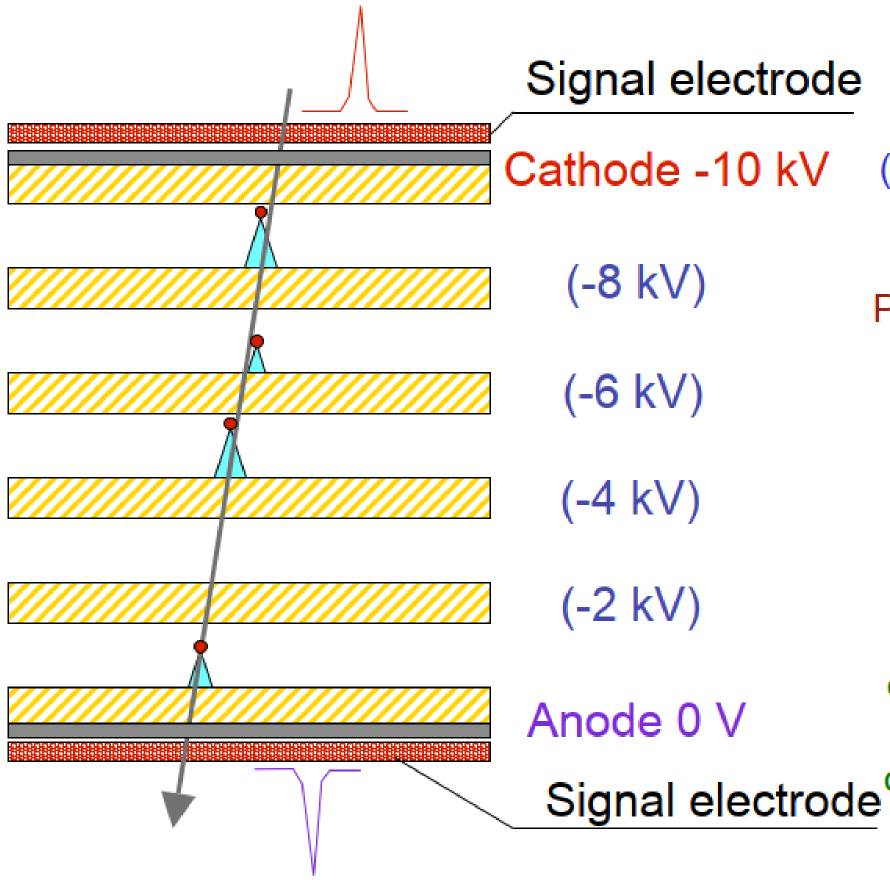

Stack of equally-spaced resistive plates with voltage applied to external surfaces (all internal plates electrically floating)

Pickup electrodes on external surfaces (resistive plates transparent to fast signal)

Internal plates take correct voltage - initially due to electrostatics but kept at correct voltage by flow of electrons and positive ions - feedback principle that dictates equal gain in all gas gaps

crispin.williams at cern.ch TOF detector slide 11

https://indico.cern.ch/event/415278/contributions/997124/attachments/848946/1183143/Williams.pdf

ALICE TOF MRPC

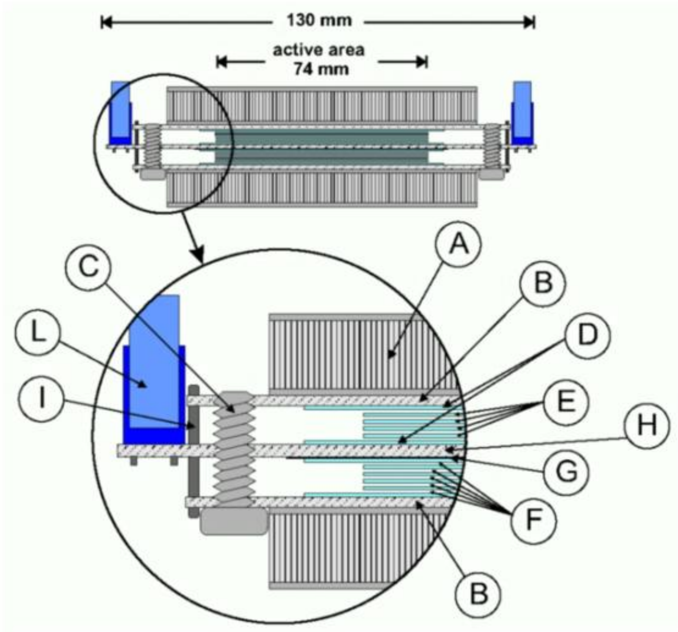

MRPC used by ALICE to instrument a large area TOF detector at LHC.

Operated in Run1 and Run2, upgraded for upcoming Run 3.

Double stack five-layer MRPC with 250um gaps

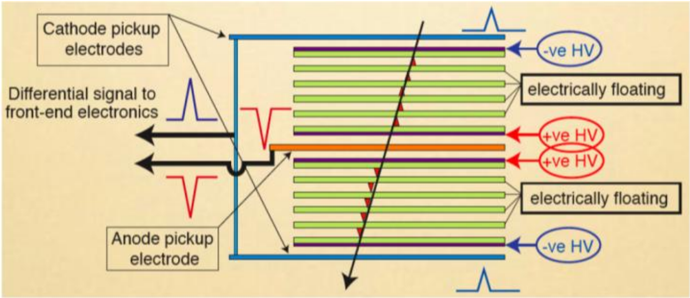

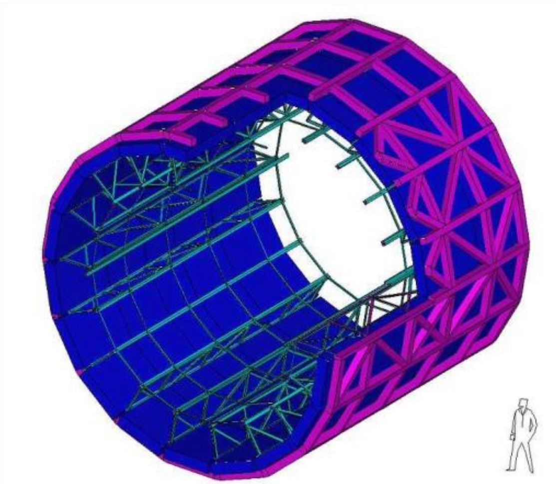

Readout: NINO + HPTDC

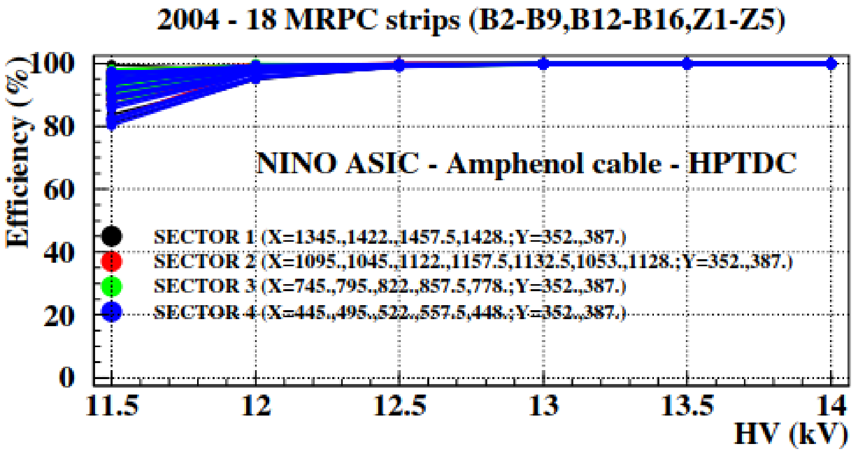

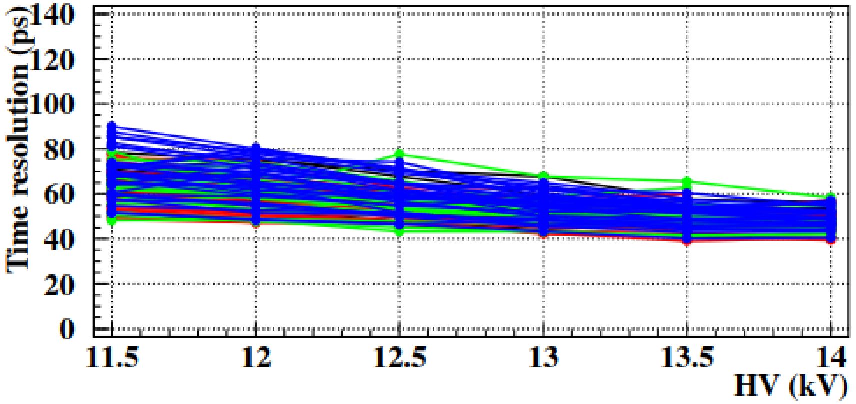

Test beam results @ at CERN PS (10 GeV μ/π/p beam)

Nuclear Physics B (Proc. Suppl.) 158 (2006) 60–66

ALICE TOF performance @ LHC

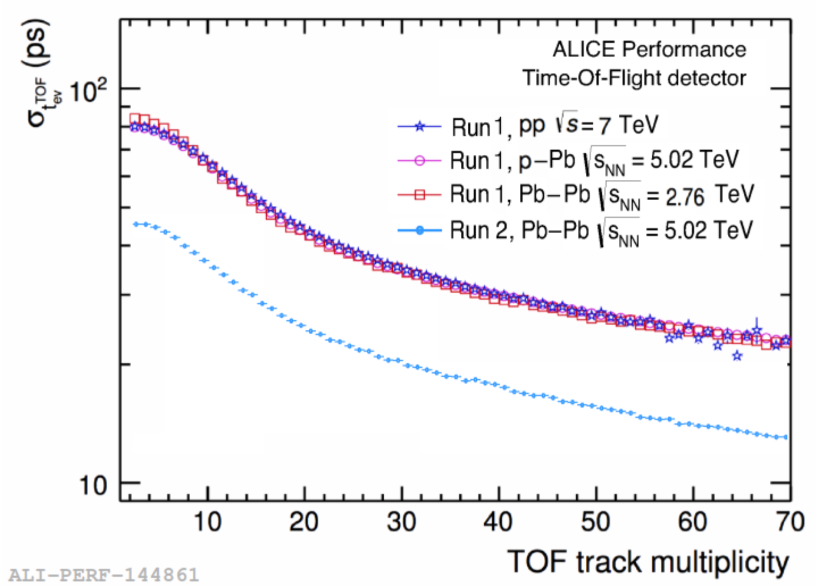

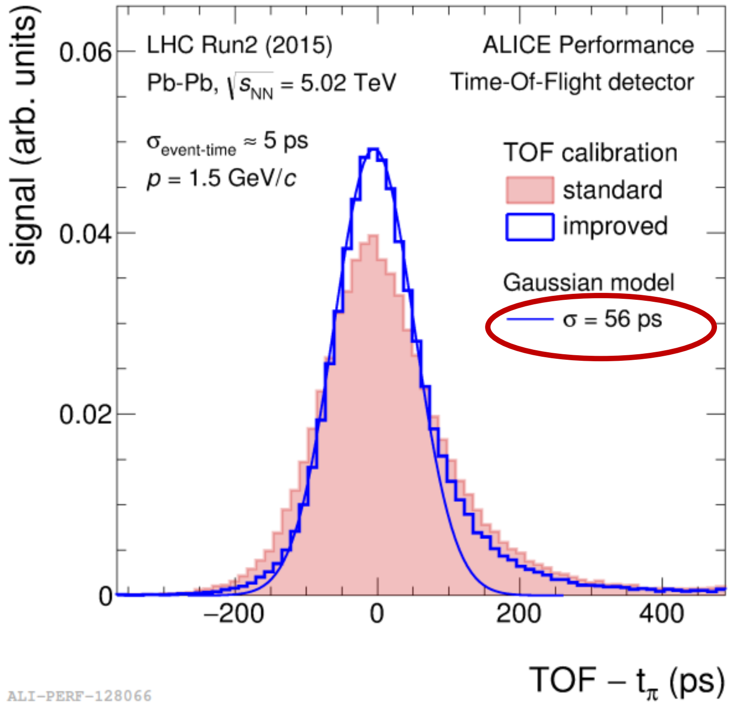

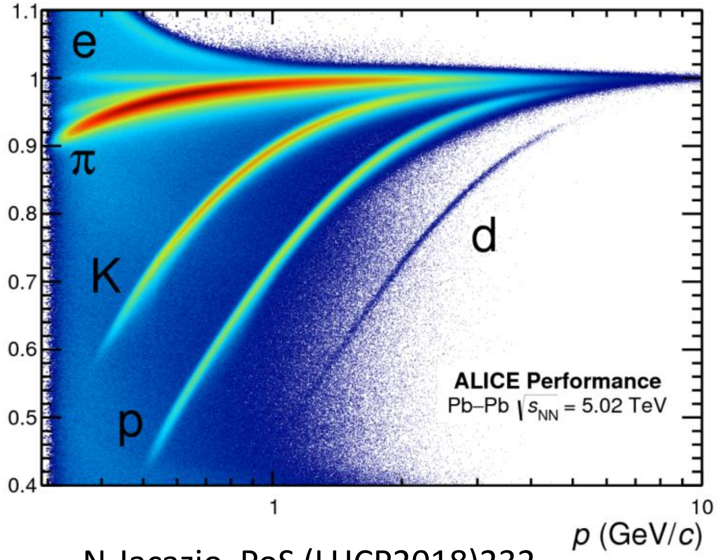

N.Jacazio, PoS (LHCP2018)232

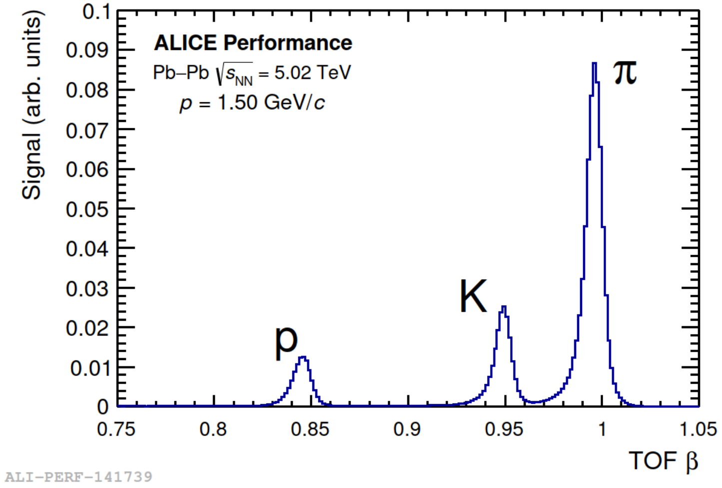

Momentum measurement through Time Projection Chambers (TPC)

In Run 2 max rate of 500 Hz/cm^2 with ~50-60 ps precision on MIP
Goal for Run 3: 50 KHz/cm^2 with ~20 ps precision on MIP

MicroMegas

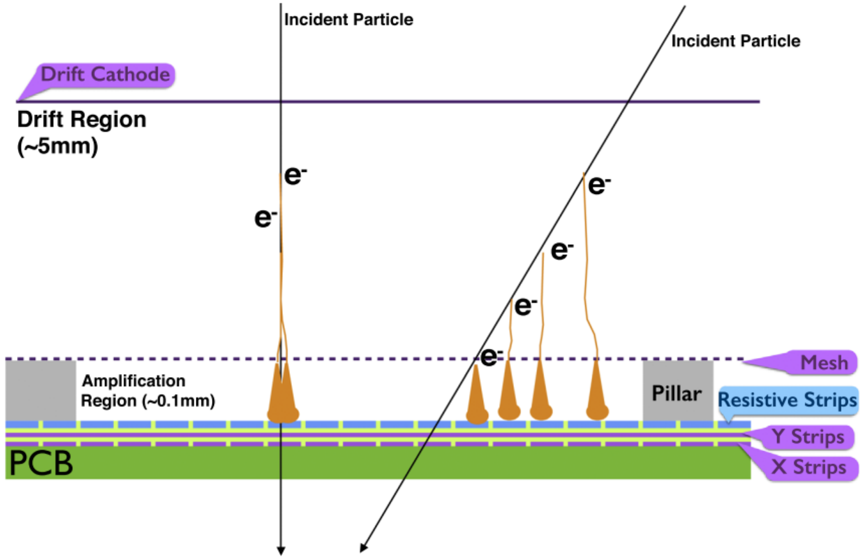

NIMA, Volume 767, 2014, Pages 281-288

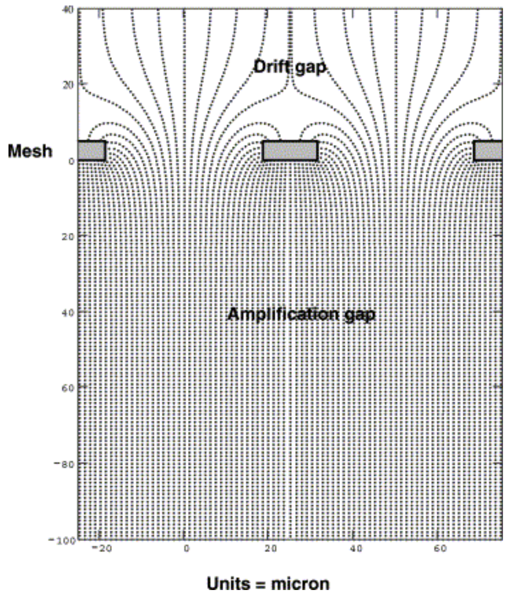

NIMA, Volume 478, Issues 1–2, 2002, Pages 26-36

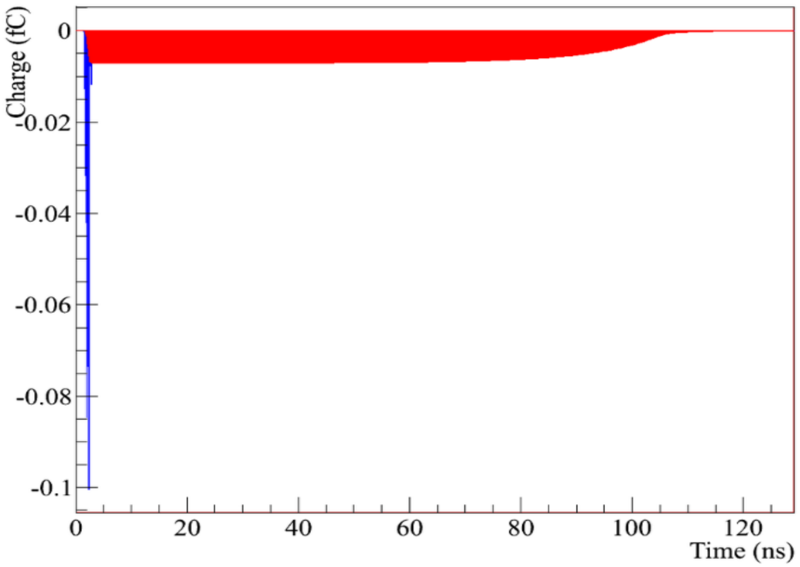

Picture from Wikipedia

Different strategy: add a mesh to divide the volume

- Thick conversion layer for detection and charge transport
- Thin amplification volume
- Mesh create an intense parallel field

Result is a fast and compact electron pulse with a long ion tail (can be cut with differential readout)

Timing Uncertainties

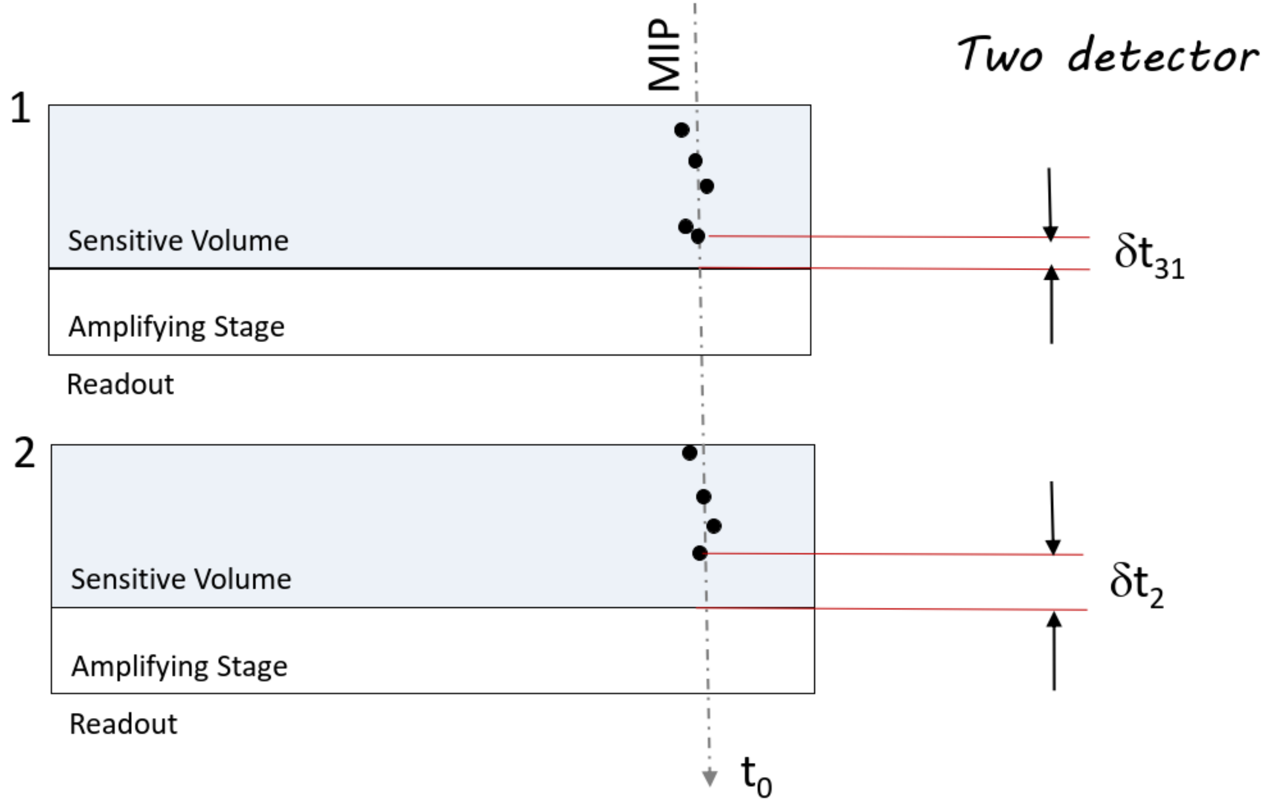

E.Oliveri, Frascati detector school 2018 , https://agenda.infn.it/event/15138/contributions/28611/attachments/20406/23149/EOliveri_FrascatiDetectorSchool2018.pdf

Time uncertainty given by the position of the first interaction point + slow drift time (5mm gap -> 1 ns for electrons)

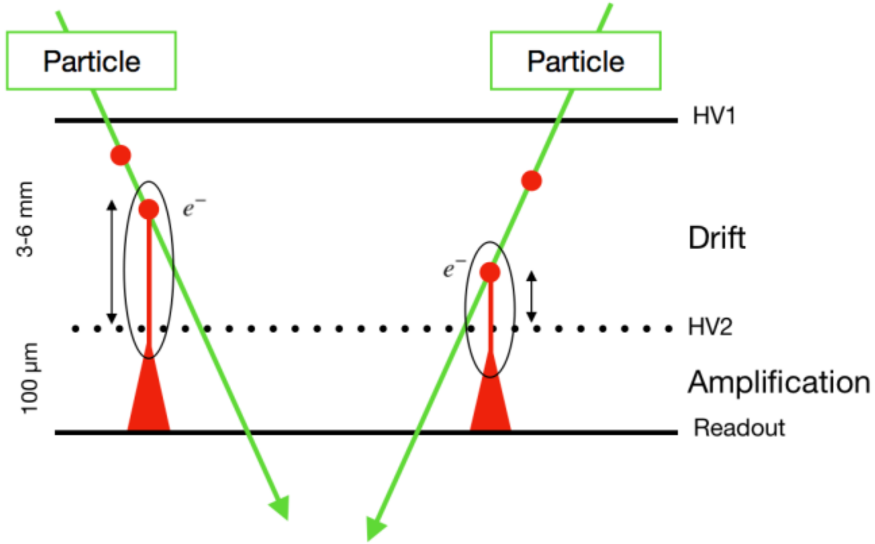

L.SOHL, RD51 miniweek 2020, https://indico.cern.ch/event/872501/contributions/3726013/attachments/1984848/3306891/PicosecRD51.pdf

Solution

E.Oliveri, Frascati detector school 2018 , https://agenda.infn.it/event/15138/contributions/28611/attachments/20406/23149/EOliveri_FrascatiDetectorSchool2018.pdf

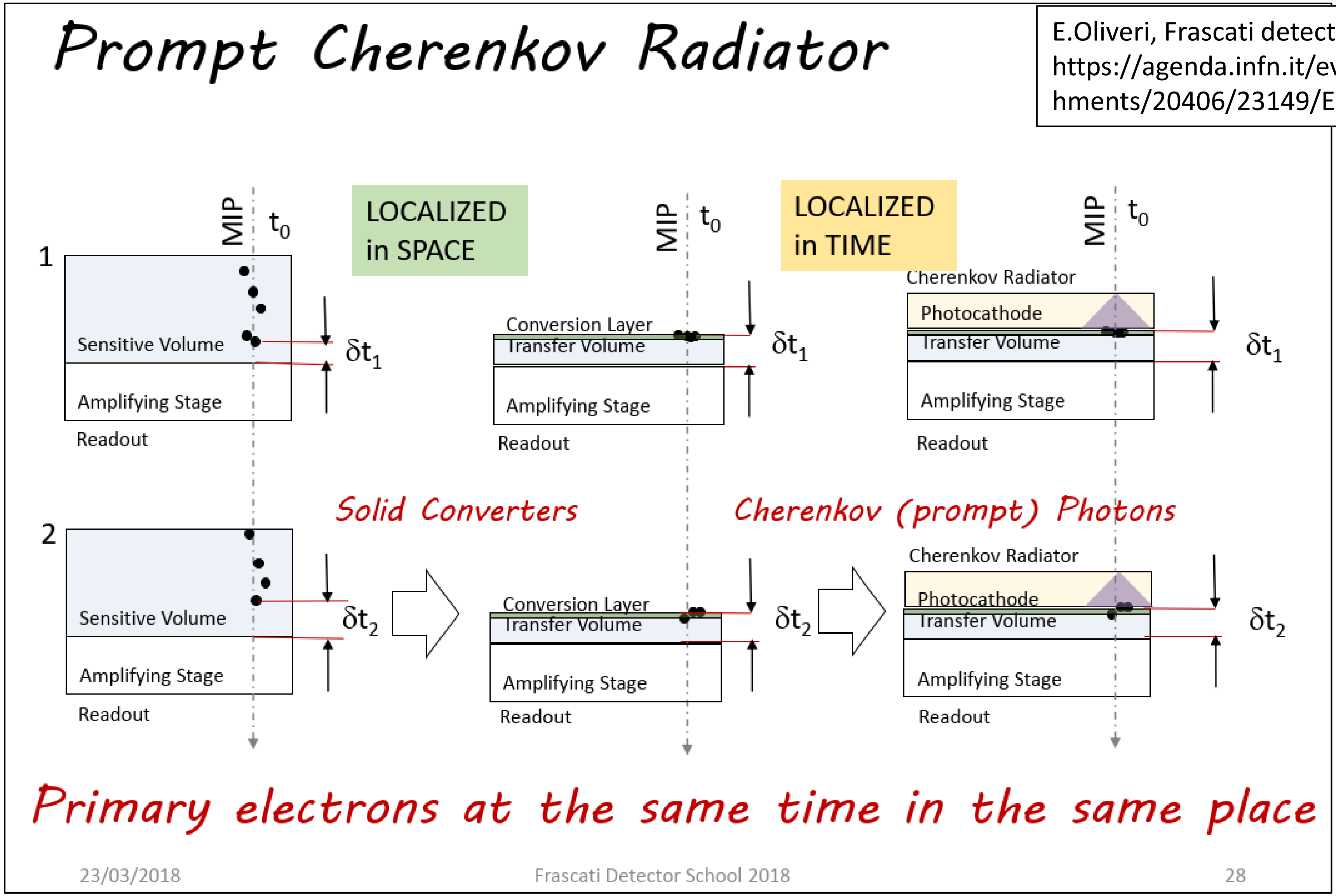

Preamplification

E.Oliveri, Frascati detector school 2018 , https://agenda.infn.it/event/15138/contributions/28611/attachments/20406/23149/EOliveri_FrascatiDetectorSchool2018.pdf

Pre-amplification in the first transfer.. The last step toward the results shown before

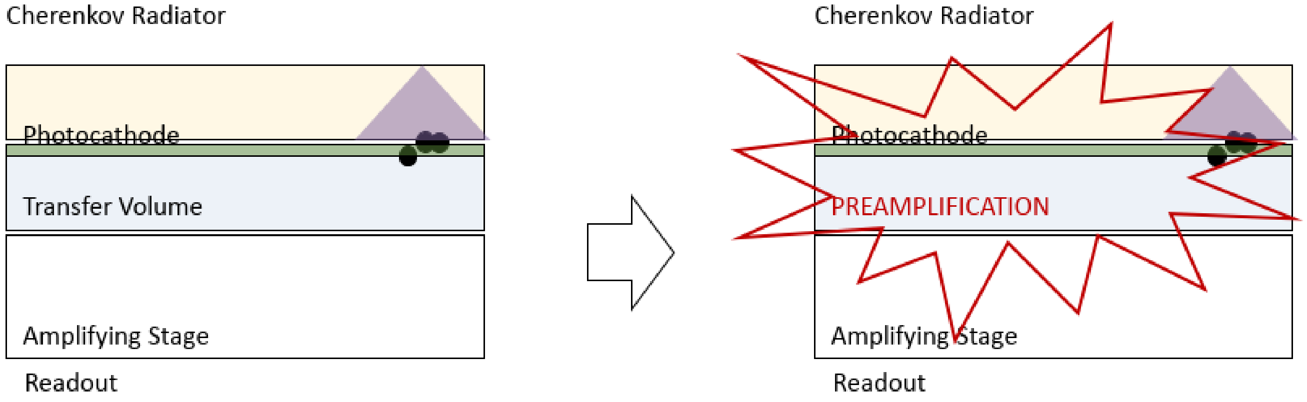

Sensitive volume reduced in order to:

- *Avoid direct gas ionization*
- *Reduce diffusion*

Pre-amplification: direct gas ionization and diffusion effect even more reduced, initial differences of pe levelled in the avalanche processes

23/03/2018 Frascati Detector School 2018 30

Single channel prototype

NIMA 903 (2018) 317–325

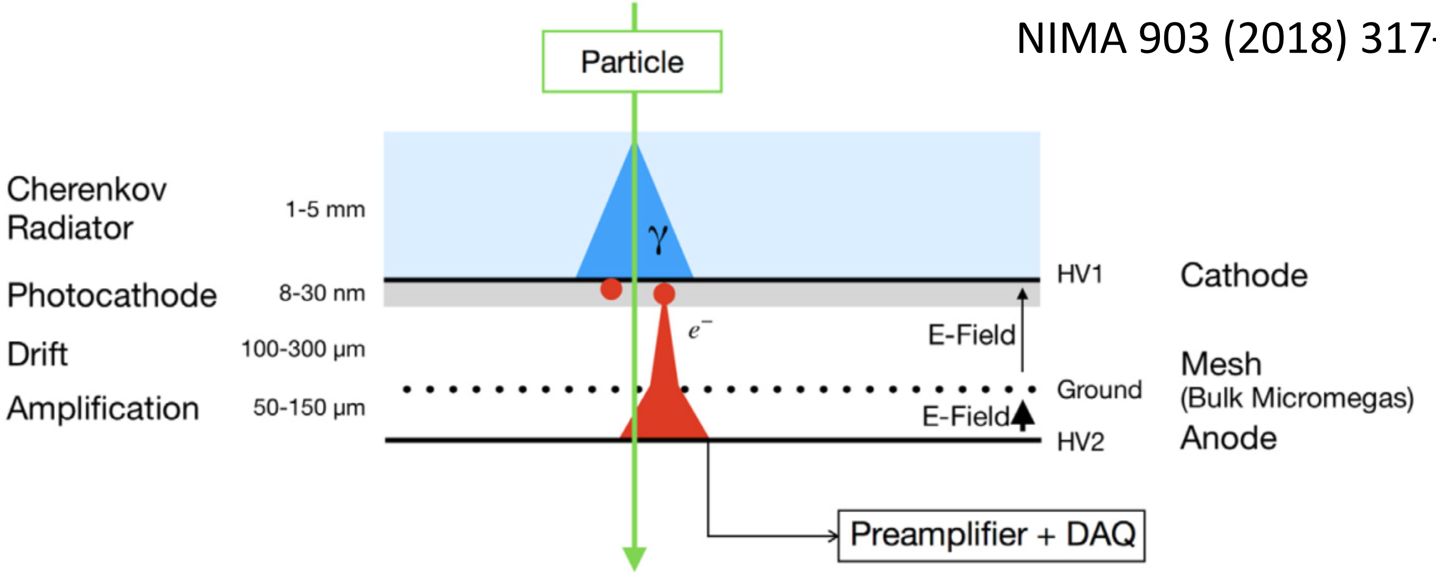

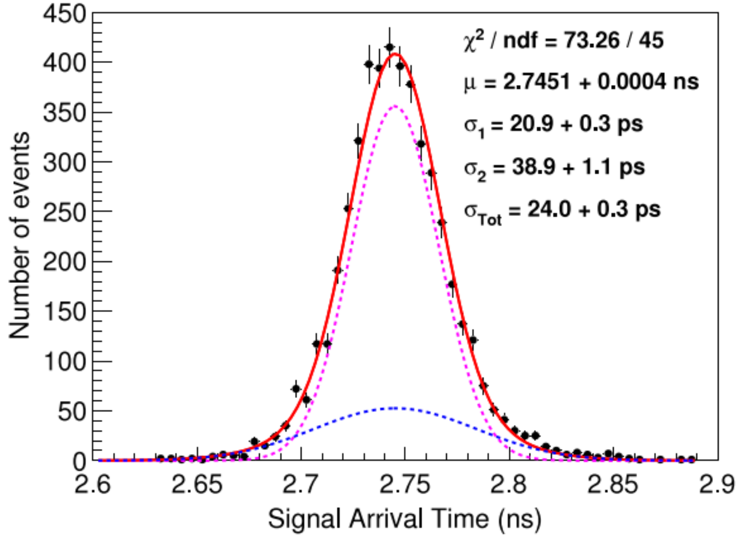

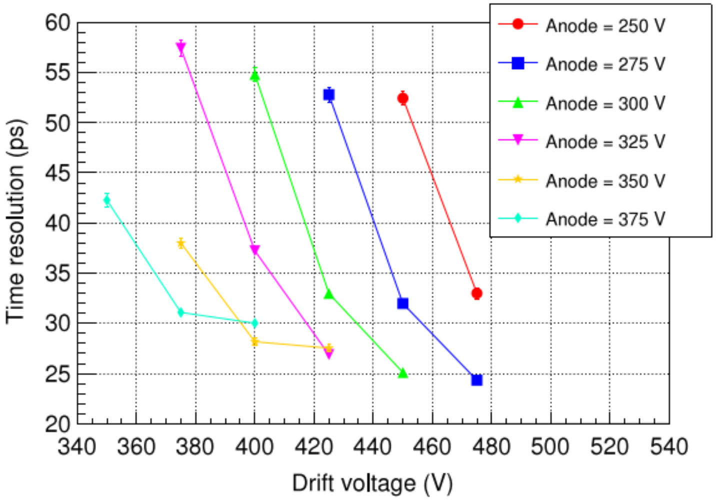

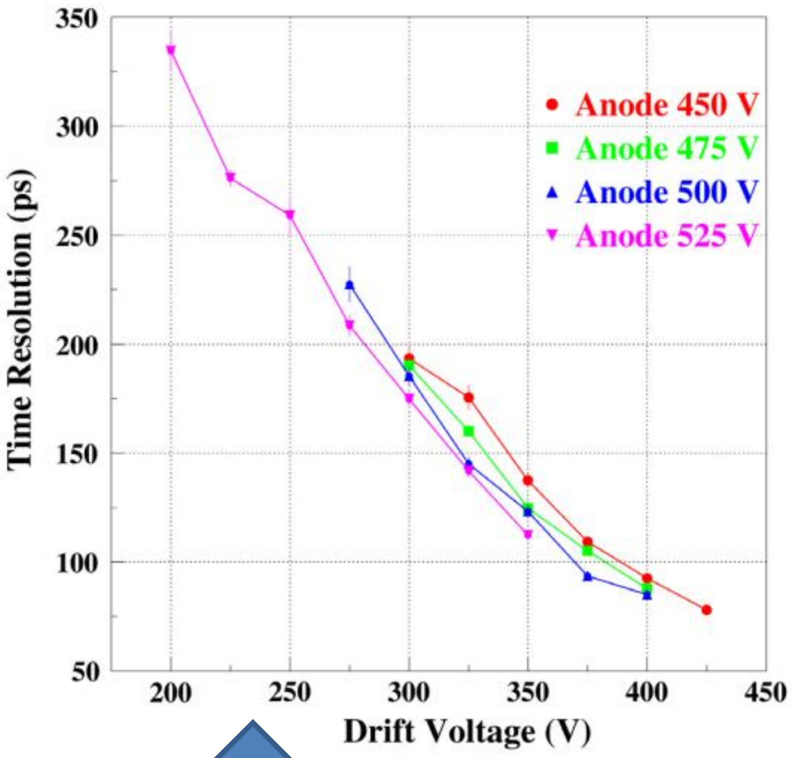

Laser (SPTR)

180 GeV Muons @ CERN SPS

Multi channel

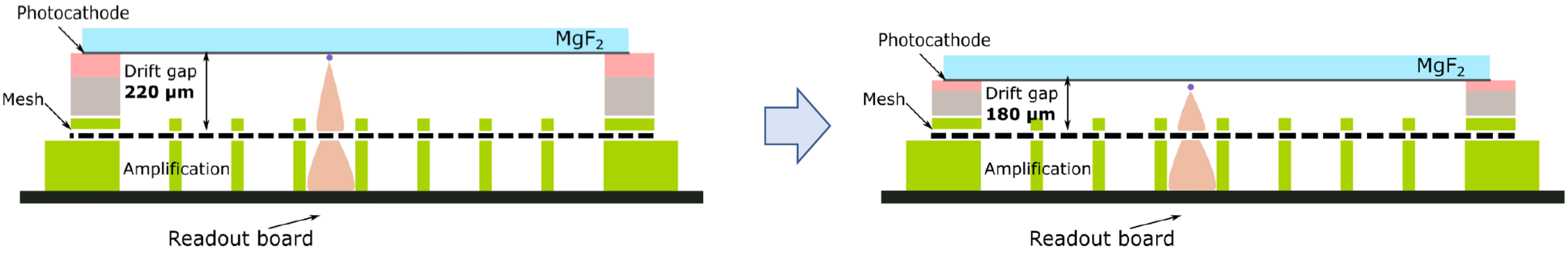

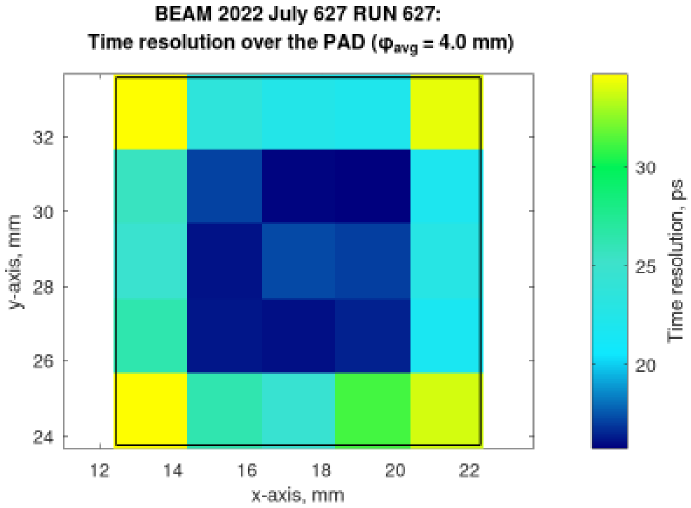

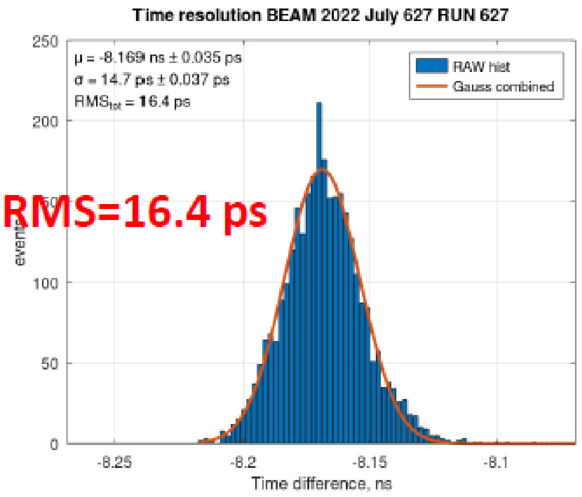

Custom made 10 channel preamplifier board for PICOSEC MM
detector

- Gain 38.5dB @100MHz
- HF -3dB cut-off 650 MHz, LF -3dB cut-off 4 MHz
- Input impedance 44 Ohm
- Negative pulses linear up to -1 V.
- Tested to sparks by shorting the input at 350 V bias.
- Power dissipation 75 mW per ch., Single supply 4 V.

First prototype with 100 channels (10x10 cm2) and improved performance.

A. Utrobicic on behalf of PICOSEC Micromegas Collaboration, “A large area 100 channel PICOSEC Micromegas detector with sub 20 ps time resolution”, MPGD2022

Electronics for timing

Electronics and digitization

Grupen and Shwartz, particle detectors, Cambridge university press 2008

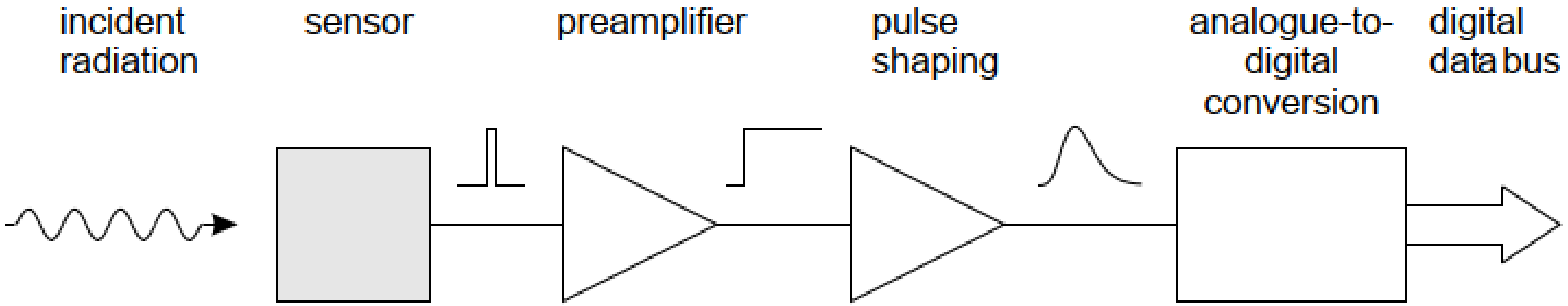

Only needed for detector with low or no internal gain (Silicon 3D, diamond, LGAD)

Not always needed but useful to have signal with constant shape and rise time.

Digitazion:

- Sampling
- Single /double measurement, typically discriminator+TDC

PreAmplifier: the classic dilemma

Charge sensitive amplifier

$$A_Q = \frac{\mathrm{d}v_\mathrm{o}}{\mathrm{d}Q_\mathrm{i}} = \frac{Av_\mathrm{i}}{C_\mathrm{i}v_\mathrm{i}} = \frac{A}{C_\mathrm{i}} = \frac{A}{A+1}\cdot\frac{1}{C_\mathrm{f}} \approx \frac{1}{C_\mathrm{f}}$$

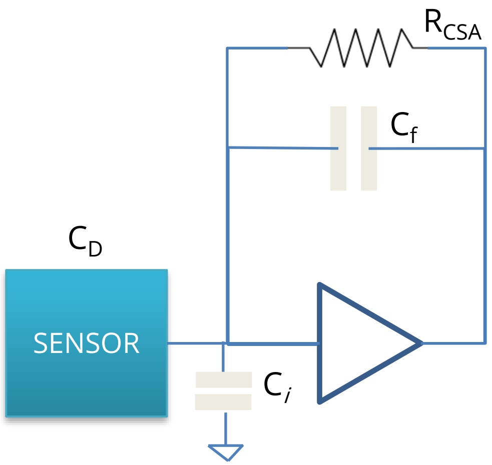

Miller effect:
$C_{if} = (A-1)C_f$

Input capacitance:
$C_i = C_{if}//C_d$

$Q_{gen} = \int i_{gen}\,dt \rightarrow$ Good solution

for:

- *Small* SNR
- *Slow* signal

Input noise $\sim$0.1fC

Broadband amplifier

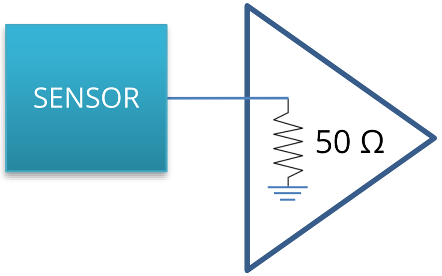

SNR for the ideal case of a read-out resistor:

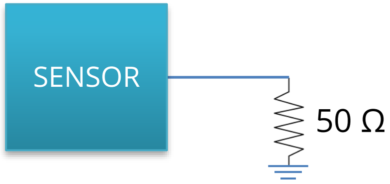

$$SNR = \frac{SNR_R}{\sqrt{F}}$$

F: Noise Factor
only contribution from the amplifier

Good solution for:

- *Large* SNR
- *Fast* signal

Input noise $\sim \mathrm{nV}/\sqrt{\mathrm{Hz}}$
With 2 GHz BW -> 50 µV

PreAmplifier: the custom way

Charge sensitive amplifier

$$A_Q = \frac{dv_o}{dQ_i} = \frac{Av_i}{C_i v_i} = \frac{A}{C_i} = \frac{A}{A+1} \cdot \frac{1}{C_f} \approx \frac{1}{C_f}$$

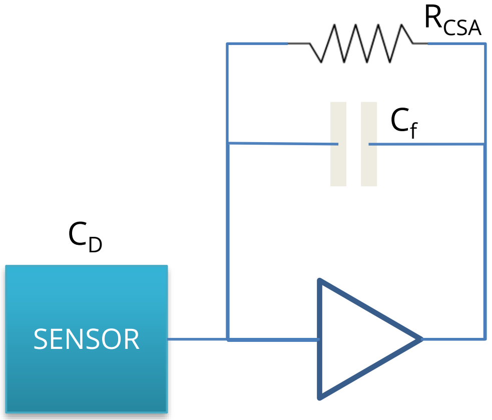

Miller effect:

$$C_i = (A-1)C_f$$

Input capacitance:

$$C_f // C_d$$

$Q_{gen} = \int i_{gen}\, dt \rightarrow$ Good solution

for:

- *Large* SNR
- *Slow* signal

Input noise $\sim 0.1\text{fC}$

It is possible to combine the advantage of the CSA (low noise) with the one of the BA (speed).

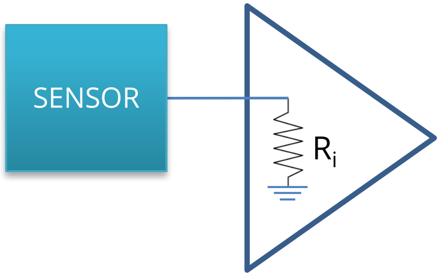

The input impedance must be selected according to the characteristics of the sensor.

A detailed simulation and understanding of the sensor is needed
Unfortunately, no commercial solutions available

More in N.Minafra, *Development of a timing detector for the TOTEM experiment at the LHC*, http://cds.cern.ch/record/2139815/

The diamond case

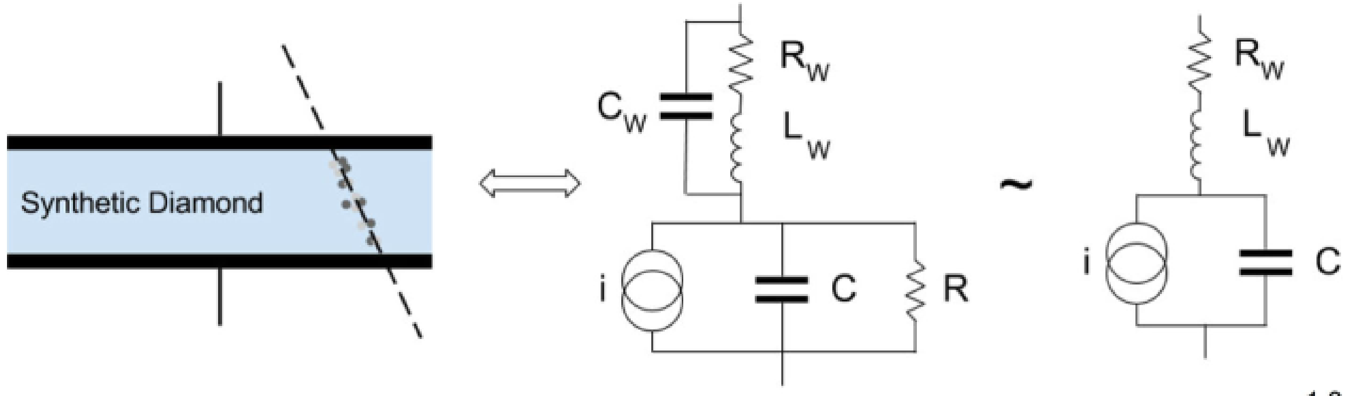

$$V_{RC}(t) = i(t) \star h_{RC}(t) = i(t) \star \frac{1}{C} e^{-\frac{t}{RC}}$$

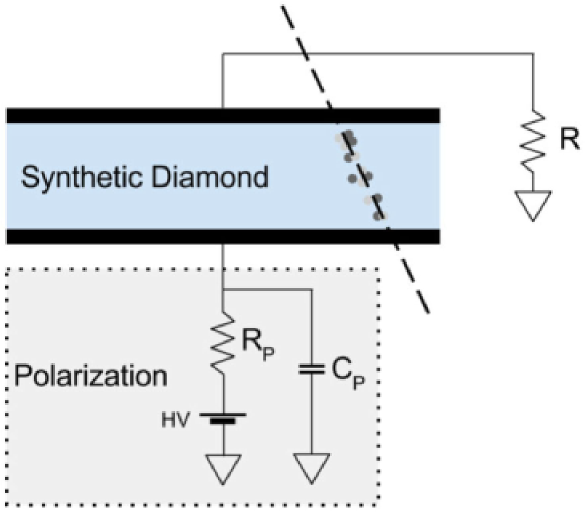

R can be the input resistance of a BA amplifier with negligible input capacitance

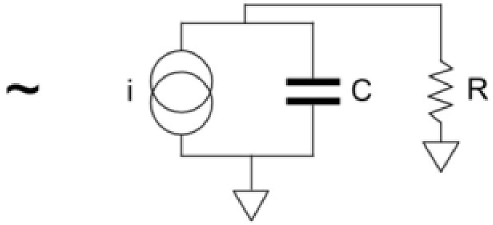

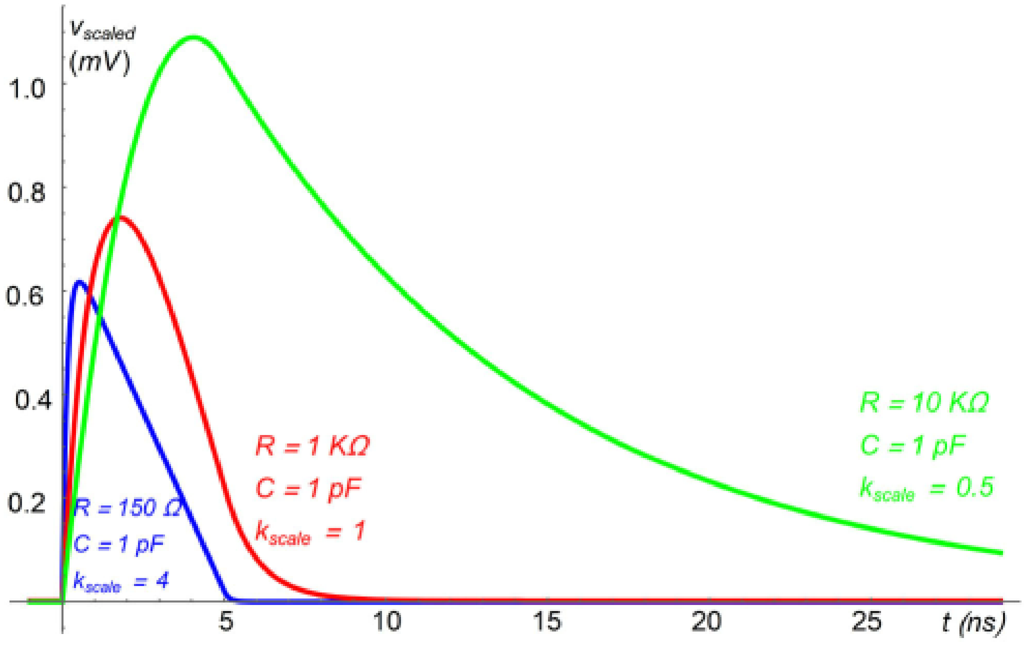

Front. Phys. 8:248. doi: 10.3389/fphy.2020.00248

The diamond case

Using the diamond signal:

Derivation: Chap.4 of N.Minafra, *Development of a timing detector for the TOTEM experiment at the LHC,* http://cds.cern.ch/record/2139815/

$$SNR = \frac{V_{max}}{\sigma_V} = \frac{2\,e\,N_{gen}}{t_{tr}^2}\frac{1}{\sqrt{k_B T}}\frac{1}{\sqrt{C}}RC\left(t_{tr} + RC\ln\left(\frac{RC}{RC+t_{tr}}\right)\right)$$

$$\lim_{R\to\infty} SNR = \frac{e\,N_{gen}}{\sqrt{k_B T}}\frac{1}{\sqrt{C}} \propto \frac{1}{\sqrt{C}}$$

Noise dominated by the thermal noise in the resistor (Johnson-Nyquist)

$$\sigma_t \sim \frac{\sigma_v}{dV/dt}\bigg|_{t=t_{th}} = \frac{\sqrt{k_B T}\,t_{tr}^2}{2\,Q_{gen}}\frac{\sqrt{C}}{RC}\frac{1}{(1+\frac{t_{tr}}{RC})\,e^{-\frac{t_{th}}{RC}} - 1}$$

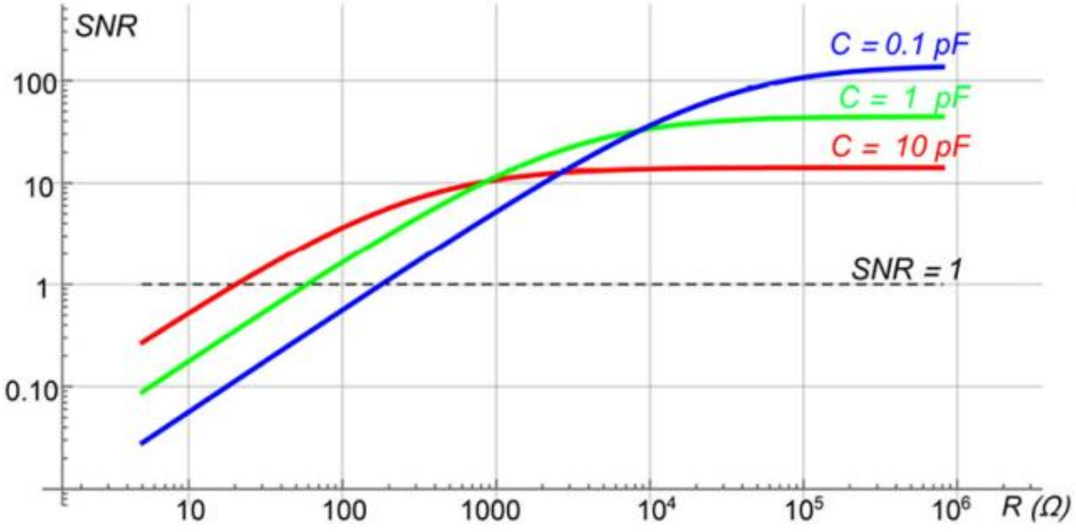

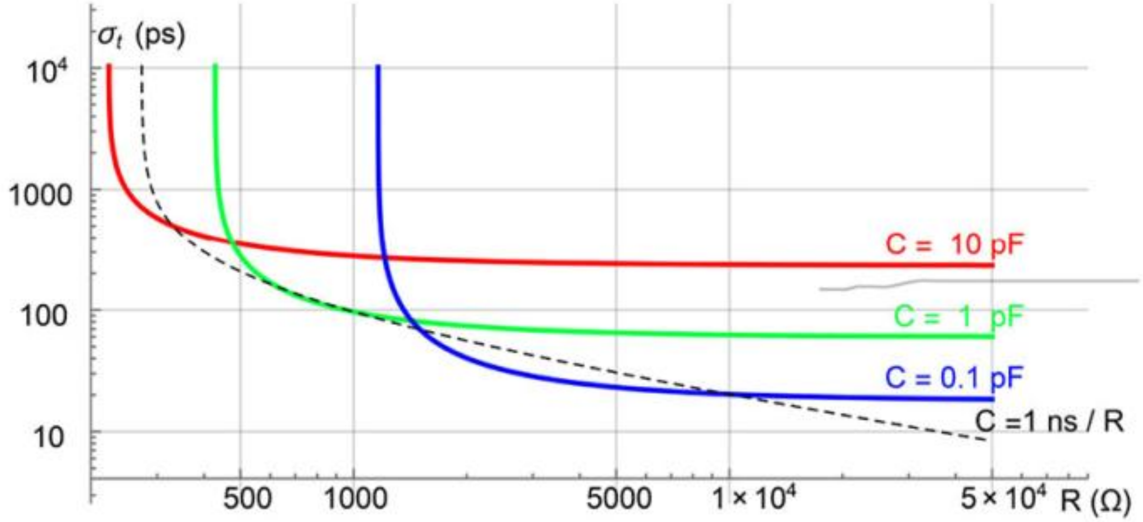

Front. Phys. 8:248. doi: 10.3389/fphy.2020.00248

Shaping: Noise

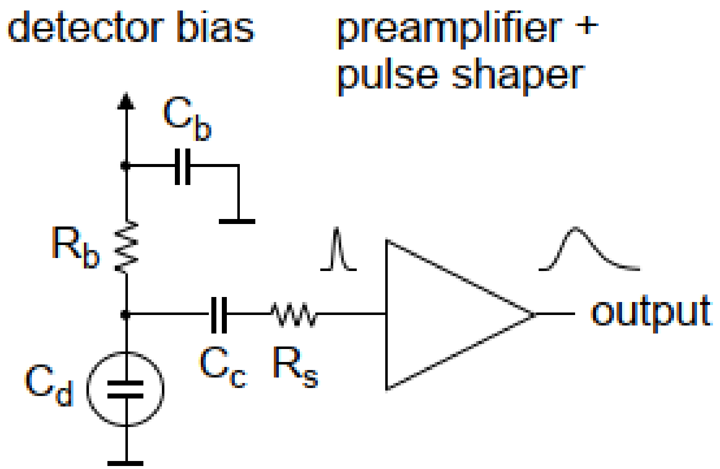

$$i = \frac{nev}{l}$$ Current flowing through a material

$$\langle \mathrm{d}i \rangle^2 = \left(\frac{ne}{l}\langle \mathrm{d}v \rangle\right)^2 + \left(\frac{ev}{l}\langle \mathrm{d}n \rangle\right)^2$$

Two components -> two mechanisms

Velocity fluctuations originate from thermal motion

$$i_{\mathrm{n}}^2 = \frac{4kT}{R}$$ White spectrum

Number fluctuations are generated by carrier flow limited by emission over a potential barrier (Shot noise):

- thermionic emission
- current flow in a semiconductor diode.

$$i_{\mathrm{n}}^2 = 2eI$$ White spectrum

A third component exists, due to carrier trapping, with frequency-dependent spectrum :

$$\frac{dP_n}{df} = 1/f^a \quad \text{(a = 0.5-2)} \rightarrow e_{\mathrm{nf}}^2 = A_{\mathrm{f}}/f$$

Usually referred to as “1/f noise”

Grupen and Shwartz, *Particle detectors*, Cambridge university press 2008
Rivetti, CMOS *Front-End Electronics for Radiation Sensors, CRC press 2015*

Shaping: Noise

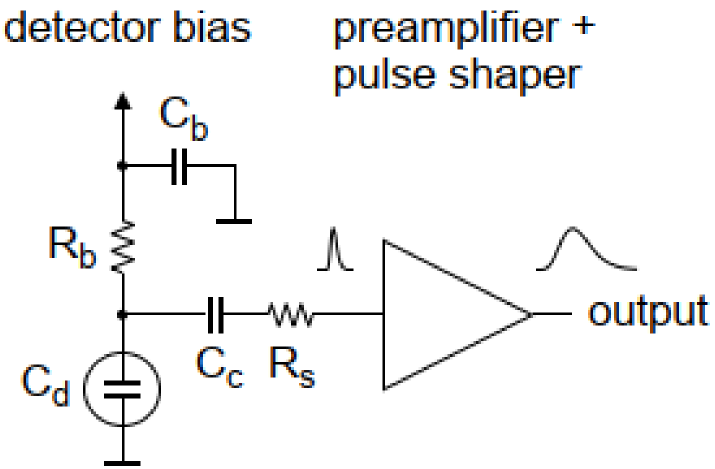

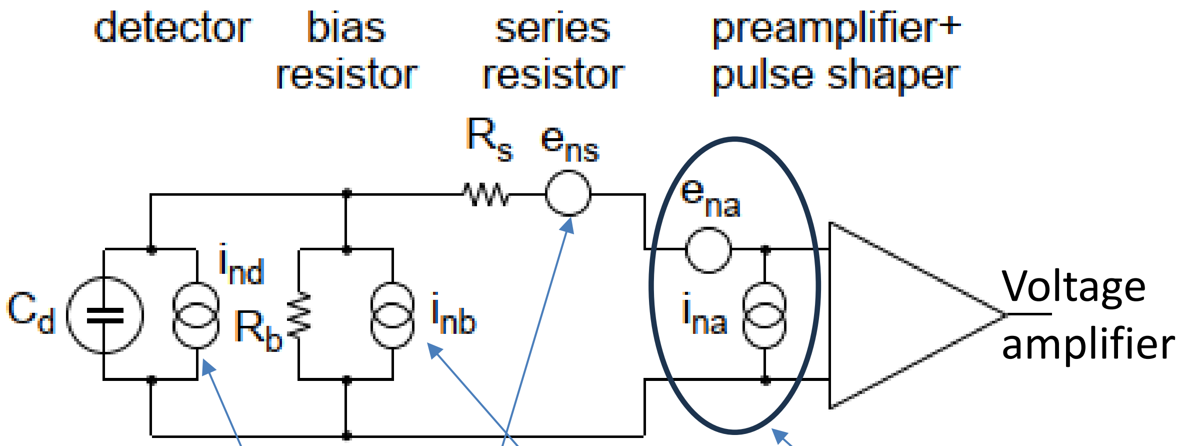

Thermal from bias resistor

Shot noise from detector (leakage current)

Thermal from series resistor

Amplifier noise model
(on datasheet)

$$i = \frac{nev}{l}$$

Current flowing through a material

$$\langle \mathrm{d}i\rangle^2 = \left(\frac{ne}{l}\langle \mathrm{d}v\rangle\right)^2 + \left(\frac{ev}{l}\langle \mathrm{d}n\rangle\right)^2$$

Two components -> two mechanisms

Parallel noise sources generate a currents through the detector capacitance (more in general through the input total capacitance)

$$\mathrm{e_n^2} = \frac{\mathrm{i_n^2}}{w^2\mathrm{C_d^2}} = \frac{\mathrm{i_n^2}\tau^2}{\mathrm{C_d^2}}$$

Grupen and Shwartz, *Particle detectors*, Cambridge university press 2008
Rivetti, CMOS *Front-End Electronics for Radiation Sensors, CRC press 2015*

Shaping: noise

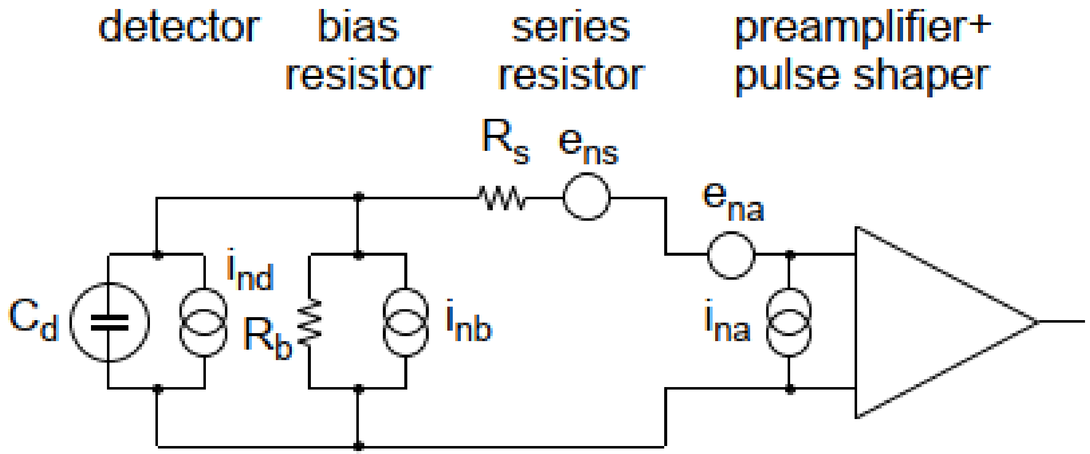

- Parallel noise source treated as voltage through a resistance $1/2\pi f C$
- Al voltages integrated over the detector (+parasitic) capacitance
- Maximize SNR is not all for timing!

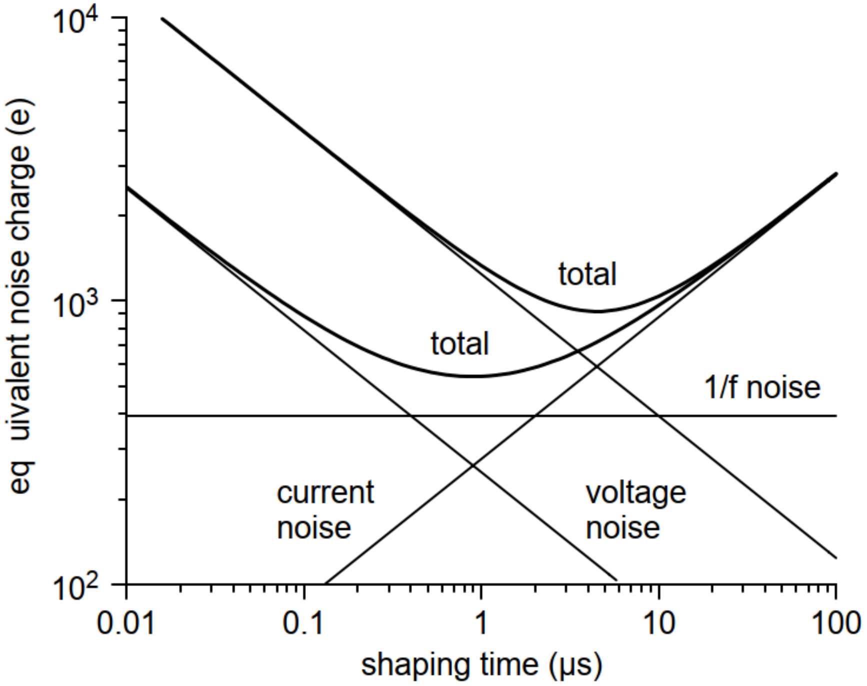

If *A(f)* constant over the amplifier BW and the noise have white spectrum

$$Q_n^2 = C_d^2 v_{on}^2 = C_d^2 \int_0^\infty e_n^2 A^2 (f) df = e_n^2 A^2 \, C_d^2/\tau$$

⇓

$$Q_n^2 = \left(\frac{e^2}{8}\right)\left[\left(2eI_d + \frac{4kT}{R_b} + i_{na}^2\right)\cdot\tau + \left(4kTR_s + e_{na}^2\right)\cdot\frac{C_d^2}{\tau} + 4A_f C_d^2\right]$$

Grupen and Shwartz, *Particle detectors*, Cambridge university press 2008
Rivetti, CMOS *Front-End Electronics for Radiation Sensors, CRC press 2015*

UNIVERSITÀ DI SIENA 1240

SAMPIC

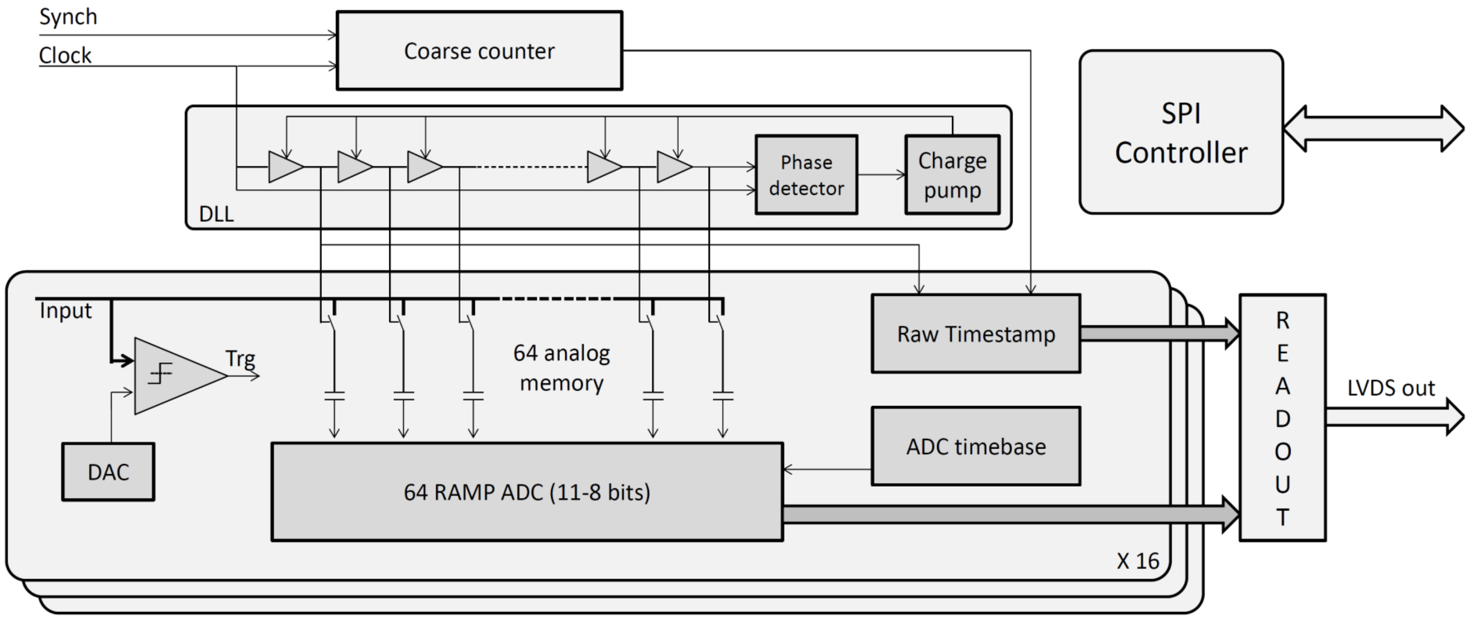

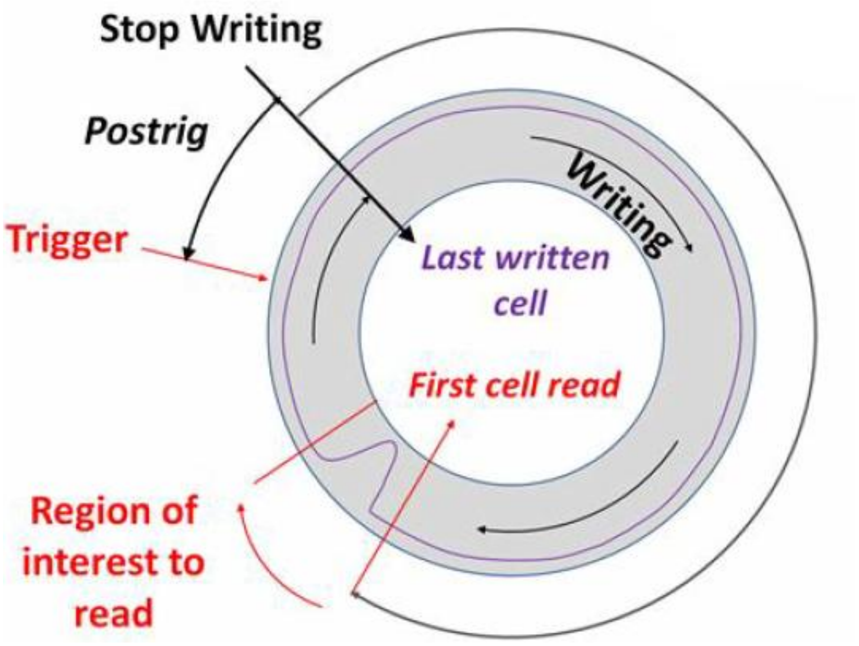

- 16 channel/chip
- 64 sample/hit up to 10 GSa/s
- 1.5 GHz bandwidth
- 8-11 bit resolution
- 0.25-1.6 µs channel dead time
- Resolution of few ps

- Self trigger or central trigger with poor latency capability
- No event building
- Each sampled signal sent out

arXiv:1503.04625
arXiv:1604.02385

HPTDC

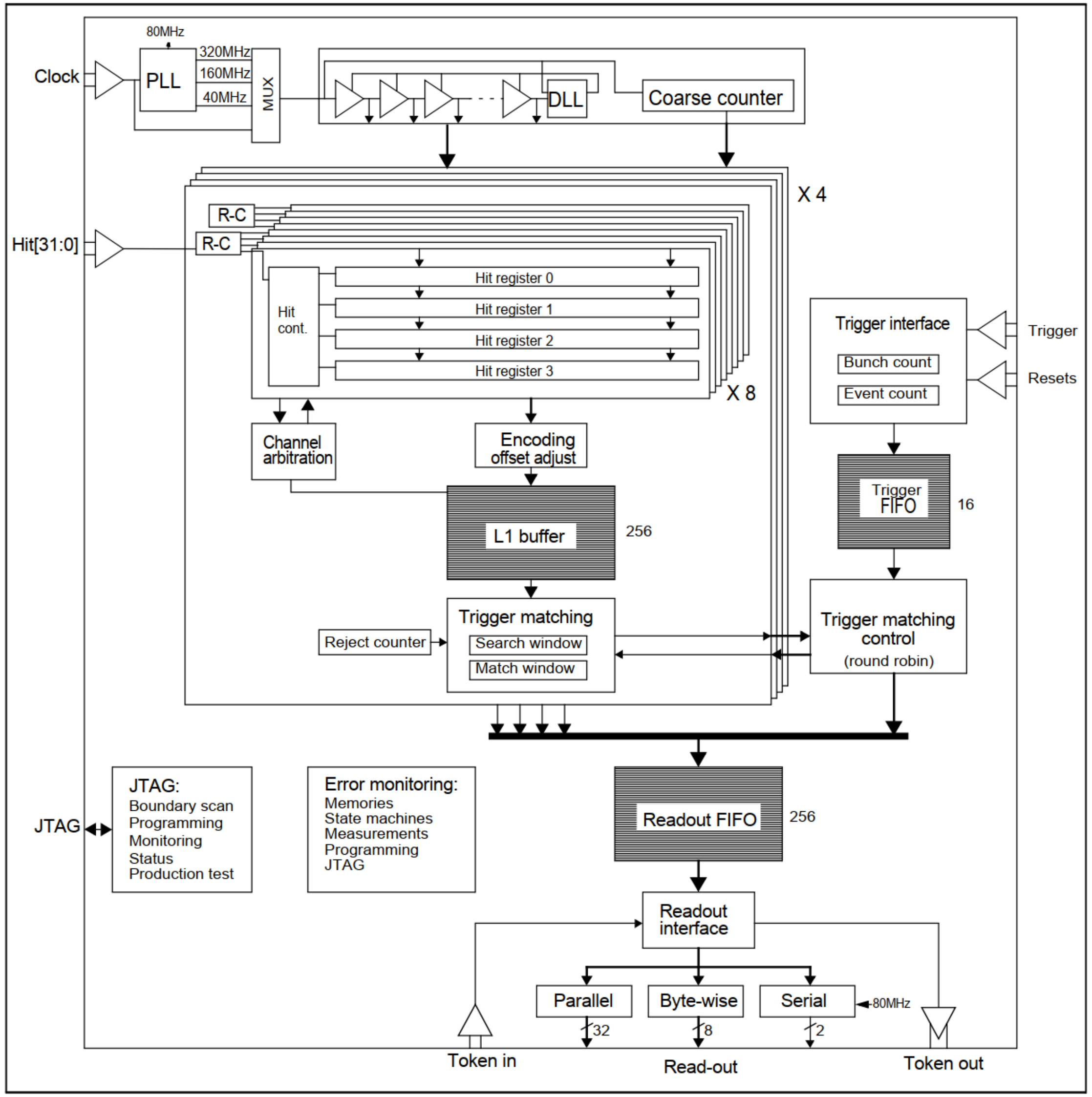

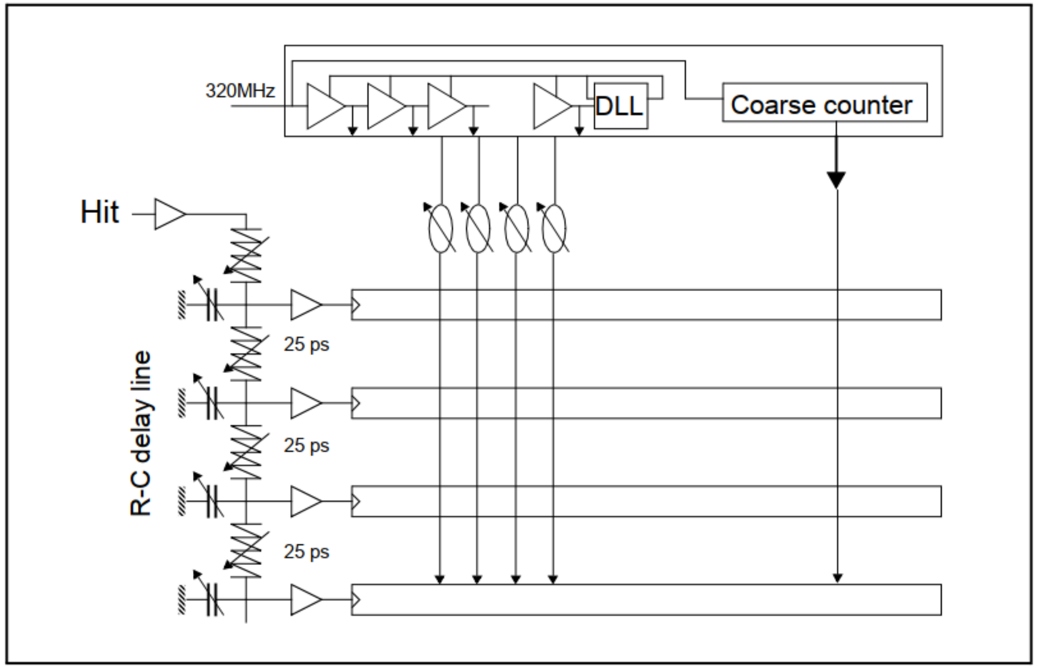

- 32 channels (100 ps bin) or 8 channel (25 ps)
- Rate capability up to few MHz/channel
- Optimize for LHC bunch structure
- Advanced event building capability
- Resolution better than 10 ps
- Double edge capability
- Multiple readout interface

3D readout example: ALTIROC

ATLAS LGAD Timing Integrated ReadOut Chip:

- ➢ Target time resolution ~25 ps
- ➢ Latency up to 35 µs @ 1MHz trigger
- ➢ Low power dissipation
- ➢ 15x15 channels (pixels)
- ➢ Time over threshold (ToT) and Time of Arrival (ToA) information
- ➢ Event building

Preamp+discriminator+double TDC